CHARACTERIZING GROUNDWATER FLOW THROUGH MEROKARST, NORTHEAST KANSAS, USA

By



Emily R. Barry
B.S., State University of New York at Oneonta, 2016

Submitted to the graduate degree program in Geology and the Graduate Faculty of the University of Kansas in partial fulfillment of the requirements for the degree of Master of Science.

_____

Chair: Gwendolyn L. Macpherson

_____

Pamela Sullivan

_____

Randy Stotler

Date Defended: June 27, 2018

The thesis committee for Emily R. Barry certifies that this is the approved version of the following thesis:

CHARACTERIZING GROUNDWATER FLOW THROUGH MEROKARST, NORTHEAST KANSAS, USA

Chair: Gwendolyn L. Macpherson

Date Approved: August 30, 2018

**Abstract**

Karst aquifers are a significant source of groundwater supply worldwide, yet are known for unpredictable flow paths and rapid groundwater velocity. Characterizing the complex nature of karst aquifers though dye tracing is essential to confronting problems, like contamination, that may threaten groundwater/drinking water supply. The aquifers this study focuses on are the Cottonwood, Morrill, and Eiss Limestones underlying the Konza Prairie Long-Term Ecological Research Site in Northeastern Kansas, USA. These aquifers are merokarst and consist of thin limestone beds that alternate with shales. Watershed N04d is drained by the northward flowing South Fork Branch of Kings Creek. Potentiometric surface maps of the Morrill Limestone indicate groundwater is flowing south in this unit. Overlying the Morrill, in the Eiss Limestone, potentiometric surface maps indicate groundwater flowing north. Here, the unusual contrasting groundwater flow directions of these units are investigated using dye-tracing to better understand the nature of merokarst aquifer systems.

Fluorescein, eosine, and rhodamine WT were used as groundwater tracers to aid in the understanding of groundwater flow at Konza. Dyes were injected into monitoring wells on July 29$^{th}$, 2017 and monitored via charcoal packets and water samples from wells and the South Fork Branch of Kings Creek. Low flow conditions dominated in this study period, both in the stream and in the aquifer. Groundwater velocity measurements from this tracer test suggest this is a diffuse flow system. The results of the tracer test show that groundwater is flowing north in the Eiss Limestone and Cottonwood Limestone, and south in the Morrill Limestone. The presence of dye in underlying limestone units suggests groundwater is leaking from the upper aquifers through shales that act as leaky aquitards. I propose that a collapse feature in the units at this site is causing groundwater to flow south in the Morrill Limestone, while springs in the Eiss

Limestone and Cottonwood Limestone discharge groundwater in these units where groundwater flows northward. Trends in fractures also influence the direction of groundwater flow. The tracer-test revealed travel times comparable to those in epikarst, suggesting the results of this study may be widely applicable.

**Acknowledgments**

I would like to thank my incredible husband, Joe, for being my rock during my time as a graduate student and for always bringing out the best in me. I would not have been able to do this without you. I would also like to thank my parents and siblings for always being only a phone call away and for always believing in me.

I would also like to thank my advisor, Dr. Gwen Macpherson for her incredible guidance and mentorship on this project. Additionally, I would like to thank my committee members Dr. Pamela Sullivan and Dr. Randy Stotler for their assistance on this project. Thank you to the KU Department of Geology and the countless professors that have mentored me throughout my graduate and undergraduate education. Thank you all for your commitment to training the next generation of scientists.

I would like to thank the friends I have made during my time at KU and for their emotional and physical support. Chantelle Davis, Mackenzie Cremeans, Matthew Downen, Adam Yoerg, Brock Norwood, and many others have always provided me with help in the field and throughout the writing process.

My sincerest thanks go to Tom Aley and the staff at the Ozark Underground Lab for their guidance on conducting a tracer test and assistance with analyses. Additionally, this project would not have been possible without funding and support from the Tumbling Creek Cave Foundation, Ozark Underground Lab, Crawford Hydrology Lab, the Leaman Harris Fund, KU Endowment, and the National Science Foundation.

Lastly, I would like to thank the Konza Prairie Long-Term Ecological Research Site for allowing me to conduct research at this site and for the use for their online data base: DOI: AGW01: 10.6073/pasta/1676db0329aee780b60ae993e22662d2.

Table of Contents

## Chapter 1: Introduction

This master's thesis is based on field data collected from July through December of 2017 at the Konza Prairie Long-Term Ecological Research Site (Konza). Laboratory analyses were completed at Ozark Underground Laboratory in Missouri. Background fluorescence tests were conducted at Crawford Hydrology Lab.

Approximately 20% of the United States relies on karst aquifers for water supply (Ford and Williams, 2007). Most studies focus on karst aquifers represented by massive limestone beds with rapid groundwater flow velocities. However, not all karst aquifers are massive, but rather, are referred to as "thin limestones." Thin limestones are only a few meters thick, while massive limestones can be hundreds of meters thick. Significantly less research has been conducted in thin limestone settings, yet a significant portion of the Midwestern United States is underlain by thin Permian limestones and shales (Macpherson, 1996). Thin limestones are known as merokarst, which is an imperfect karst setting with thin limestones (Monroe, 1970). These limestone aquifers are an important groundwater supply for the surrounding areas (Macfarlane, 2003). Although the storage capacity of thin limestones is typically much lower than massive limestones, thin limestone aquifers are still used as a freshwater source and are important in groundwater supply. The purpose of this study is to use fluorescent dye tracers to better understand groundwater flow through a complex merokarst aquifer at Konza.

Understanding flow through thin limestone systems is difficult due to complex flow paths and is further complicated by solution-enlarged fractures, the locations of which are often unknown. Solution enlarged conduits tend to be smaller in thinner limestones, resulting in slower flow velocities. These flow velocities are still considered rapid when compared to porous media. Therefore, karst aquifers can be subject to rapid contamination, if contaminated water flows

through their conduits. Understanding flow through karst environments is crucial when determining an aquifer's potential use as a freshwater supply.

Massive limestones typically have mature cave systems and solution enlarged conduits that carry water at rapid velocities compared to porous media. Typical flow velocities in well-developed, or mature, karst aquifers range from 220 to 9500 meters per day (Mull *et al*., 1988). The Barton Springs Edwards Aquifer, a mature karst system, can carry water miles/kilometers per day under high flow conditions and 800 meters per day under low flow conditions (Hauwert *et al*., 2002). In an immature karst aquifer, water travels through smaller conduits and flow velocities are much lower, taking months to travel tens of feet/meters (Freidrich and Smart, 1981). Konza's flow system is characterized as immature and diffuse, where groundwater moves through a network of joints, fractures, and bedding planes that are a few centimeters or less in length (Schuster and White, 1971). This immature flow system causes water to move through the system slower than in a mature karst aquifer. The driving force for groundwater flow is hydraulic gradient. Water flows along the hydraulic gradient from high points where recharge occurs to low points where discharge occurs (Toth, 1962). Tracer tests are a reliable and commonly used technique for determining flow direction in massive limestones.

The results of a tracer test are commonly used to indicate the direction of groundwater flow, groundwater flow paths between injection points and springs, and a more informed understanding of hydraulic flow in the subsurface. In Walkerton, Ontario a tracer test was conducted to determine if groundwater contaminated with *Escherichia coli*, more commonly known as *E. coli*, was traveling to a municipal water supply well and how rapid the water was traveling through the karst aquifer (Worthington *et al*., 2002). Test results indicated the travel time of the tracers injected was much faster than the travel time predicted by MODFLOW

(Worthington *et al*., 2002). The results of a tracer test usually disprove a travel time made using Darcy's law or another comparable calculation.

Another example illustrating the success/usefulness of tracer tests in karst aquifers is the Biscayne aquifer in Florida. This aquifer supplies water to over a million people, and had the potential to become contaminated if a quarry were to be opened near the well field. Tracer tests showed the velocity of the groundwater to be 366 meters per day which drastically surpassed the predicted velocity of 8 meters per day (Green *et al*., 2006).

Finally, the Clays Ferry Formation of Kentucky consists of thinly bedded limestones interbedded with shales, similar to the geology of Konza. Tracer tests show a groundwater velocity of 2160 meters per day (Mull *et al*., 1993). This aquifer is characterized as a diffuse flow system, again like Konza, so a similar groundwater flow velocity may be expected.

Tracer tests are clearly the best way to characterize groundwater flow directions in a karst system (Aley, 2002). Chapter 2 of this thesis focuses on three fluorescent tracer tests at the Konza Prairie to investigate groundwater flow dynamics in multiple karst aquifers. The dyes used were fluorescein, eosine, and rhodamine WT. Both qualitative and quantitative data were collected, and used to make conclusions regarding groundwater flow dynamics in each of the studied aquifers. Results suggest that groundwater flows in different directions in the aquifers that are stacked on top of each other.

Chapter 3 discusses future work regarding groundwater flow through thin limestone aquifers at Konza and in similar environments. The appendix contains charts, maps and tables showing the results from the tracer test, maps of geologic units and springs at the field site, detailed methods, stream information, and precipitation data that are essential to interpreting the results of this study.

The findings of this study have implications for groundwater remediation in karstic systems. Karst aquifers are very vulnerable to contamination. Groundwater flows faster in fractured aquifers than most porous media aquifers. This means that contaminants can reach a destination more rapidly in karst than in porous media. Groundwater is one of our most important resources and understanding how it flows through different types of geologic media is essential to protecting it.

**References**:


Aley, T. (2002). Groundwater tracing handbook. *Ozark Underground Labs*.

Friederich, H., & Smart, P. L. (1981). Dye tracer studies of the unsaturated zone: recharge of the Carboniferous Limestone aquifer of the Mendip Hills, England. In *Proceedings of the 8th International Congress of Speleology* (Vol. 1, pp. 283-6). Kentucky USA.

Ford, D., & Williams, P. (2007). Introduction to Karst. *Karst Hydrogeology and Geomorphology*, 1-8.

Green, R. T., Painter, S. L., Sun, A., & Worthington, S. R. (2006). Groundwater contamination in karst terranes. *Water, Air, & Soil Pollution: Focus*, *6*(1-2), 157-170.

Hauwert, N. M., Johns, D. A., Sansom, J. W., & Aley, T. J. (2002). Groundwater tracing of the Barton Springs Edwards Aquifer, Travis and Hays Counties, Texas.

Macfarlane, P.A., (2003). The hydrogeology of Crystal Spring with and delineation of its source water assessment area: Kansas Geological Survey, Open-file Report no. 2003-35, 156 p.

Macpherson, G. L. (1996). Hydrogeology of thin limestones: the Konza Prairie long-term ecological research site, Northeastern Kansas. *Journal of Hydrology*, *186*(1-4), 191-228.

Mull, D. S., et al. *Application of dye-tracing techniques for determining solute-transport characteristics of ground water in karst terranes*. No. PB-92-231356/XAB; EPA--904/6-88/001. Environmental Protection Agency, Atlanta, GA (United States). Region IV, 1988.

Mull, D. S., Liebermann, T. D., Smoot, J. L., & Woosley, L. H. (1988). *Application of dye-tracing techniques for determining solute-transport characteristics of ground water in karst terranes* (No. PB-92-231356/XAB; EPA--904/6-88/001). Environmental Protection Agency, Atlanta, GA (United States). Region IV.

Shuster, E. T., & White, W. B. (1971). Seasonal fluctuations in the chemistry of lime-stone springs: A possible means for characterizing carbonate aquifers. *Journal of hydrology*, *14*(2), 93-128.

Tóth, J. (1962). A theory of groundwater motion in small drainage basins in central Alberta, Canada. *Journal of Geophysical Research*, *67*(11), 4375-4388.

Worthington, S. R. H., Smart, C. C., & Ruland, W. W. (2002). Assessment of groundwater velocities to the municipal wells at Walkerton. *Ground and Water: Theory to Practice*, 1081-1086.

# CHAPTER 2: CHARACTERIZING GROUNDWATER FLOW THROUGH MEROKARST, NORTHEAST KANSAS, USA

**Executive Summary**

Karst terrain covers 10 % of the Earth's surface, is an important resource for groundwater supply, and is easily contaminated. Solution-enlarged fractures can make understanding flow through these aquifers difficult. Knowing how groundwater moves through these aquifers is important for developing them as a water supply and for remediating contamination. This study took place at the Konza Prairie Long-Term Ecological Research Site in Northeastern Kansas, USA and focuses on the Permian aged Morrill and Eiss Limestone Members. The underlying bedrock is made of thin limestones (1–2 m) and shales (2–4 m), which are classified as merokarst. These karst aquifers can be considered a diffuse flow system because they have slower flow than massive karst aquifers. These aquifers also demonstrate similar characteristics to epikarst aquifers. Potentiometric surface maps show that groundwater in the Morrill Limestone Member of the Beattie Limestone Formation is flowing south, while in the overlying unit, the Eiss Member of the Bader Limestone Formation, groundwater flows north. The South Fork Branch of Kings Creek, which drains the N04d watershed, flows to the north.

Dye tracing was used to characterize the flow dynamics of the aquifers during the dry season. Fluorescein, eosine, and rhodamine were injected into water wells that are screened in the Morrill and Eiss Limestones at Konza on July 29$^{th}$, 2017. This dye trace represents low-flow aquifer conditions. Charcoal packets and water grab samples were used to take concentration measurements of dye in wells and in the stream. The results of this study confirmed that groundwater flows southward in the Morrill Limestone and northward in the Eiss Limestone. It also demonstrated that groundwater moves downward into the underlying Cottonwood Limestone Member of the Beattie Limestone, bypassing the stream. The shales separating these limestones must behave as leaky aquitards, although whether this leakage is restricted to certain

focused paths or is diffuse is unknown. Detection of rhodamine both southward and northward of the injection well reveals a complex flow pattern that could be explained by groundwater flowing in different directions in different aquifers and those aquifers being vertically connected. The results of this study show that some of the rhodamine plume flowed south in the Morrill Limestone, and some moved downward through the Florena Shale and into the Cottonwood Limestone where it then flowed north, thus creating a multidirectional plume. I hypothesize this southward flow and the cross-formational flow result from a collapse feature that enhanced dissolution along joints and fractures and created a topographically low area in The Morrill Limestone.

## 1. Introduction

Approximately 20% of the United States is underlain by karst aquifers (Quinlan and Ewers, 1989). A large portion of karst aquifers, especially in Europe, underlie densely populated regions, making management of karst aquifers crucial for large populations that depend on these aquifers for water supply (Chen *et al*., 2017). Flow paths through karst aquifers are often difficult to predict because connectivity of solution-enlarged fractures. Karst features develop where limestone is dissolved during chemical weathering along preexisting joints in the rock. The enlargement of these fractures often depends on the joint orientation, spacing, and intersections. Karst aquifers transmit water more rapidly than other aquifers because the enlarged fractures have higher hydraulic conductivity than porous media and focus the flow along directed paths (Mull *et al.*, 1998). This often presents problems related to groundwater contamination as karst aquifers lack the natural filtration that most porous media aquifers have.

Holokarst is an area with little or no surface runoff and is underlain by massively bedded limestone (Monroe, 1970). Caves or large fractures develop in holokarst, this creates rapid

groundwater flow and preferential flow paths, which can be challenging to predict. In contrast, merokarst is an imperfect karst area with thin, impure limestones that has surface drainage and dry valleys that contain some karst features (Monroe, 1970). The major difference between the two, for the purpose of this study, is that merokarst has a more immature fracture network and a slower travel time than typically observed in holokarst. A large portion of central North America is underlain by strata similar to those that underlie Konza (Macpherson, 1996). Although holokarst and merokarst differ in scale, the same principles related to groundwater flow apply, and both present challenges in developing conceptual models for predicting groundwater flow.

Tracer tests are a common method used to determine the direction and velocity of groundwater flow. In this study, we use strategies and precautions similar to those discussed in Benson and Yuhr (2016). We performed well hydraulic tests and evaluated potentiometric surfaces to gain insight into groundwater flow directions and rates before beginning a five-month long fluorescent dye trace after a single-day injection of three different dyes at three shallow monitoring wells.

The field site is located on a tallgrass prairie with wooded riparian zones within the Flint Hills, the Konza Prairie Long-Term Ecological Research Site (Konza). The Flint Hills in northeastern Kansas (Figure 1) are underlain by Permian bedrock in which thin limestones and shales alternate (Macpherson, 1996). These strata are characterized as a humid climate karst, consisting of carbonate rocks at or near the land surface that are part of the Flint Hills Aquifer system (Weary & Doctor, 2014; Macfarlane, 2003). This region has a temperate mid-continent climate with a mean annual temperature of 12° Celsius and an average precipitation of 835 millimeters (CLIMDB/HYDRODB). Although the average precipitation classifies Konza as a humid climate karst (30 inches/762 millimeters or more of rain), the precipitation was less than

762 millimeters during this study, therefore this study represents dry conditions. The 60 watersheds on Konza form the experimental framework for ecological research. Watershed N04d was the focus of this study. It is one of the few watersheds that contain observations wells and a gauged stream (Figure 2).

The objectives of this study were to determine the direction and velocity of groundwater flow through N04d, to determine if the Morrill and Eiss aquifers are connected, to understand more about how groundwater flows through thin limestones, and to discover how the results of a merokarst study compare to holokarst.

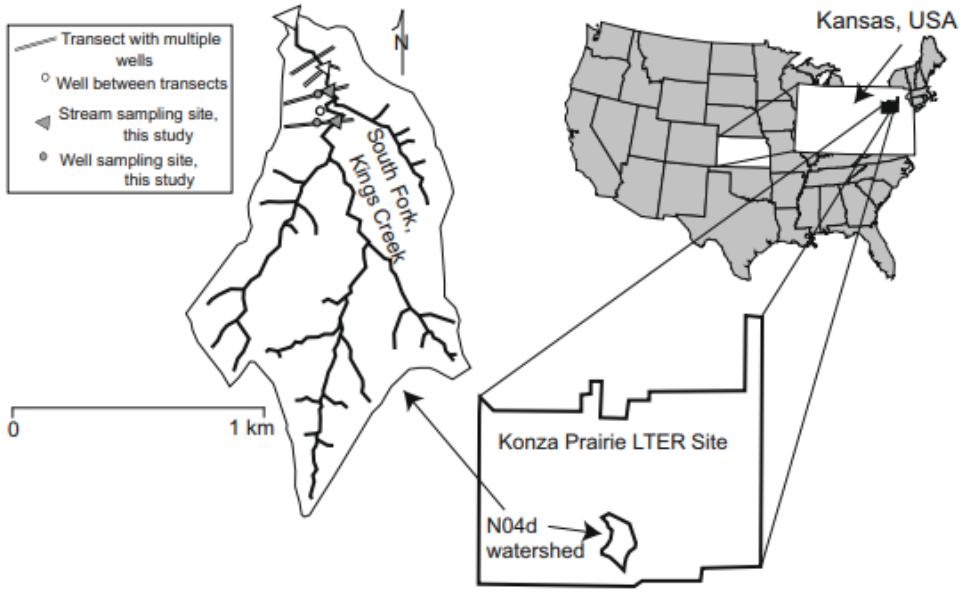


Figure 1: Watershed N04d located in the Konza Prairie LTER Site in Northeastern Kansas, U.S.A. (Macpherson *et al*., 2008).

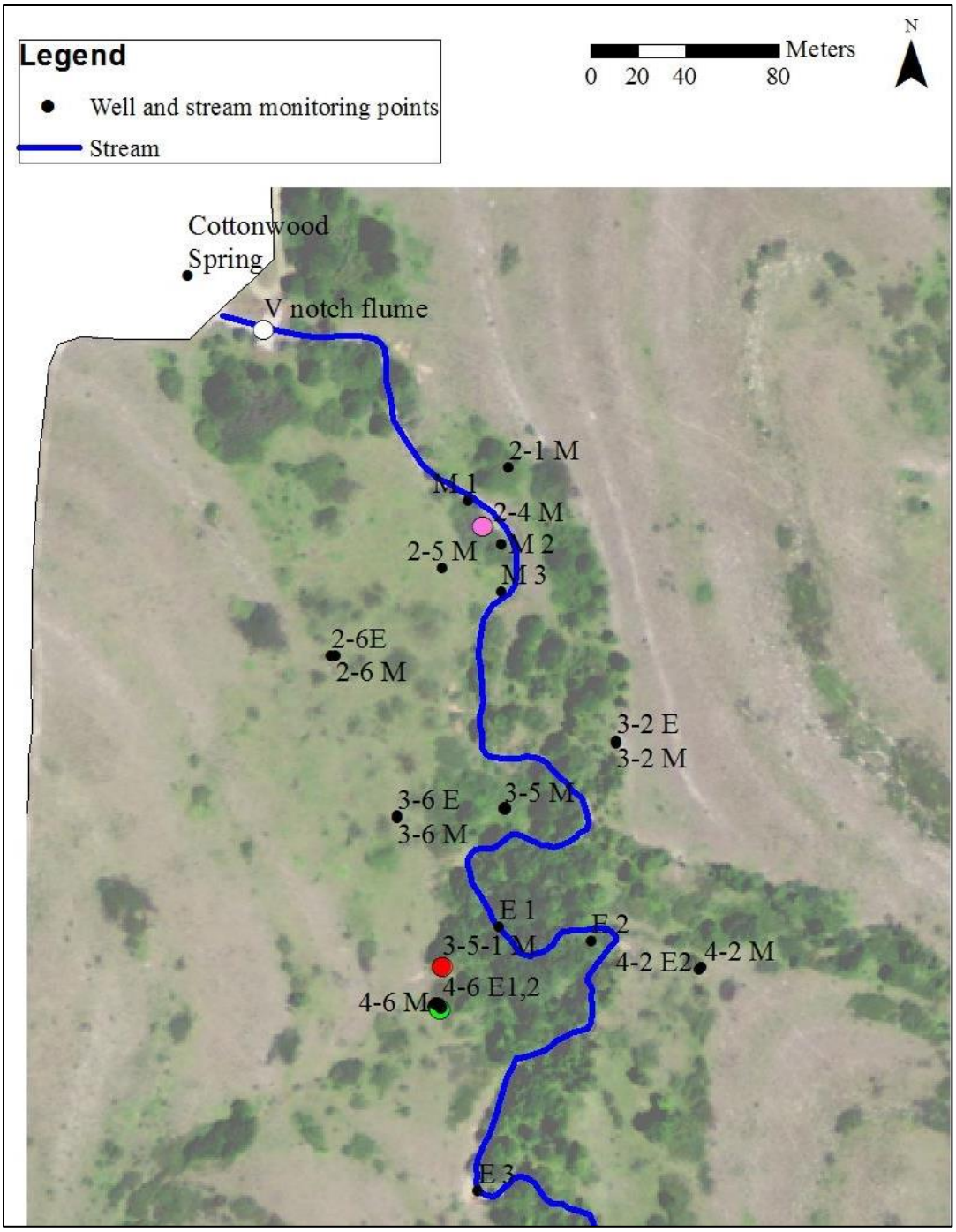


Figure 2: Map of monitoring wells, stream monitoring points, injection wells (colored circles). Color of circle indicates dye type. Red is rhodamine (3-5-1M), green is fluorescein (4-6E2), and pink is eosine (2-4M). Modified from B. Norwood, 2016.

## 2. Field Site

### 2.1 Geology

The geologic units in this study are Permian limestones and shales from the Council Grove Group and Chase Group of the Wolfcampian Series (Figure 3; Jewett, 1941). The regional strata are nearly horizontal with a dip of 0.1-0.21$^0$ NW (Smith, 1991). In a core examined by Twiss (1991), it was discovered that the depth to weathering is 40m in this area. The wells in N04d are no deeper than 15 m and therefore are within the zone of weathering, which contributes to karstification. The examination of this core also showed that only 74% of it was recovered, which is likely due to karstification. Evaporite minerals have been found in cores but are lacking in outcrop which suggest the dissolution of these minerals and aiding the karstification of these units (Twiss, 1991). This type of karst aquifer is likely classified as a discontinuous carbonate rock (Chen *et al*., 2017). The thicknesses listed are general, but the actual thicknesses of the units are highly variable. The Cottonwood Limestone Member of the Beattie Limestone, the Morrill Limestone Member of the Beattie Limestone and the Eiss Limestone Member of the Bader Limestone are all included in the Council Grove Group, and were the aquifers investigated in this study (Figure 3). For this study, the Cottonwood Limestone, Morrill Limestone, and Eiss Limestone will all be referred to as aquifers. The Cottonwood Limestone member of the Beattie Limestone is the lowest unit monitored in this study. The Cottonwood Limestone is 1.8 m thick and is distinguished surficially by massive ledges. Springs are common beneath these massive ledges (Jewett, 1941). The Florena Shale member overlies the Cottonwood Limestone, is 3 m thick, and is a gray argillaceous shale. Overlying this, the Morrill Limestone is approximately 1 m thick and is brownish gray with many distinct calcite crystals in it. The Morrill Limestone weathers into an irregularly pitted, granular brown limestone. The weathered pits are partially filled with crystalline calcite (Jewett, 1941). Because it is easily weathered, outcrops of the Morrill are difficult to find, but can be identified by locating the Cottonwood Limestone, which

the Morrill overlies by 3 m. The Morrill is overlain by the Stearns Shale. The Stearns Shale is overlain by the Eiss Limestone. The Eiss Limestone is made up of three parts: 1) a lower gray, thinly bedded limestone unit which is 0.5 m thick, 2) a middle unit of gray shale which is 0.75 m thick, and 3) the upper limestone unit which is 0.9 m thick. (Jewett, 1941). Quaternary deposits of alluvium and colluvium overlie these Permian units. A thin layer of loess covers most of the region (Smith, 1991).

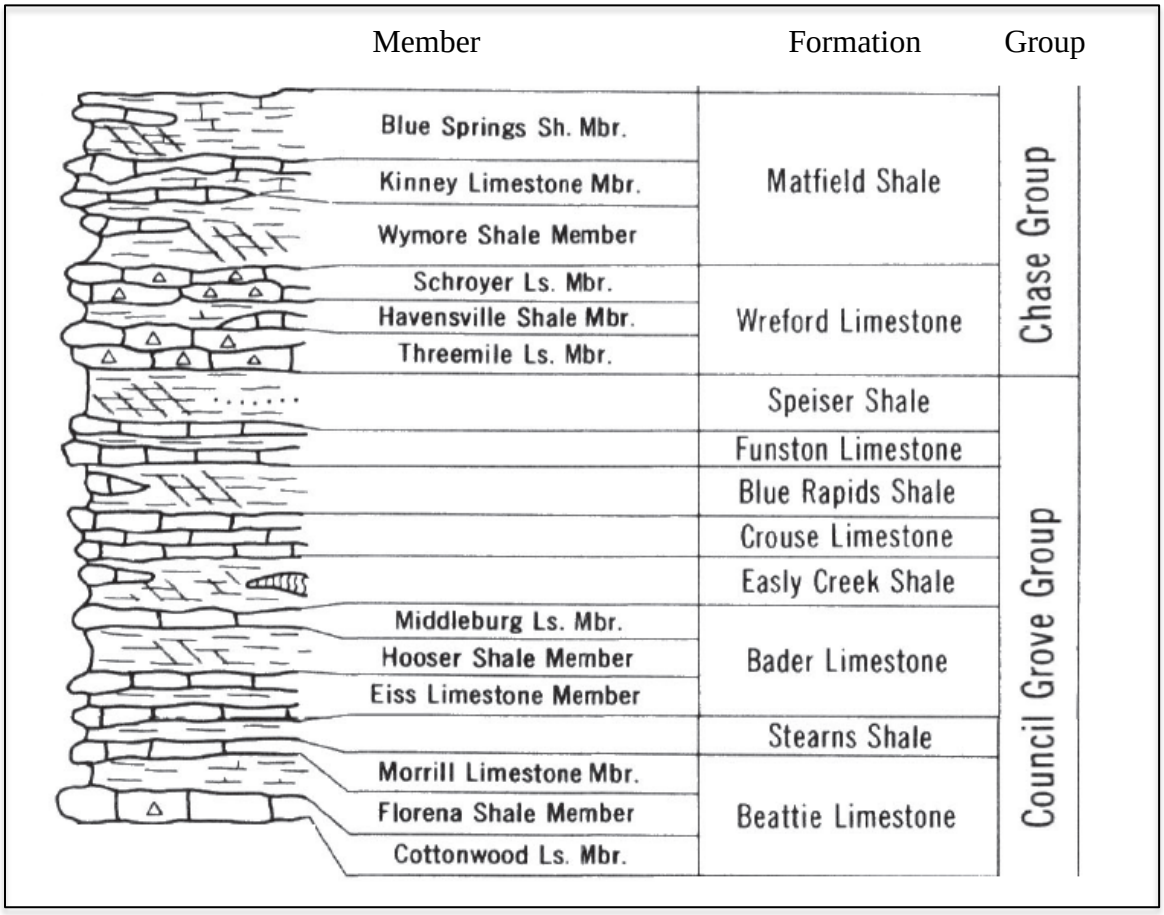


Figure 3: Stratigraphic column (Zeller, 1968).

## 2.2 Springs

The term "springs" in this project refers to groundwater springs, seeps, or any point where groundwater is discharging at the surface. Springs were previously mapped by Ken Ross and Graham Smith on an analog map and were transferred to Google Earth for this project (Ross,

unpublished data; Smith, 1991; Figure 4). The springs in N04d were mapped by Ross in great detail, while the springs at Konza outside this watershed were mapped by Smith with less detail. Springs commonly occur within the stream where the limestones crop out. The springs that are located in the Cottonwood Limestone (Figure 5a) and the Eiss Limestone (Figure 5b) were used as monitoring points (Figure 2). There are no known springs in the Morrill Limestone in N04d. No springs outside of N04d were monitored because this is a diffuse karst system where water moves more slowly than in holokarst, allowing sampling points to be closer to the injection locations (e.g. Schuster & White, 1971). The majority of the springs mapped in the N04d watershed are in units that are stratigraphically higher than the units being studied. The number of springs in each unit and the unit thickness are shown in Table 1. In general, the units that have a thickness of 5 meters or less have fewer springs in them. The relationship between the number of springs and the thickness of the unit increases linearly with a thickness of less than 5m, above this the thickness and number of springs reaches a maximum of 12. These units with a greater thickness have a higher degree of karstification, can transmit more groundwater, which causes and increased number in springs. For the duration of this study, the Flint Hills was drier than average. If climate change caused precipitation to increase, I predict that the number of springs would increase as well and the 12-spring maximum I observed for unit thicknesses greater than 5m would change to some higher maximum at some greater thickness.

| Unit | Number of springs | Limestone unit thickness (m) |
|---|---|---|
| Florence Limestone & Blue Springs Shale | 11 | 13 |
| Kinney Limestone & Whymore Shale | 5 | 1.2 |
| Shroyer Limestone & Havensville Shale | 12 | 5.4 |
| Threemile Limestone & Speiser Shale | 9 | 2.7 |
| Funston Limestone & Blue Rapids Shale | 2 | 1.5 |
| Crouse Limestone & Easly Creek Shale | 11 | 3 |
| Middleburg Limestone & Hooser Shale | 3 | 1.2 |
| Eiss Limestone & Stearns Shale | 2 | 2.2 |
| Beattie Limestone & Eskridge Shale | 4 | 2.8 |

Table 1: Number of springs in each limestone unit at Konza. In the geologic map (figure 4), limestone and shale units are grouped together as a shapefile. Only the thicknesses of the limestones are shown in this table.

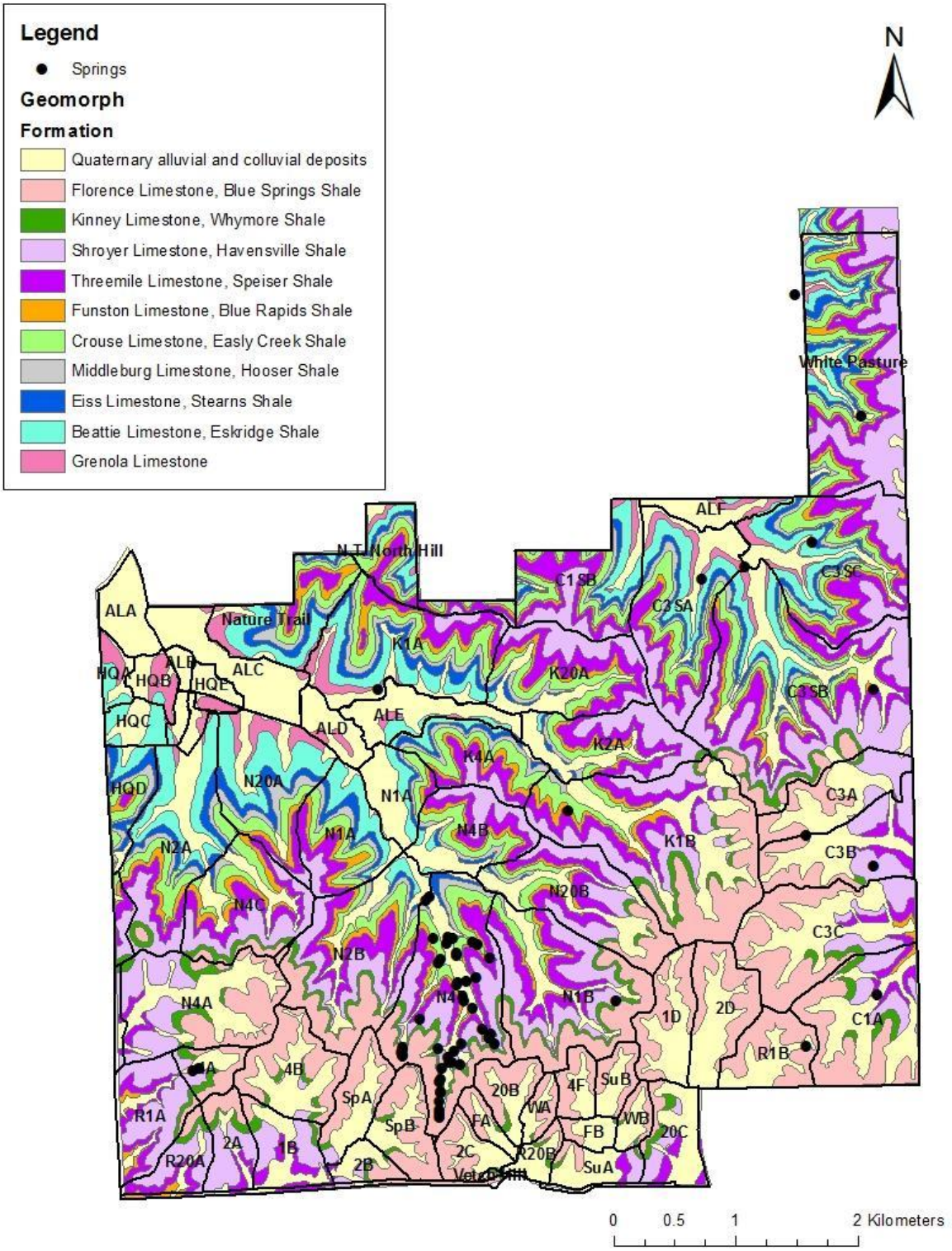


Figure 4: Springs and geologic units within Konza. Springs in N04d were mapped by Ross in great detail, while the springs outside this watershed mapped by Smith and lack the same level of detail. N04d has the largest number of springs and is the focus of this study (Yang Xia, Konza Information Manager, personal communication, 2016)

A

B.

Figure 5: A. Spring at the base of the Cottonwood Limestone in the stream facing south. Field assistant is 1.6 m tall. B. Spring in the Eiss Limestone portion of the stream facing west. Field assistant is 1.6 m tall.

## 2.3 Precipitation

Precipitation contributes to groundwater recharge at Konza. Precipitation data is collected at the field site at a location that is 2.7 km northwest of the study watershed (HQC, Figure 4). In a typical year, most rainfall occurs in the spring and fall months and is sporadic in the summer and winter, although this varies depending on the year (Figure 6). Precipitation that falls during the growing season is typically taken up by vegetation quickly (Brookfield *et al*., 2016).

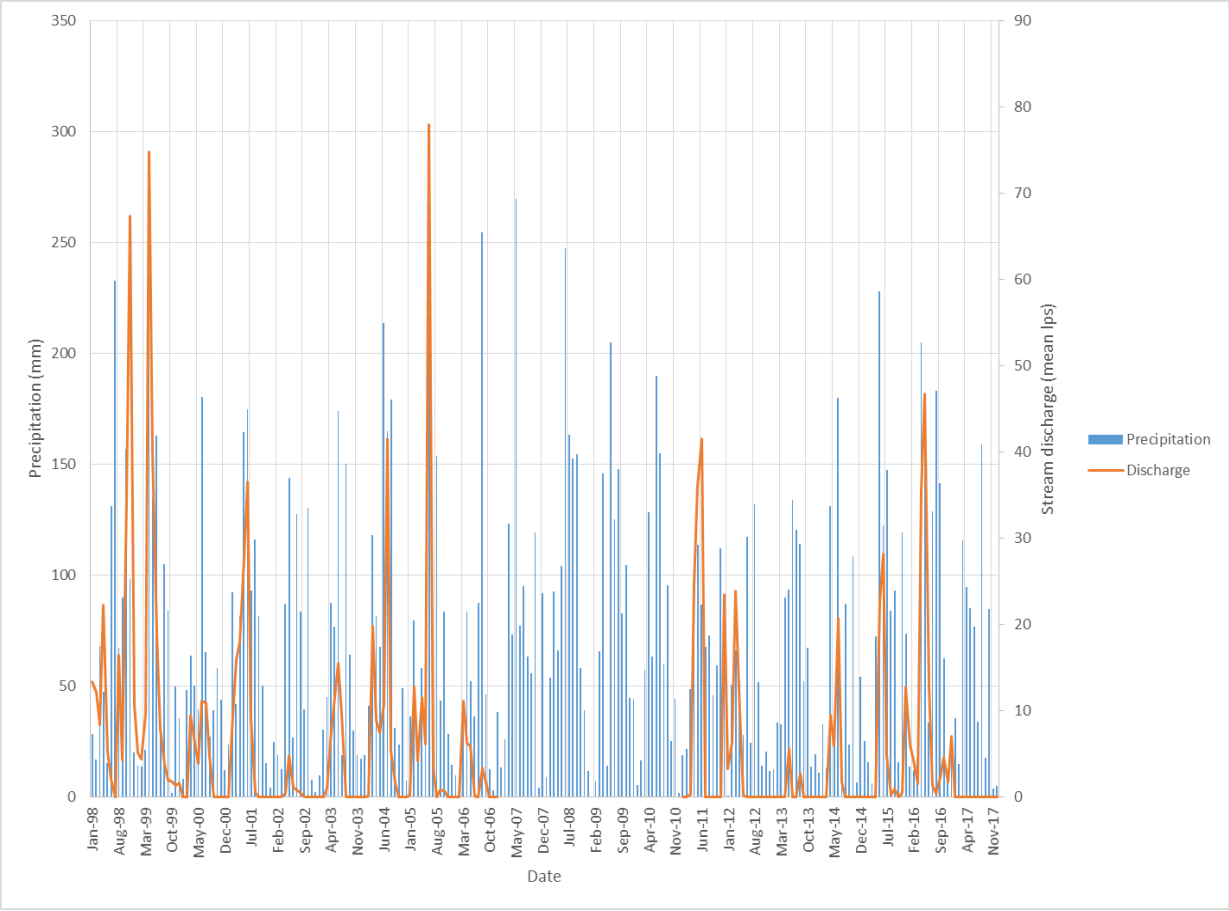


Figure 6: Konza stream discharge and monthly precipitation from January 1998 to December 2017. Stream discharge data are missing from 2007 through 2010 because of equipment malfunction. A comparison of the 2017 average precipitation and the average monthly precipitation can be found in figure 18. (CLIMDB/HYDRODB)

## 2.4 Streamflow

Stream flow is mostly fed by groundwater in N04d. Though it is groundwater-fed, during dry months flow stops before it reaches the v-notch flume in N04d. Most sampling points for the

tracer test are upstream of the flume in N04d but one is downstream (labeled "Cottonwood Spring" in Figure 7). For the first week of the study, the stream was flowing over the flume. Throughout the remainder of the monitoring period, the stream became progressively drier upstream of the flume. The geologic units that crop out in the stream dried out in this order: Cottonwood Limestone (except for the location of the spring at the base of the limestone), Florena Shale, Morrill Limestone, and Stearns Shale. The part of the stream underlain by Eiss Limestone did become dry during this study. Additionally, the downstream sampling location where the Cottonwood Limestone crops out has a pool (Figure 5a) fed by springs draining the Cottonwood. This pool did not dry during the duration of this study despite the lack of surface-water flow and apparent lack of water flowing through the portion of the Cottonwood Limestone immediately upstream of the pool. This information will become important later, in the discussion of the tracer-test results.

The stream was used to sample dye concentrations and to observe groundwater entering the stream via springs. Although the stream became progressively drier upstream during the monitoring period, as described above, it never dried out completely. To summarize, sampling points that had water throughout the entire study were in the Cottonwood Limestone (at the downstream sampling point) and all sampling points in the Eiss section of the stream (Figure 7). Additionally, when the stream is flowing, it alternates between gaining and losing depending on the geologic unit that crops out in the stream (C. Davis, personal communication, 2017). In the portion of the stream where the Eiss Limestone crops out, the stream is gaining. Where the Stearns Shale and Morrill Limestone crop out, the stream is a losing stream. This type of gaining and losing behavior is comparable to sinking streams in holokarst.

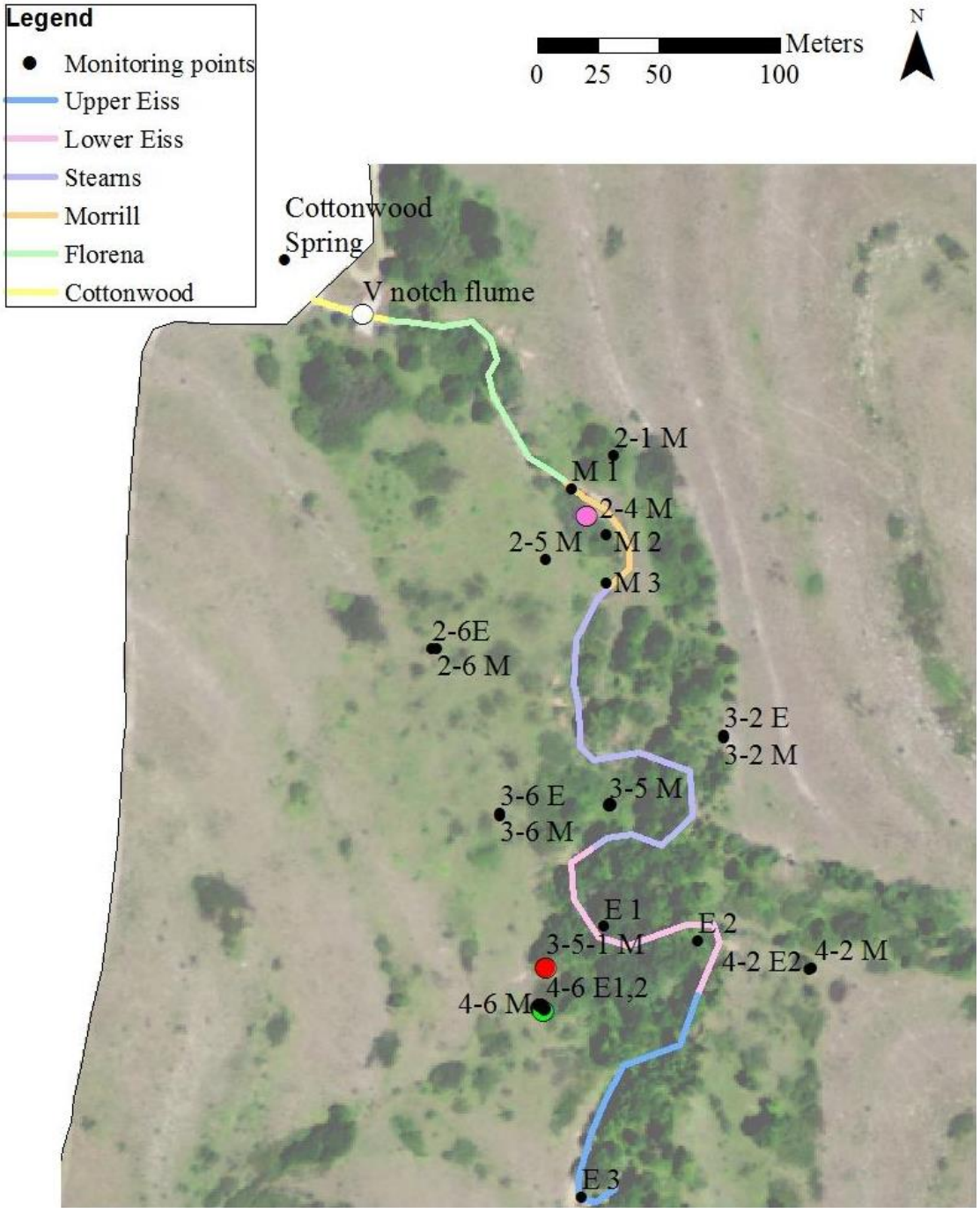


Figure 7: Map of sampling locations (black circles), injection wells (colored circles: red is rhodamine (3-5-1M), green is fluorescein (4-6E2), and pink is eosine (2-4M)) and geologic outcrops in the stream. Stream outcrop map altered from B. Norwood, 2016.

## 2.5 Hydrogeology and water well network

Four transects of 5-cm (2-inch) PVC-cased water wells with 0.61-m (2-foot) screens were installed in N04d from 1988 through 1997 by the USGS and the Konza Prairie LTER. These are monitored approximately monthly to study aqueous geochemistry and monitor groundwater levels in the Morrill and Eiss Limestone aquifers. In this study, a total of 13 wells and 8 stream sampling locations were monitored for the presence of dye, including 5 wells screened in the Eiss Limestone ("E") and 8 wells screened in the Morrill Limestone ("M"). Eiss 1 ("E1") wells are screened in the Lower Eiss Limestone, Eiss 2 ("E2") wells are screened in the Upper Eiss Limestone. The Eiss Limestone ranges in elevation from 367.47 – 372.64, and the Morrill Limestone ranges in elevation from 362.56 – 366.21 m. The chemistry of these aquifers suggests that they are separate aquifers (Macpherson, 1996). However, in some locations, the Upper Eiss and Lower Eiss are not differentiable, the wells screened in these locations are labeled with a general "E". During construction, some of the wells were drilled partially into the shale that is below the limestone in which the wells are screened to create a reservoir for drought periods. This fact will become important later in the discussion.

Both the Morrill and Eiss Limestones can be considered perched aquifers because the shales between the limestones are often dry, rather than wet. Previous slug tests in the Morrill have a range in hydraulic conductivity from $10^{-3}$ m $s^{-1}$ to $10^{-8}$ m $s^{-1}$ (Pomes, 1995), and a previous pumping test resulted in a hydraulic conductivity value of $10^{-7}$ m $s^{-1}$ (Kissing, 2005, unpublished data). Slug tests of the Morrill aquifer (3-5-1M) in February 2017 resulted in a hydraulic conductivity of $10^{-5}$ m $s^{-1}$, which is within the range of previous tests. Well productivity and hydraulic conductivity in this merokarst system likely vary depending on whether or not the well intersects a fracture or fractures, and the degree of secondary porosity developed in the fractures. Little is known about the hydrology of the Cottonwood Limestone because there are no wells

screened in this unit at this site. Springs (Figure 4) are fed by groundwater from these aquifers. In general, groundwater in these units flows towards these springs in order to discharge. Several springs occur outside of the stream on hillslopes; however, these springs were dry for the duration of this study with the exception of the first week, after a heavy rainfall.

**3. Methods**

A groundwater tracing study was conducted in the Cottonwood, Morrill, and Eiss limestone aquifers from July 29th, 2017 through December 16th, 2017, using three separate traces. Fluorescein, eosine, and rhodamine WT (water tracing) were used to determine the direction of groundwater flow in these aquifers. These dyes were chosen for their lack of toxicity (Field *et al*., 1995). Fluorescent dyes were also chosen because they can be detected at low concentrations (Aley, 2017), which is important in a diffuse karst system. Background samples (4 samples from wells and 2 samples from the stream) were analyzed at Crawford Hydrology Laboratory. Three times the amount of water in the injection wells was bailed from the aquifer the day prior to injection to avoid introducing foreign water into the aquifer, serving to push from the well and into the aquifer. Fluorescein and eosine powders were mixed with distilled water, but rhodamine was injected in liquid form, as supplied. Following their preparation, the dyes were injected into monitoring wells 2-4M, 3-5-1M, and 4-6E2 at Konza. Dye injections occurred within several hours of each other. Following introduction of the dye, water that was bailed the previous day was added to flush the dye into the aquifer. Activated charcoal receptors were placed in monitoring wells and the stream surrounding the injection wells for qualitative analysis. Water grab samples (a total of 21 sampling locations) were also collected from these locations for quantitative analysis (Figure 1). Samples were collected weekly for the first two months of the study (168 samples), monthly for the third month (21 samples), and bimonthly for the fourth and

fifth months (21 samples) of the study. Post dye-injection charcoal receptors and water grab samples were analyzed at the Ozark Underground Laboratory, using methodology described by Aley (2002).

When samples were ready to be analyzed, the activated charcoal receptors were washed with unchlorinated water to remove sediment and organic matter (Aley, 2002). Once washed, samples were eluted in a 5% aqua ammonia and 95% isopropyl alcohol solution mixed with hydroxide flakes that saturate the solution. Water samples were not treated except to adjust pH. After the samples were eluted, they were analyzed using a spectrofluorophotometer (Shimadzu RF 5000U) and software developed by the Ozark Underground Laboratory.

## 4. Results

### 4.1 Geology

Isopach maps (Figures 8, 9) for the Morrill and Eiss Limestones were made using ARCMAP from well log data collected during well installation (Pomes, unpublished data; Macpherson, unpublished data). The isopach map of the Morrill Limestone indicates that the unit decreases in thickness near the wells that are closest to the stream (Figure 8). The thickest portion of the Morrill surrounds well 3-5-1M. The isopach map of the Eiss Limestone, however, shows that the thickness is greater near wells to the east of the stream and decreasing in thickness towards the southwest (Figure 9). These maps show the variable thickness in the different units being studied. The thickness in the Morrill Limestone ranges from 2.8 meters in thickness and the Eiss Limestone varies from 1.2 meters in thickness. Changes in thickness may be representative of the challenges of obtaining accurate depths of lithology changes from well cuttings. Several wells (3-5-1M, 3-7M, E, 4-7M, E) have full cores that were available so the depths for these wells are more accurate.

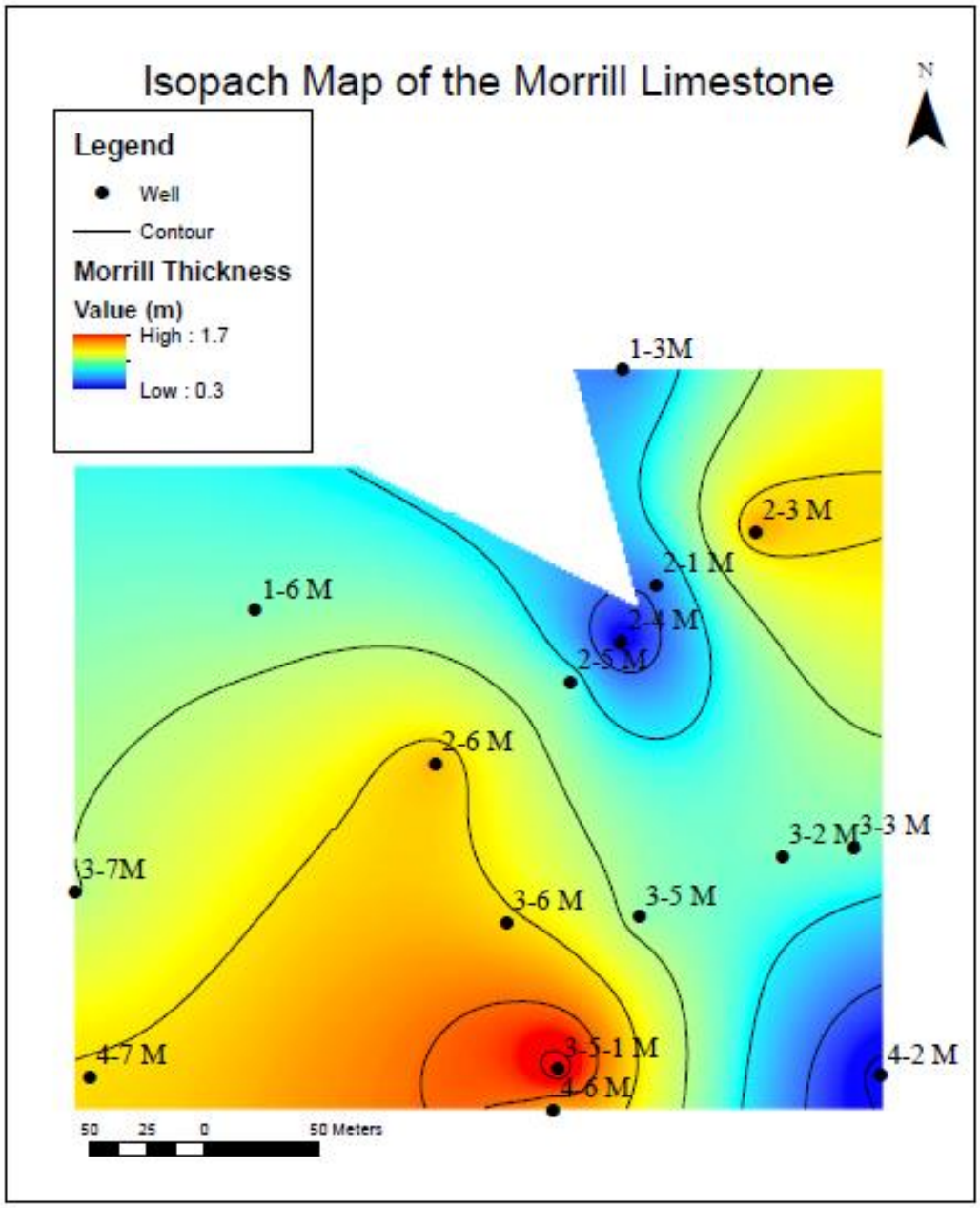


Figure 8: Isopach map of the Morrill Limestone

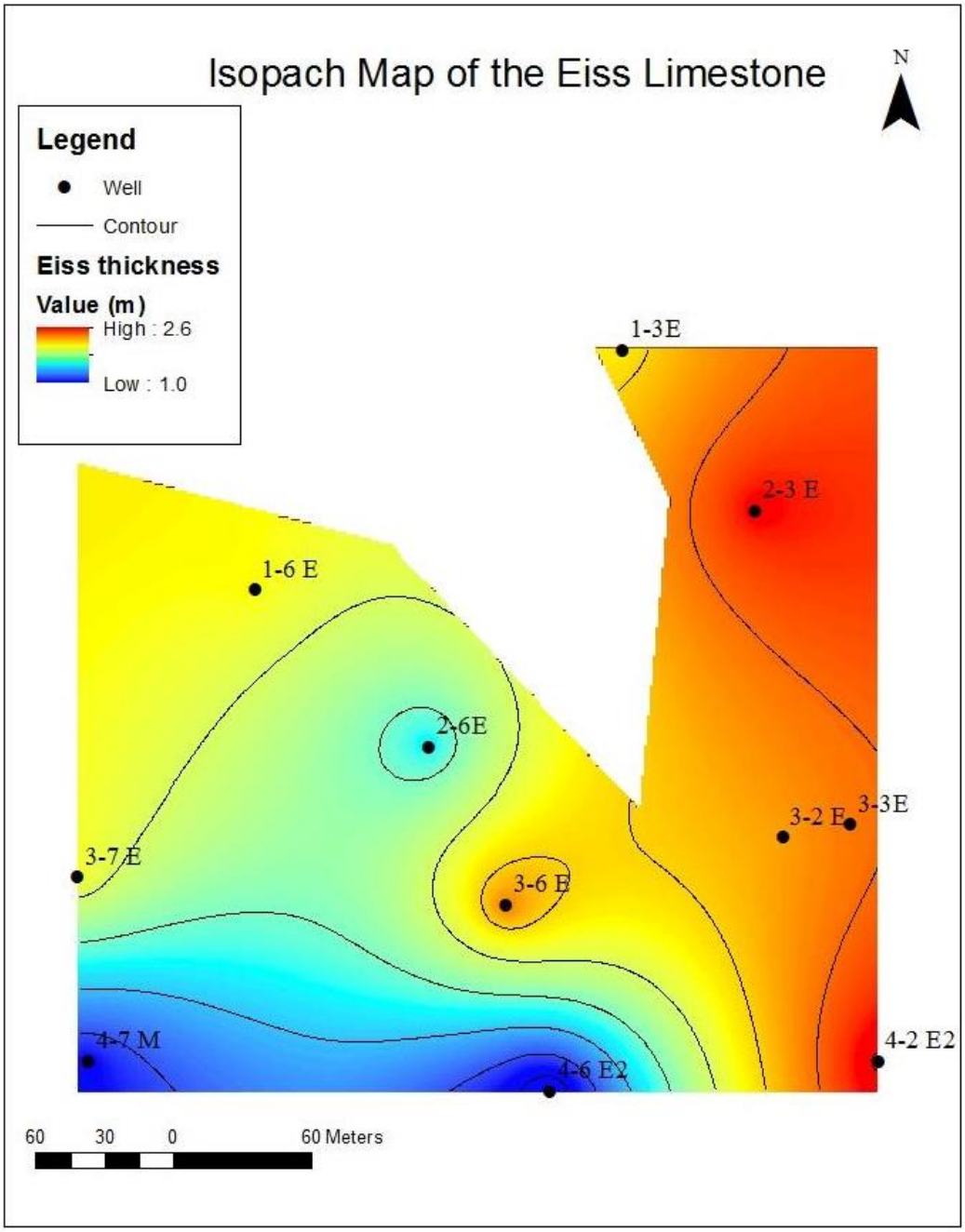


Figure 9: Isopach map of the Eiss Limestone.

Structural contour maps (Figures 10, 11) were created to visualize the base of the Morrill and the Eiss. The Morrill Limestone dips 0.3° south to southwest within N04d. This trend is demonstrated in Figure 10, in which the base elevation of the Morrill decreases to the south/southwest. The Eiss Limestone dips 0.1° south to southwest within N04d. This is observed

in Figure 11, in which the base elevation of the Eiss is higher to the north and decreases to the south/southwest. Surrounding well 3-5-1M, there is a depression in the contours, which may represent a collapse feature. A cross section of wells 1-6M/E, 2-6M/E, 3-6M/E, 3-5-1M, and 4-6M/E (Figure 12a) also demonstrates the same pattern in the units. Error bars were added to the well elevations to show error associated with well installation. The contour map (Figure 11) and the cross section (Figure 10) of the base of the Morrill Limestone shows the low point is well 3-5-1M, however tracer test data do not support this. Error bars were added to this cross section to demonstrate that the elevation of the Morrill in well 4-6M must be lower than the elevation of well 3-5-1M, as tracer data suggests. A regional map of the base of the Morrill was made to determine if the trends seen in N04d is local or regional. The regional map around Konza shows that the strata dip to the west/southwest (Figure 13).

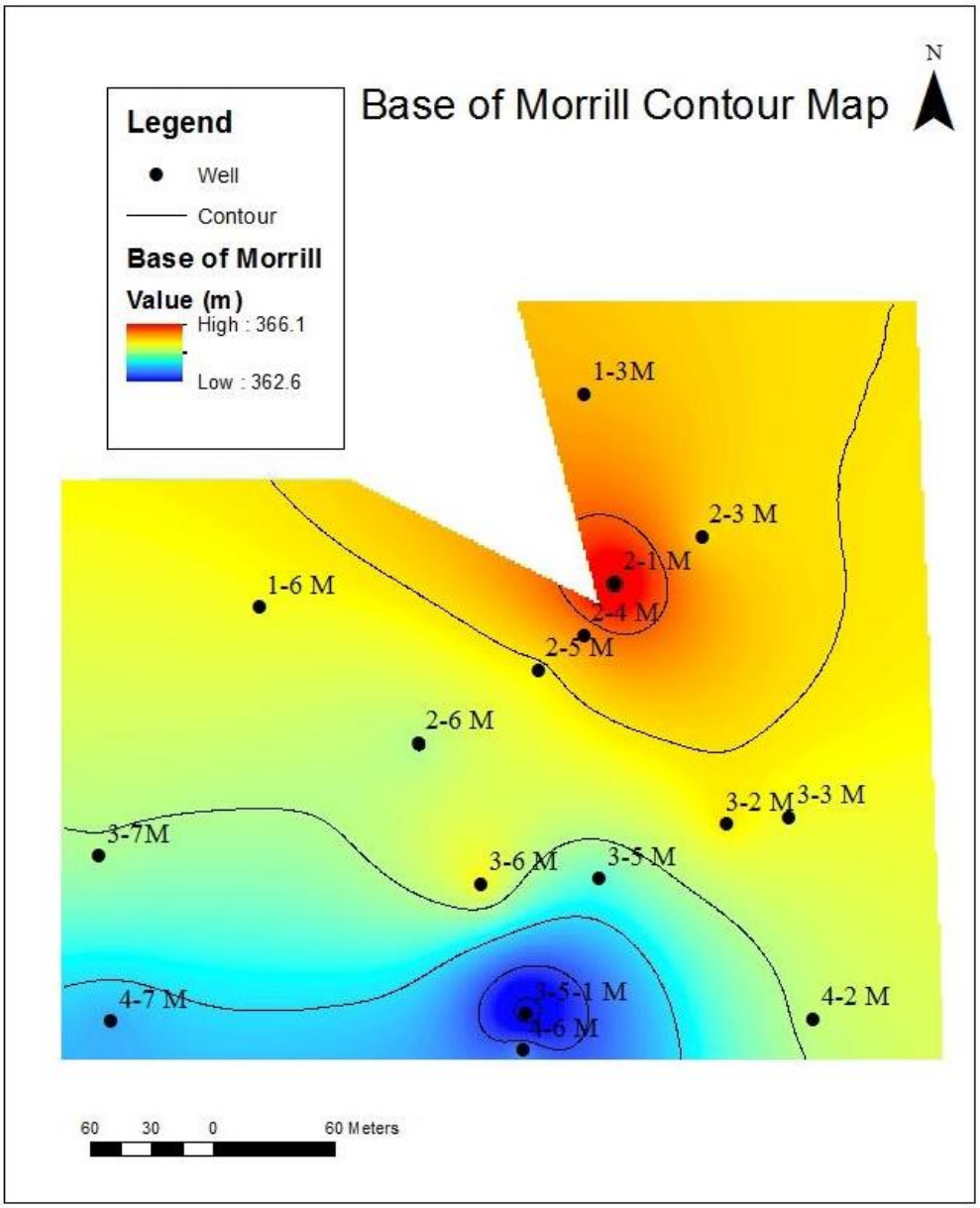


Figure 10: Structural contour map of the base of the Morrill Limestone.

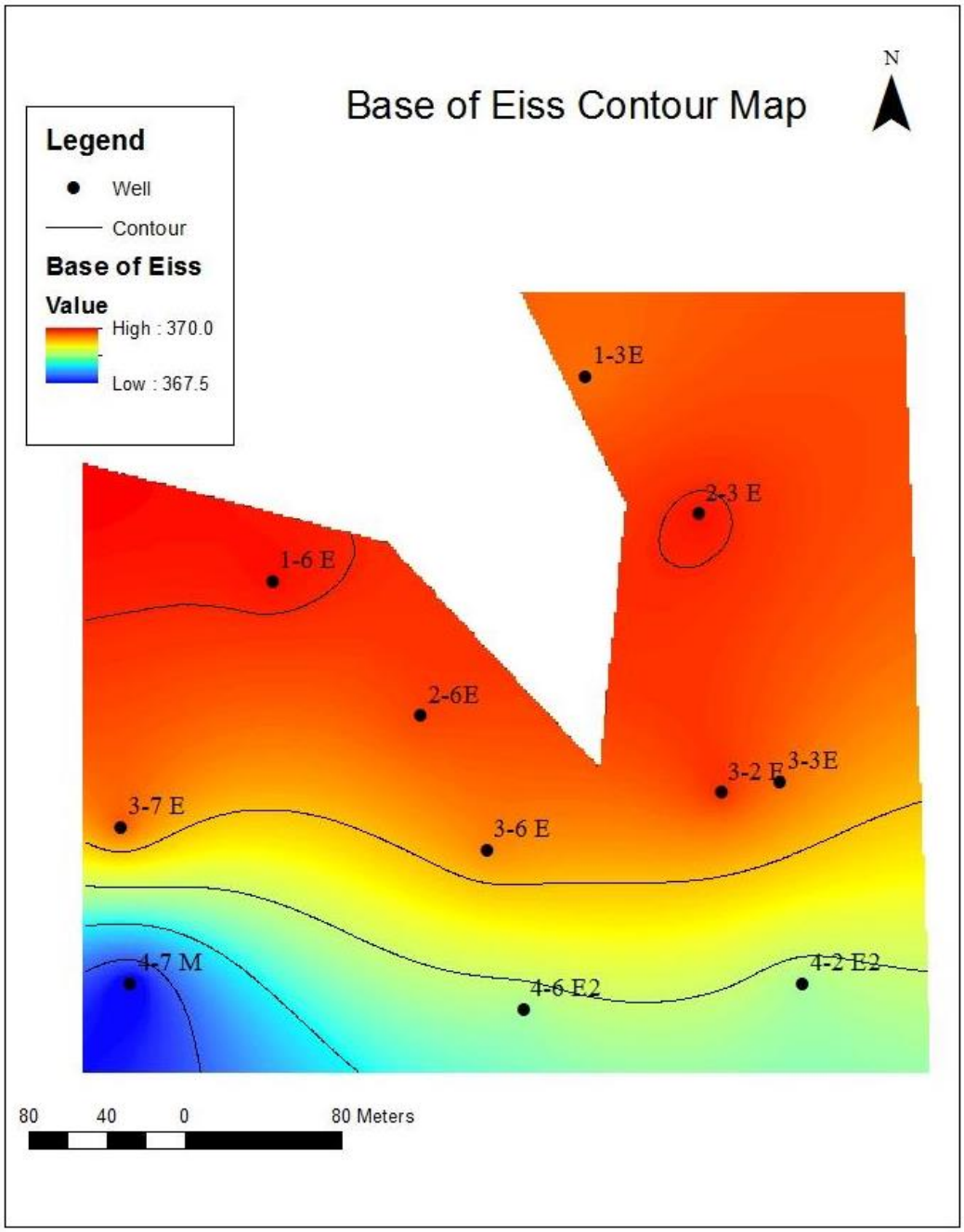


Figure 11: Structural contour map of the base of the Eiss Limestone.

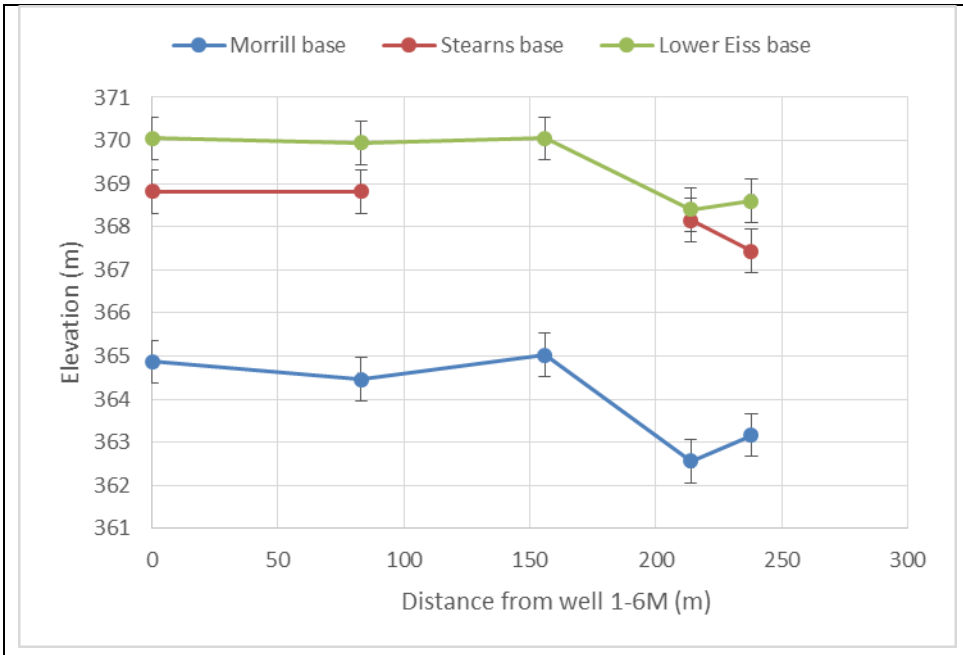


A.

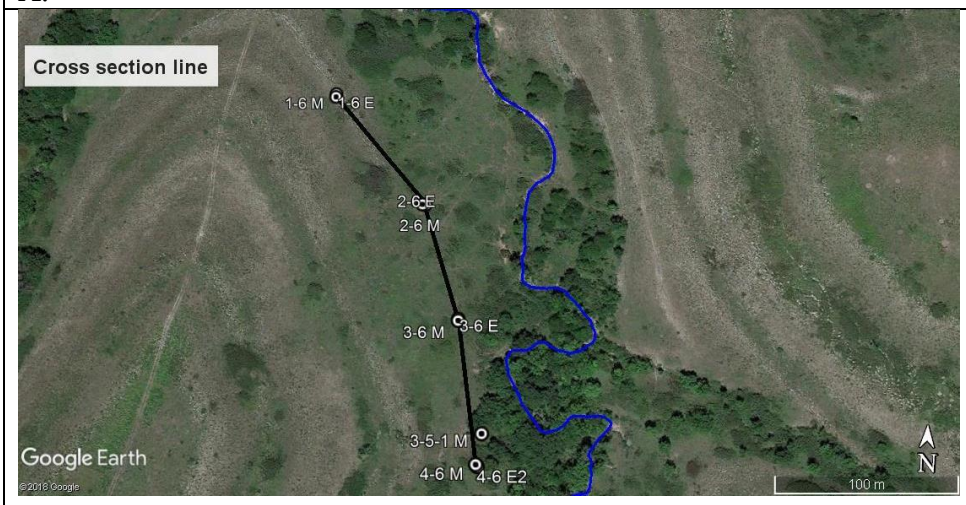


B.

Figure 12: A: Cross section of the base of the Morrill, Eiss, and Stearns beginning at well 1-6, ending at well 4-6. Error bars are 0.5 meters and represent the error in well cuttings measurements. B: Cross section line (black).

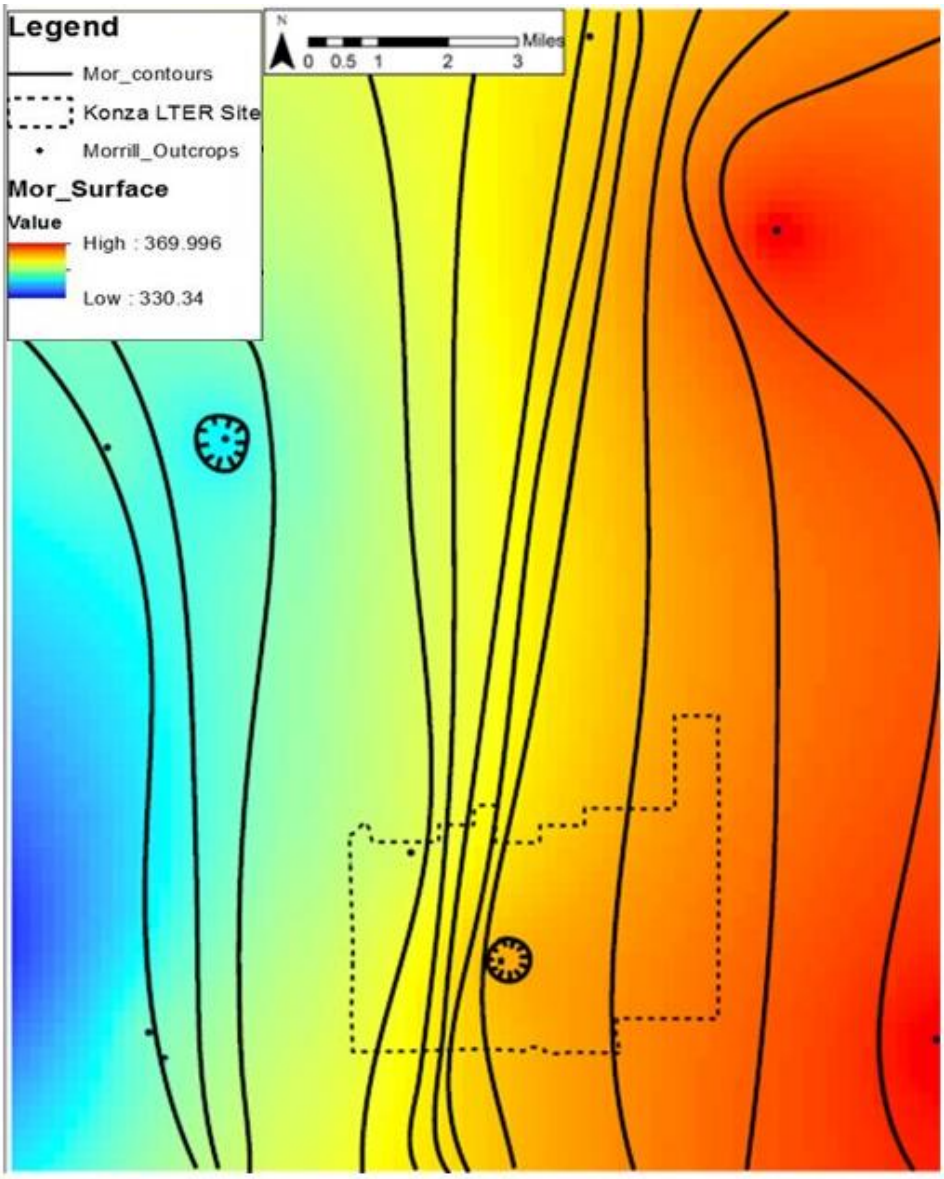


Figure 13: Regional contour map of the base of the Morrill Limestone.

The orientation of joints in these units were measured in this study along with their spacing and width at one location within N04d, one location outside on N04d but on Konza, and three locations outside of Konza using Strabospot (Figure 14). Since preexisting joints weather into larger solution enlarged fractures, determining their direction is important for predicting

groundwater flow. The dominant fracture set in the area strikes N 35° W in this area (Chelikowsky, 1972). There are a series of parallel faults to the southeast of the field site, but no known faults within the field site itself. A dominant strike trend is not seen in the fractures of the Cottonwood Limestone (Figure 15). Fractures in the Cottonwood Limestone range in size from 1 – 5 cm and several fractures can occur within 1 m of each other. In the Morrill Limestone, the fractures strike to the northwest to southeast (Figure 16). Fractures range in size from less than 1 – 5 cm and approximately 4 fractures occur within 1 m of each other. In the Eiss Limestone, fractures strike to the northwest to southeast (Figure 17). Fractures are generally 1 – 5 cm, approximately 3 fractures occur within 1 meter of each other. Spacing of fractures in the Eiss are difficult to identify because it does not crop out well. Straight segments of the stream appear to follow the orientation of fractures as well. There is a great deal of evidence, such as highly variable hydraulic conductivity (Pomes, 1995), rapid response time of wells to precipitation (Brookfield *et al*., 2016), and rapid ground water velocity (as seen in this study), that support the idea that there are solution-enlarged fractures in these aquifers and that these fractures influence the direction of groundwater flow.

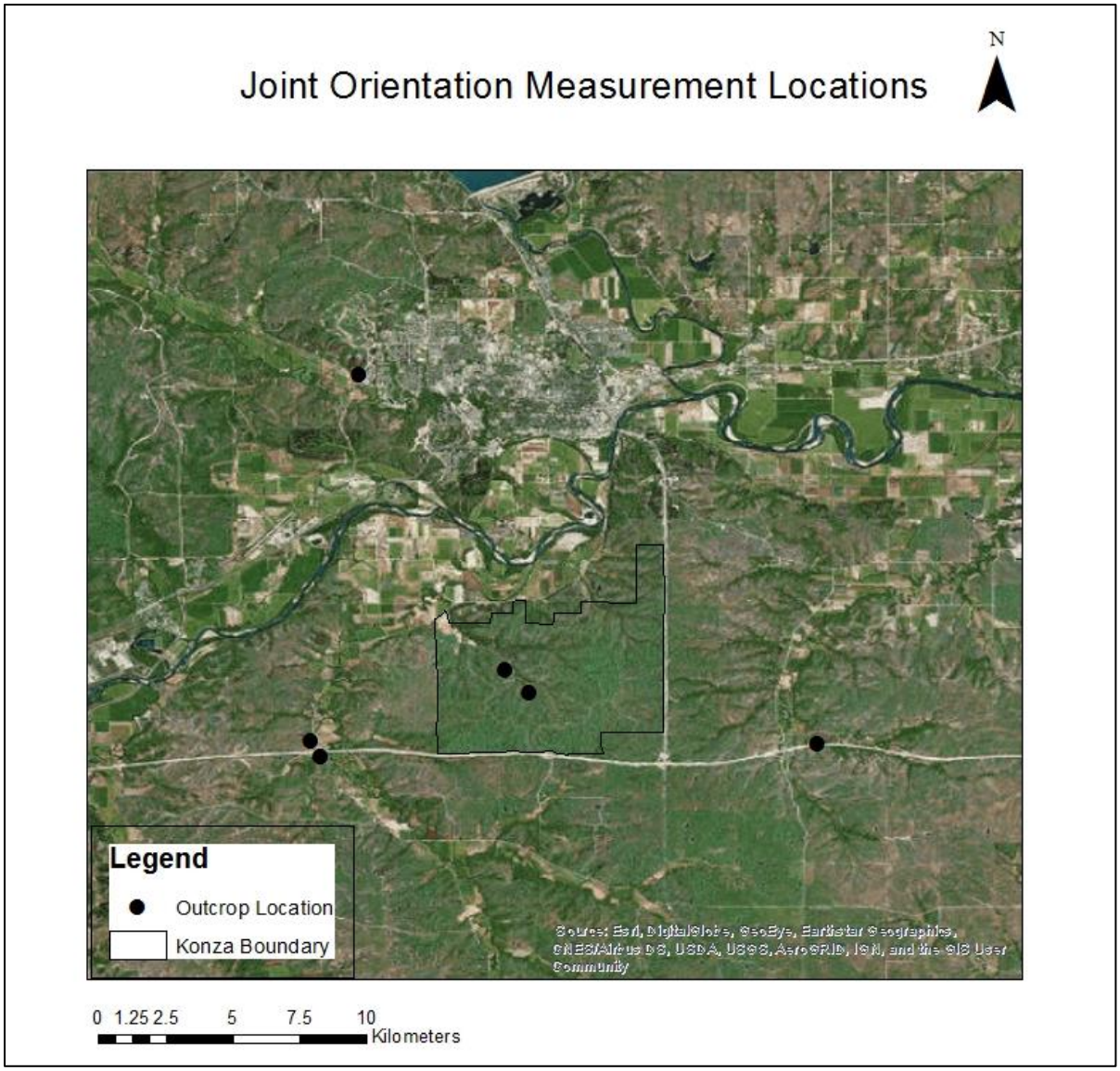


Figure 14: Location map of joint orientation measurements

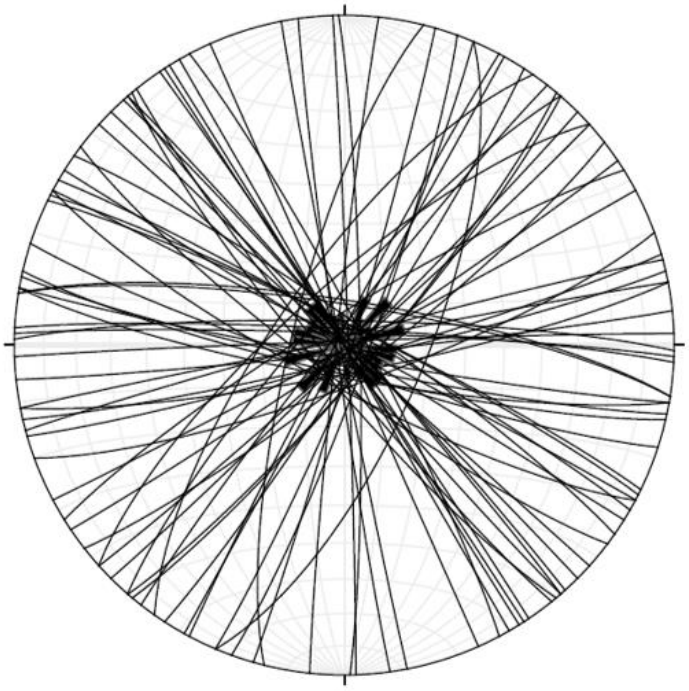

Figure 15: Fracture orientations of the Cottonwood limestone. Longest filled isosceles triangle represents the dominant direction of fracture orientations.

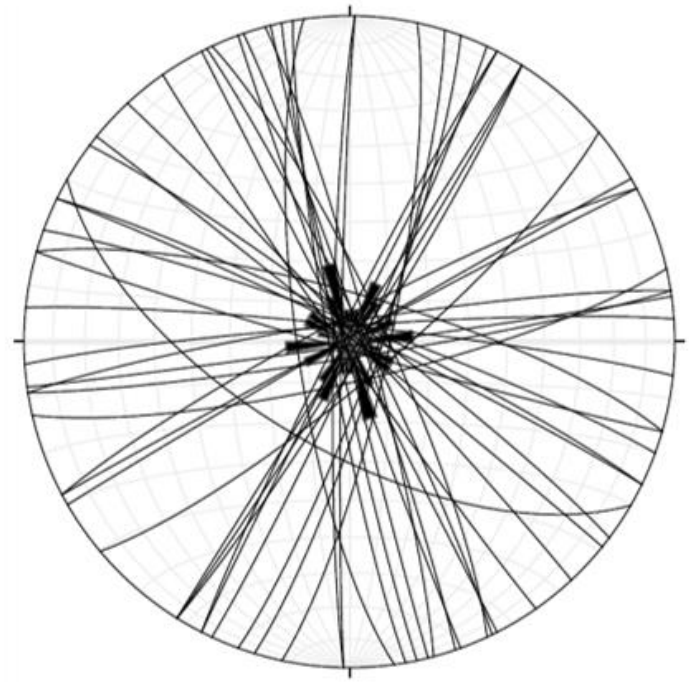

Figure 16: Fracture orientations of the Morrill Limestone. Longest filled isosceles triangle represents the dominant direction of fracture orientations.

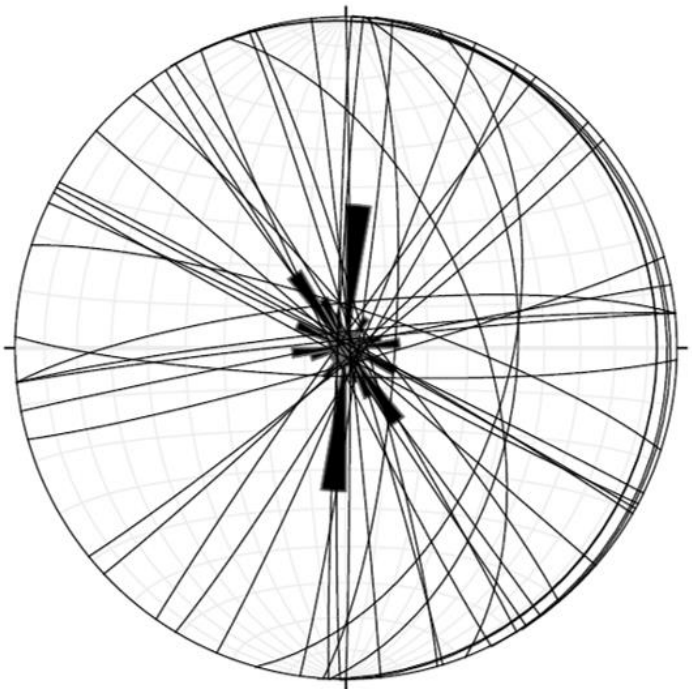

Figure 17: Fracture orientations for the Eiss Limestone. Longest filled isosceles triangle represents the dominant direction of fracture orientations.

### 4.2 Precipitation

The average meteoric precipitation at Konza over the past 20 years is approximately 850 millimeters per year (CLIMDB/HYDRODB). In 2017, there were 726 millimeters of rain, which is 85% of the 20-year average. Though the annual precipitation was less than average, the monthly precipitation varied in comparison with long-term precipitation (Figure 18). During this study, there was little precipitation, with the exception of a large rainfall event on August 5$^{th}$ that produced 85 millimeters of rain. The months of February, May, June, July, September, November, and December received less precipitation than their monthly averages. Typically, spring and summer months (April – August) receive the most precipitation. The 2017 precipitation during these months, however is less than their 20-year averages. All other precipitation events during three out of five months of this study were less than 20 mm. Because

the rainfall was below average for most months during the growing season, it is more likely that precipitation was used by vegetation than it is for it to have recharged groundwater.

### 4.3 Streamflow response to precipitation

Streamflow in this watershed is unpredictable and varies greatly depending on the year and the amount of rainfall from previous years (Figure 18). After precipitation occurs, the stream responds with very flashy, rapid flow, which dissipates quickly. During 2017, most precipitation occurred during the spring months from March through June. The stream, however, flowed from March through May and declined from June through July. There was no flow in the stream at the gauging station from August through December (the time period of the tracer test in this study) (Figure 18). Even though a large rainfall event occurred in August, it was not enough to make the stream flow for more than one day.

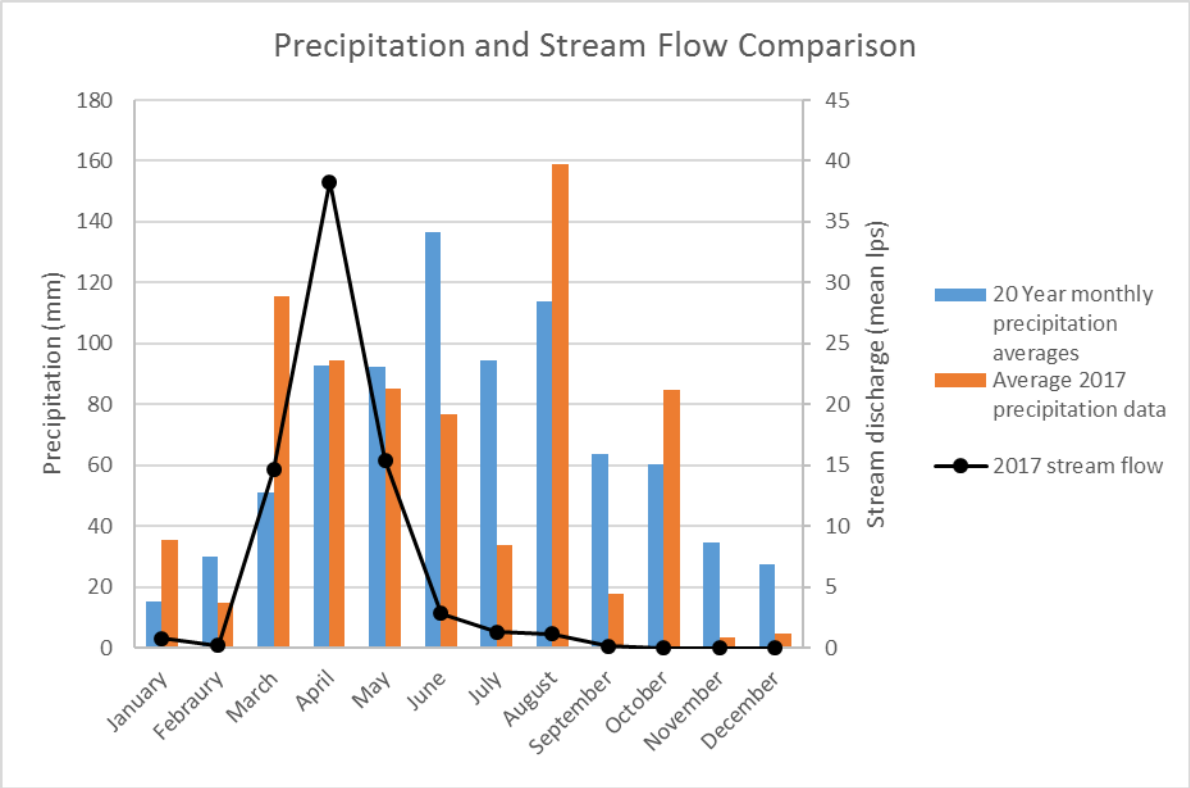


Figure 18: Stream flow response to precipitation in N04d. (CLIMDB/HYDRODB)

### 4.4 Groundwater response to precipitation

As is common in karst settings, the velocity and recharge rate of the groundwater are more rapid than in porous media. At Konza, groundwater recharges rapidly during rainfall events. The response time of the groundwater level after a significant precipitation event is between 2 and 5 hours (Brookfield *et al*., 2016). Wet years tend to have a stronger response time to precipitation than drier years (Brookfield *et al*., 2016). This rapid recharge of groundwater indicates that groundwater flows rapidly at Konza, and recharge is strongly event-driven, rather than continuous. Figure 19 demonstrates the variability in the water table in response to precipitation. The spring of 2016 had 16% more than the average precipitation, while the spring of 2017 had 25% less than the average precipitation. These graphs show the comparison in water level response to precipitation during a wet period and a dry period. It is clear that during a dry period, the groundwater levels are less responsive to precipitation than during periods with more precipitation.

The water table elevations in both the Morrill and the Eiss show a great amount of variability. The range in water table elevations is 1.2 m in the Morrill and 1.5 m in the Eiss in April 2017. The water levels in both aquifers sometimes rise above the top of the aquifer, showing that the Eiss and Morrill aquifers act as semi-confined aquifers depending on the season (Macpherson, 1996).

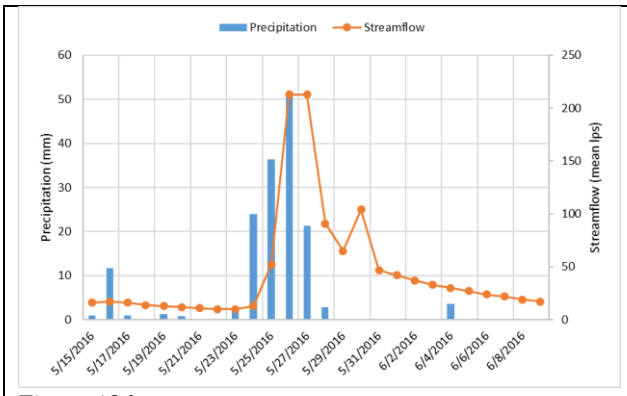


Figure 19A.

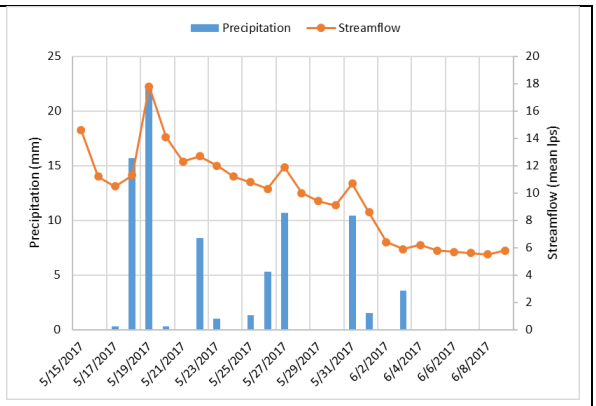


B.

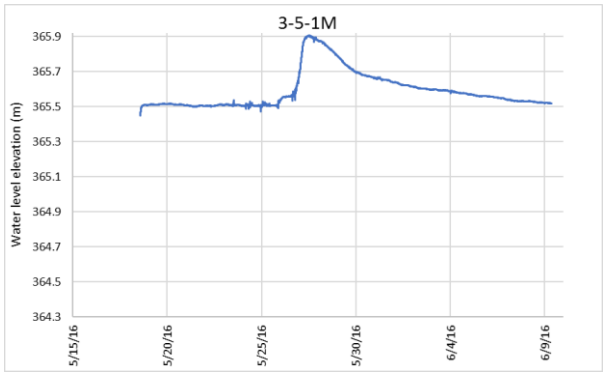


C.

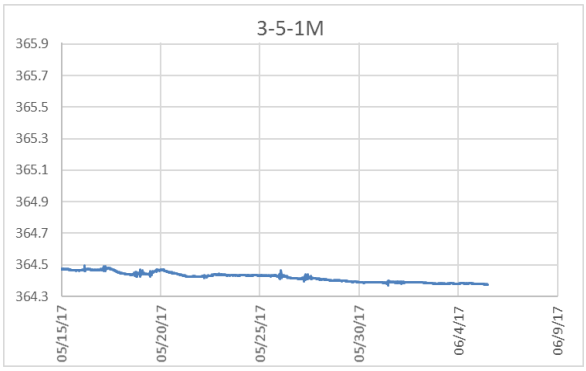


D.

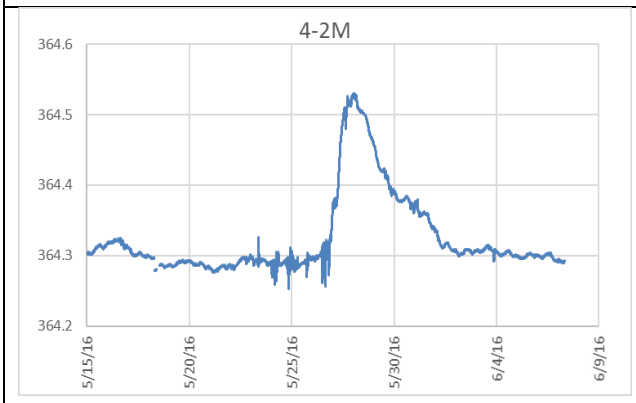


E.

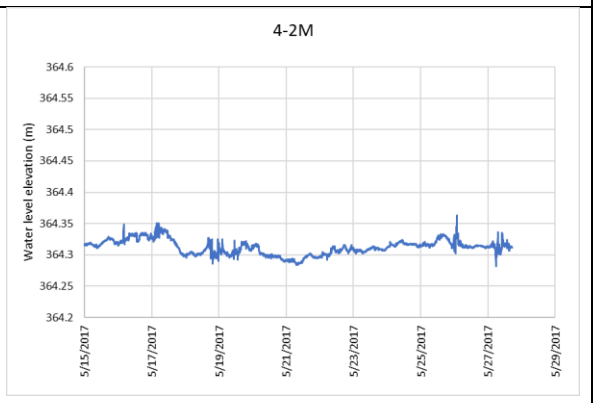


F.

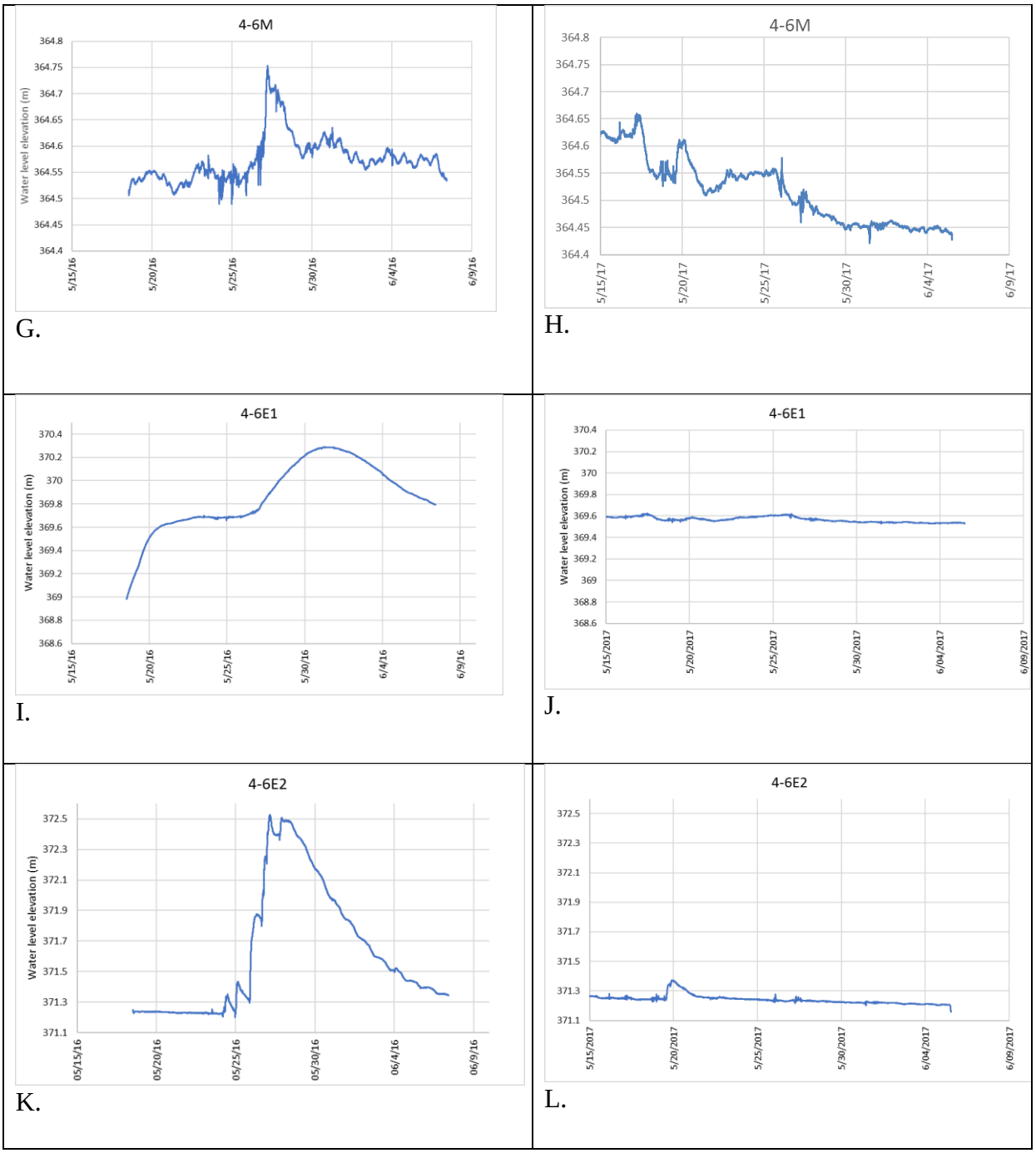


Figure 19: Contrasts between meteoric precipitation at Konza (HQC) and water-level response in well 3-5-1M. A. 2016 precipitation and streamflow from May 15 to June 9. B. 2017 Precipitation and streamflow from May 15 to June 9. C. 2016 water level response in well 3-5-1M from May 15 to June 9. D. 2017 water level response in well 3-5-1M from May 15 to June 9. E. 2016 water level response in well 4-2M from May 15 to June 9. F. 2017 water level response in well 4-2M from May 15 to June 9. G. 2016 water level response in well 4-6M from May 15 to June 9. H. 2017 water level response in well 4-6M from May 15 to June 9. I. 2016 water level response in well 4-6E1 from May 15 to June 9. J. 2017 water level response in well 4-6E1 from May 15 to June 9. K. 2016 water level response in well 4-6E2 from May 15 to June 9. L. 2017 water level response in well 4-6E2 from May 15 to June 9. K. 2016 water level response in well 3-5-1M from May 15 to June 9. L. 2017 water level response in well 3-5-1M from May 15 to June 9.

| Well | Peak time | Head change (m) | Recovery time (days) |
|---|---|---|---|
| 3-5-1M | 5/27/2016 14:17 | 0.4 | 12 |
| 4-2M | 5/28/2016 3:35 | 0.2 | 5 |
| 4-6M | 5/27/2016 5:30 | 0.2 | 7 |
| 4-6E1 | 5/31/2016 12:21 | 0.6 | >11 |
| 4-6E2 | 5/27/2016 4:48 | 1.3 | >7 |

Table 2: The response of the water level to precipitation events on May 24-27, 2016 taken from pressure transducer data shown in figure 20. The year 2016 had a total of 991mm of precipitation. The response time of the aquifer to a peak in the water table after the first precipitation event took place on May 24th. The head change is the rise in water level cause by precipitation. The recovery time represents the time it takes the water level to recover back to a static level after the peak in the water table.

| Well | Peak time | Head change (m) | Recovery time (days) |
|---|---|---|---|
| 3-5-1M | 5/19/2017 19:13 | 0.02 | 4 |
| 4-2M | 5/18/2017 4:27 | 0.02 | 3 |
| 4-6M | 5/20/2017 4:12 | 0.06 | 3 |
| 4-6E1 | 5/20/2017 4:16 | 0.03 | 10 |
| 4-6E2 | 5/19/2017 22:05 | 0.13 | 2 |

Table 3: The response of the water level to precipitation events on May 18-20, 2017 taken from pressure transducer data shown in figure 20. The year 2017 had a total of 725mm of precipitation. The response time of the aquifer to a peak in the water table after the first precipitation event took place on May 18th. The head change is the rise in water level cause by precipitation. The recovery time represents the time it takes the water level to recover back to a static level after the peak in the water table.

Figure 19 demonstrates the water-level variability in wells 3-5-1M, 4-2M, 4-6M, 4-6E1,2 in 2016 and 2017 in comparison to stream flow and precipitation. For the purpose of this comparison, we consider 2016 a “wet” year and 2017 a “dry” year. The Morrill and Eiss well responses vary depending on the aquifer and the amount of precipitation received. Certain wells show similar response curves to each other. For example, in 2016, wells 3-5-1M and 4-6E2 have curves that show a peak with a tail that takes 7 days or more to reach a static water level (Figure 19 C, K). In 2016, wells 4-2M and 4-6M also have similar shaped curves, with a more rapid decline (5-7 days) back to a static water table (Figure 19 F, H). Well 4-6E1 responds seven days after the precipitation event, which is much slower than other wells, and its curve does not match any other wells (Figure 19 I). However, in 2017, these wells have very different responses from

those recorded in 2016. Wells 3-5-1M and 4-6M have almost identically shaped curves while 4-6E2 demonstrates a slight variation from these two (Figure 19 D, H, L). Well 4-6E1 responds uniquely again in 2017 and shows a delayed rise in the water table than other wells do (Figure 19 J). The stream hydrographs show an almost instant rise in stream flow after a precipitation event. Groundwater takes longer to respond than the stream, but mimics the shape of the stream hydrograph (Figure 19 A, B).

Tables 2 and 3 demonstrate the differences in water level response from precipitation events shown in Figure 19 during 2016, a year with 991mm of precipitation, and 2017, a year with 725mm of precipitation. During 2016, well 4-6E2 responded the fastest to rainfall, and had the greatest change in hydraulic head (Table 2). During 2016, 4-6M peaks before 3-5-1M, but has a secondary peak several hours after 3-5-1M has its peak (Table 2). However, in 2017, 3-5-1M peaks several hours before 4-6M does (Table 3). During 2017, well 4-2M responded the fastest to rainfall, but had the smallest change in head (Table 3). Well 4-6E2 had the largest change in head in both 2016 and 2017. The Morrill wells (3-5-1M, 4-6M, and 4-2M) and well 4-6E2 respond within a day of each other, while 4-6E1 is delayed by several days (Table 2, 3).

**4.5 Potentiometric Surface Maps for Morrill and Eiss**

Potentiometric surface maps were hand-contoured for the Morrill and Eiss Limestones, using unpublished data that will become part of the Konza LTER database, doi: AGW01 (Macpherson, unpublished data). The range in hydraulic head in the Morrill Limestone is 1.2 m based on the potentiometric surface map of the Morrill Limestone from April of 2017 (Figure 20), and groundwater potential is high in the north and low in the south with a possible groundwater mound around well 3-5M. The range in hydraulic head in the Eiss Limestone is 1.5 m based on the potentiometric surface map from April 2017 (Figure 21), and groundwater

potential is high in the south and low in north. Three additional potentiometric surface maps were made for both the Morrill and Eiss (not shown) to determine if groundwater flow direction changes depending on the amount of precipitation. Maps from wet, dry, and average years show that the direction of groundwater is consistent with the maps provided below.

There is some level of uncertainty associated with the potentiometric surface maps. The monitoring wells used to take water level measurements are unevenly spaced, which creates some uncertainty in the contouring of the potentiometric surface maps. The location of the outcrops on this map may also be slightly distorted because the location of each outcrop is not always visible and these maps were hand contoured.

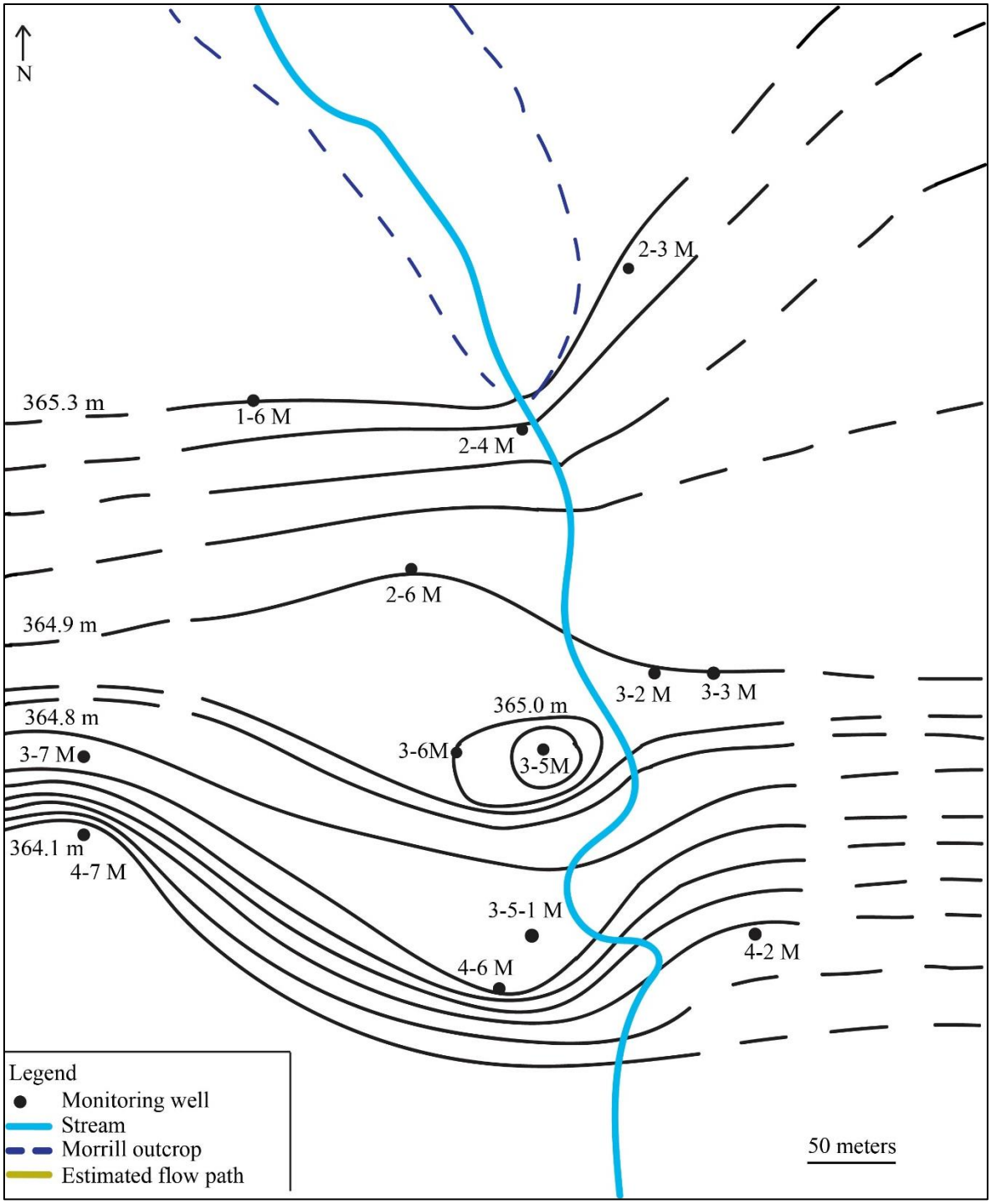


Figure 20: Potentiometric surface map of the Morrill Limestone from April 2017. Isolines become dashed when unconstrained.

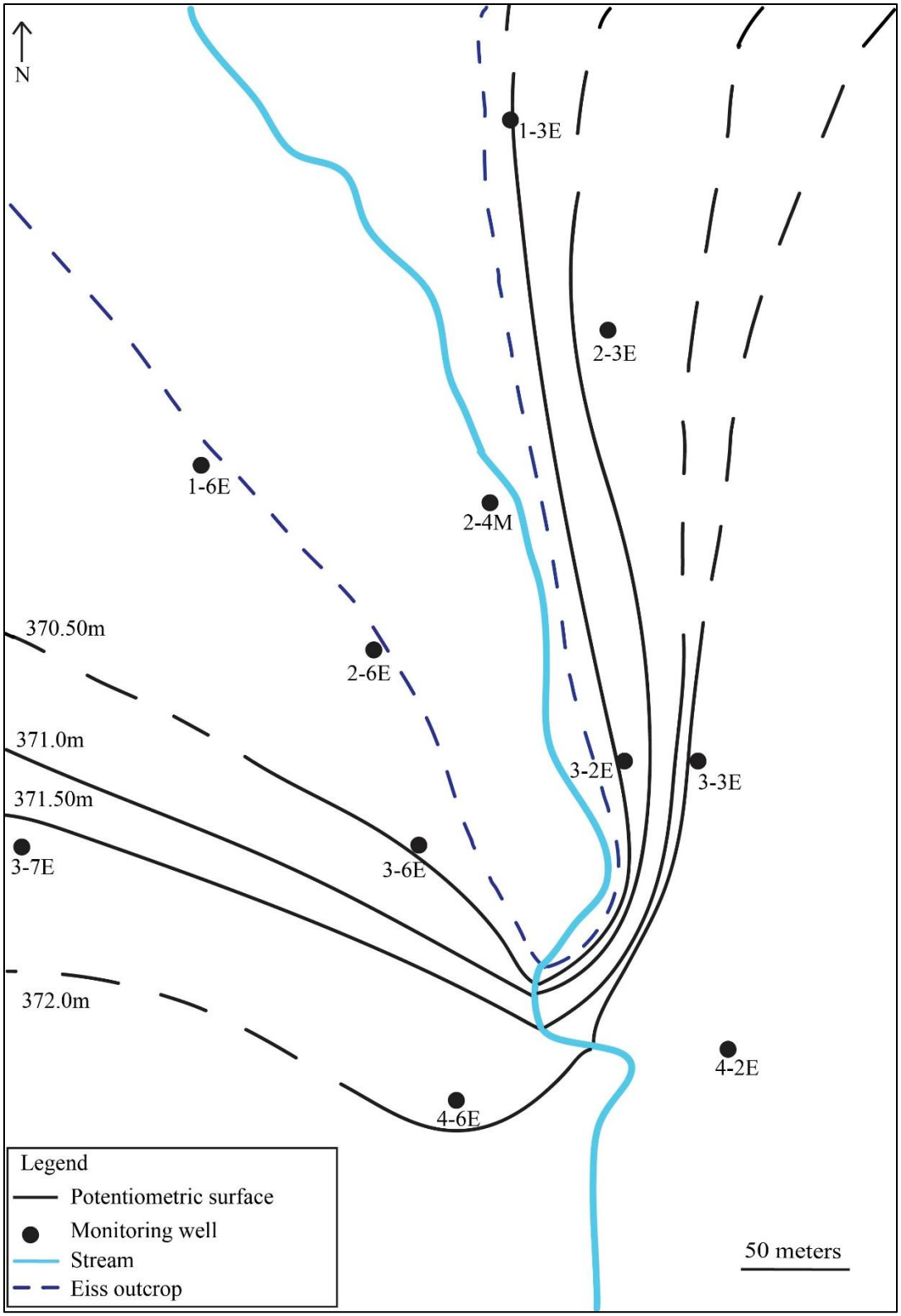


Figure 21: Potentiometric surface map of the Eiss Limestone from April 2017. Isolines become dashed when unconstrained.

## 4.6 Dye traces

### 4.6.1 Eosine

Eosine was injected into the Morrill aquifer in well 2-4M. This well was chosen for its proximity to the stream and to monitoring wells. It was also chosen because in the background fluorescence test conducted, rhodamine was detected that had been used into the stream by a different research group. A direct connection between the stream and this well seemed very likely. The volume of water used to mix the dye and flush the dye into the well created an induced hydraulic head increase of 3.8 m. Eosine was initially detected at the Cottonwood Spring one week after injection, and then consistently at the same location for the duration of the monitoring period (Figure 22). Breakthrough curves are shown in section 4.6.4. The injection well is approximately 160 m from the detection point. Eosine was not detected in any other sampling location during this study. Eosine was observed in the roots of plants in the stream 10 m away from the injection well at the end of sampling period 3 (week 3) of sampling. These roots were growing out of the Morrill Limestone nickpoint that is approximately 1m high; the nickpoint is formed above the pool in which sampling point Morrill 1 is located (Figure 1). Eosine was not detected in the charcoal sampler at the Morrill 1 sampling point. During the first week of the study, the stream was flowing for at least one day.

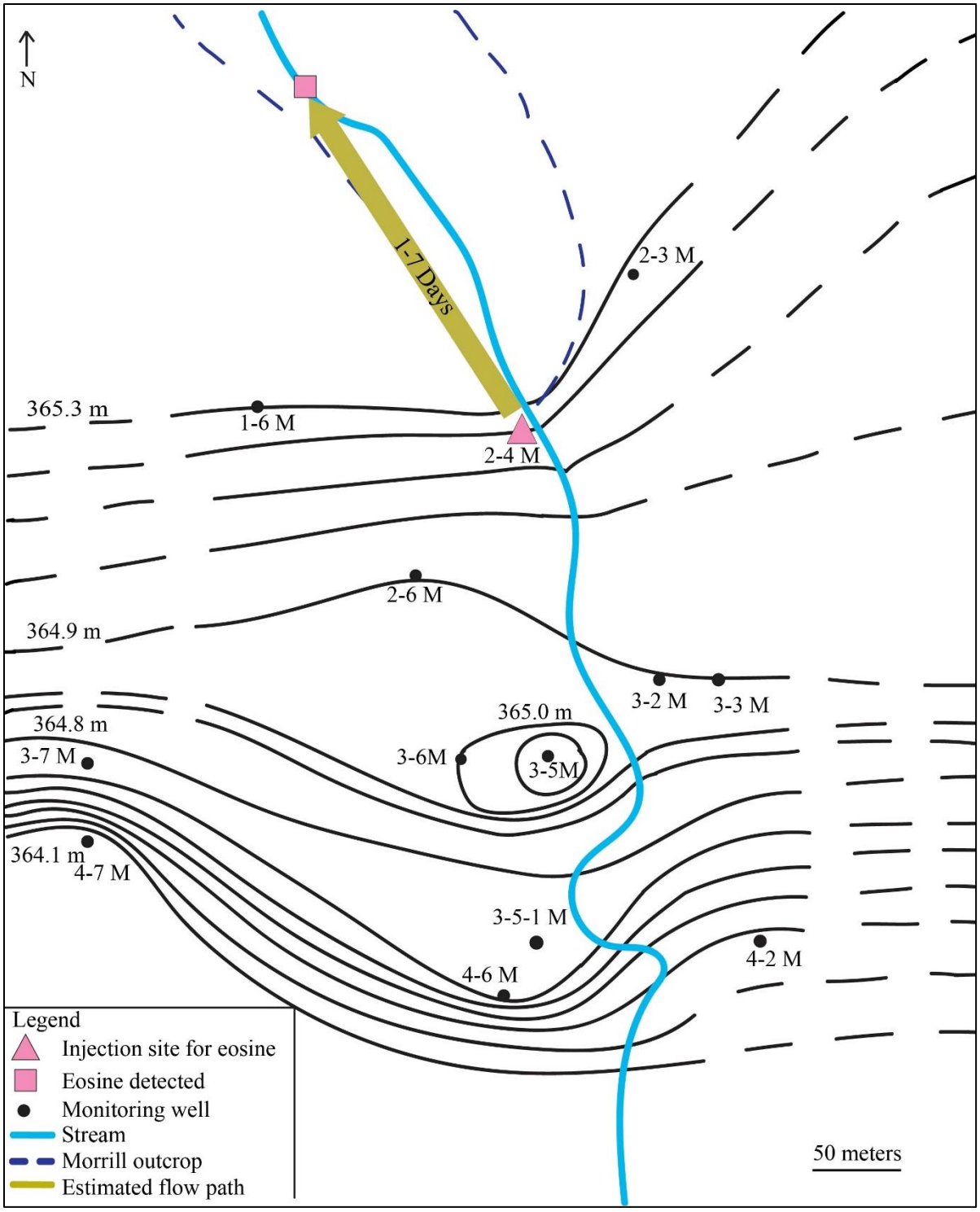


Figure 22: Summary of Eosine injection overlying Morrill potentiometric surface map.

### 4.6.2 Fluorescein

Fluorescein was injected into the upper Eiss aquifer in well 4-6E2. This well was chosen because it is surrounded by wells to the north where potentiometric surface maps indicate groundwater would flow. It is also one of the only Eiss wells that consistently has water in it. Additionally, this well occurs in a nest with wells 4-6E1 (completed in the lower Eiss) and 4-6M (completed in the Morrill), so that this tracer test was also used to test if these three wells are vertically connected. The volume of water used to mix the dye and flush the dye into the well created an induced head increase of 5.8 m. Fluorescein was initially detected (Figure 23) at the end of the first week post-injection at the Eiss 1 sampling point, at a distance of 40 m, as well as in all stream sampling points downstream of that point (Morrill 3, 2, 1, and Cottonwood Spring) and in wells 4-6E1 and 4-6M (Figure 1). The tracer could have arrived between one and seven days after injection, the exact timing unknown because of the weekly sampling interval.

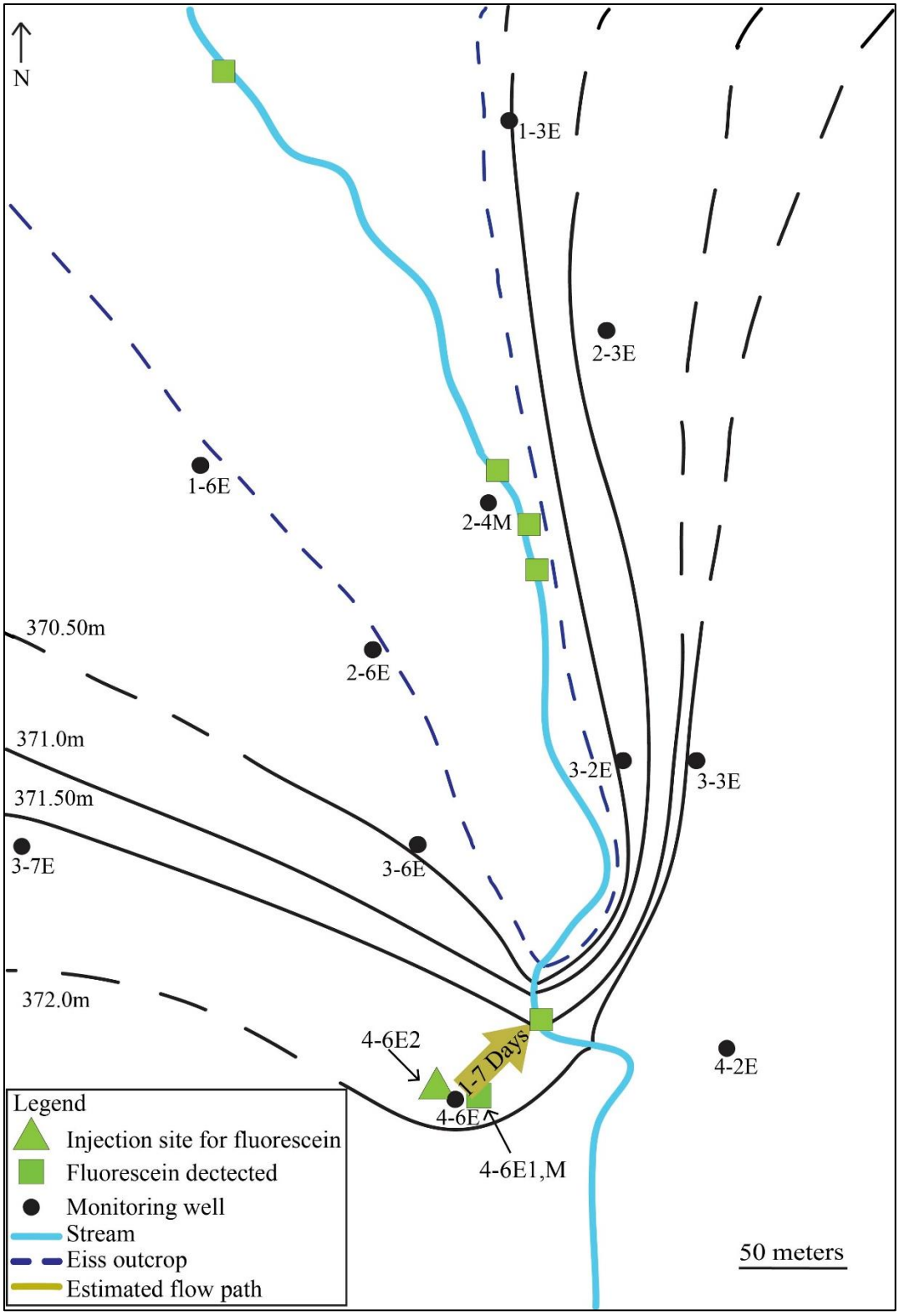


Figure 23: Summary of fluorescein injection overlying Eiss potentiometric surface map. All stream detections of fluorescein were detected at the first sampling period and only the shortest flow path is shown. The lack of upstream monitoring locations makes it impossible to know the travel direction more precisely.

### 4.6.3 Rhodamine WT

Rhodamine WT was injected into the Morrill aquifer in well 3-5-1M. This well was chosen because it is a very productive Morrill well that regularly has water in it. This well has Morrill wells near it to the north and south, so it the direction of flow could be determined in this aquifer. The volume of liquid used in the dye and to flush the dye created an induced head increase of 6.6 m. Rhodamine WT was detected (Figure 24) at well 4-6M at the end of the second sampling period (week 2) in water samples and was consistently detected at this location for the duration of the study. In charcoal receptors, rhodamine was detected at this location at the end of the 8$^{th}$ sampling period week 8. The detection of rhodamine in water samples 6 weeks before it was detected in charcoal samples is likely because the rhodamine was masked by the high concentration of fluorescein also in the water. Rhodamine WT was also detected at the downstream sampling point at the end of the 6$^{th}$ sampling period (week 6) in charcoal receptors and every week after that for the duration of the study with the exception of week 9 and the monthly sampling period during October 2017. Rhodamine appeared again downstream during the final sampling period at the end of the 5$^{th}$ month.

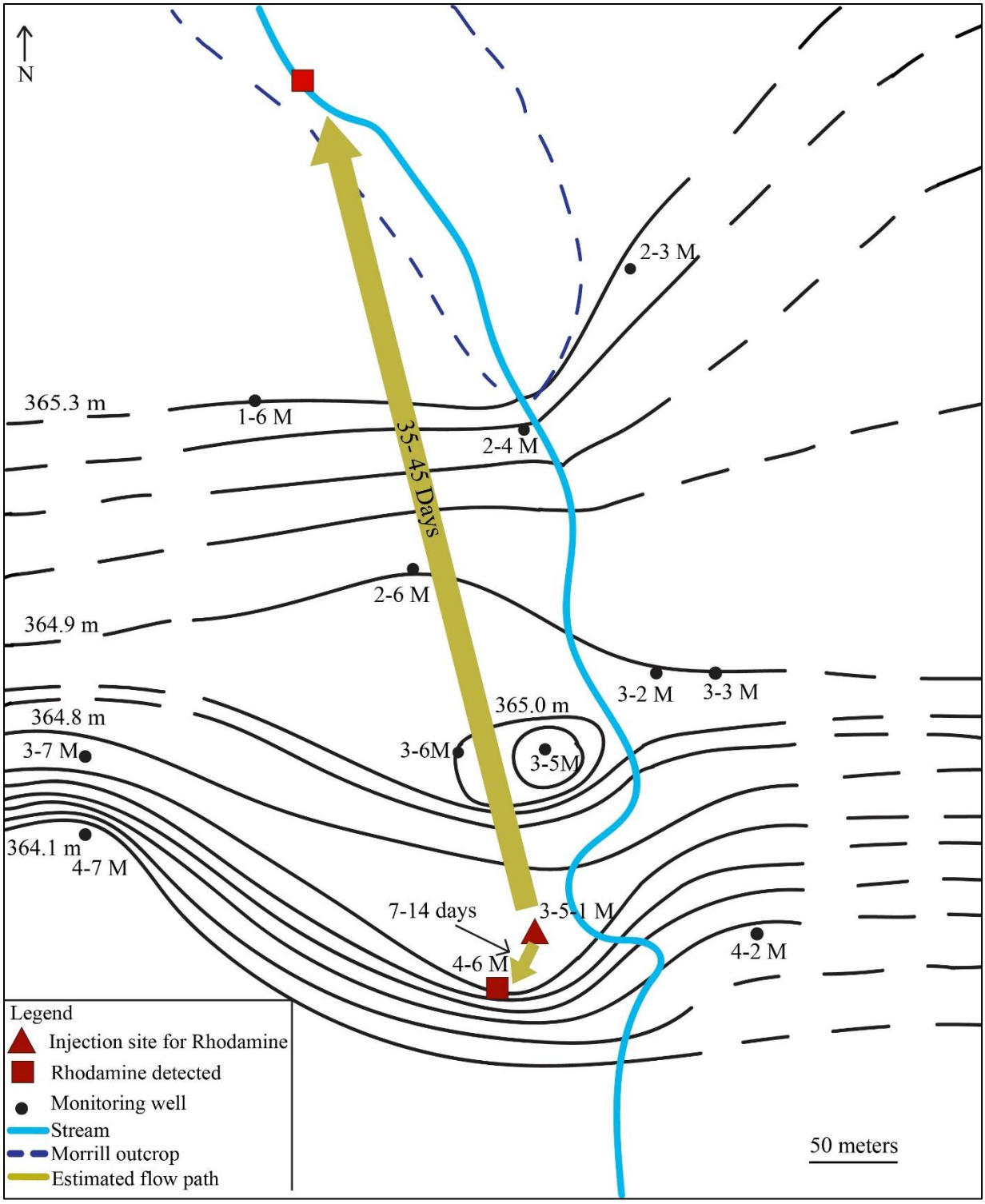


Figure 24: Summary of rhodamine injection overlying Morrill potentiometric surface map. Estimated flow paths connect injection and detection points, and are not intended to be interpreted as actual flow paths.

### 4.6.4 Dye break-through curves

Dye was detected at multiple sampling points at different times and in different quantities. The following figures are examples of dye breakthrough curves from this study. The remaining breakthrough curves from this study are in the Appendix. Precipitation data from the study period is shown below (Figure 25), as well to demonstrate the effect of precipitation on the breakthrough curves.

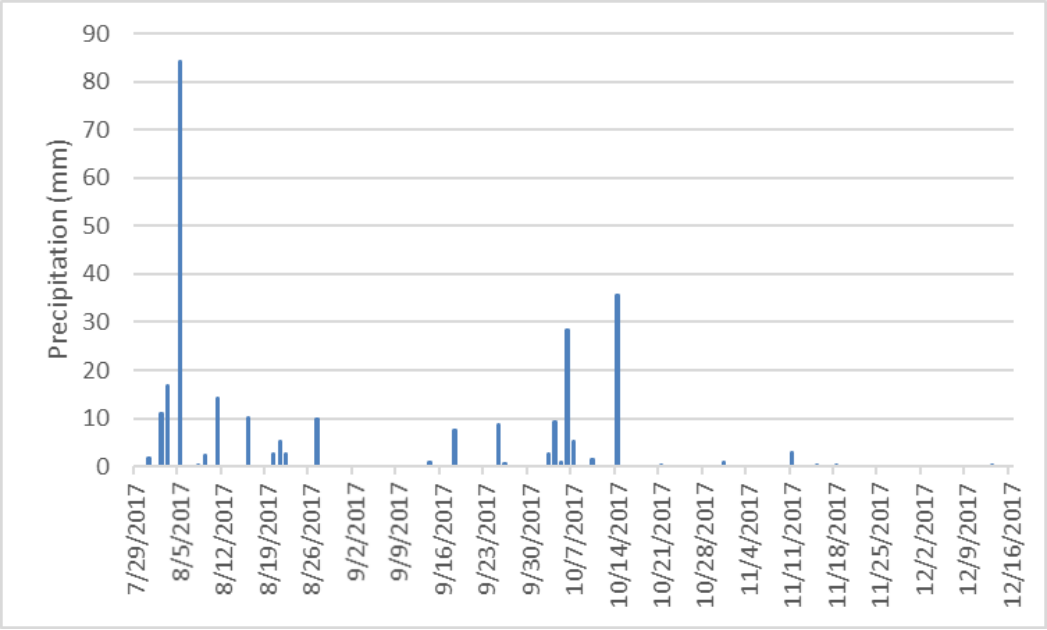


Figure 25: Precipitation data for the duration of this study.

The breakthrough curves for 4-6M (Figure 26) show a peak in fluorescein at the beginning of the study which is likely due to the proximity of 4-6M to the injection well, 4-6E2. The gap in data at the downstream sampling site (Figure 27) is likely due to the charcoal packet not being fully submerged in water for the entire month of sampling.

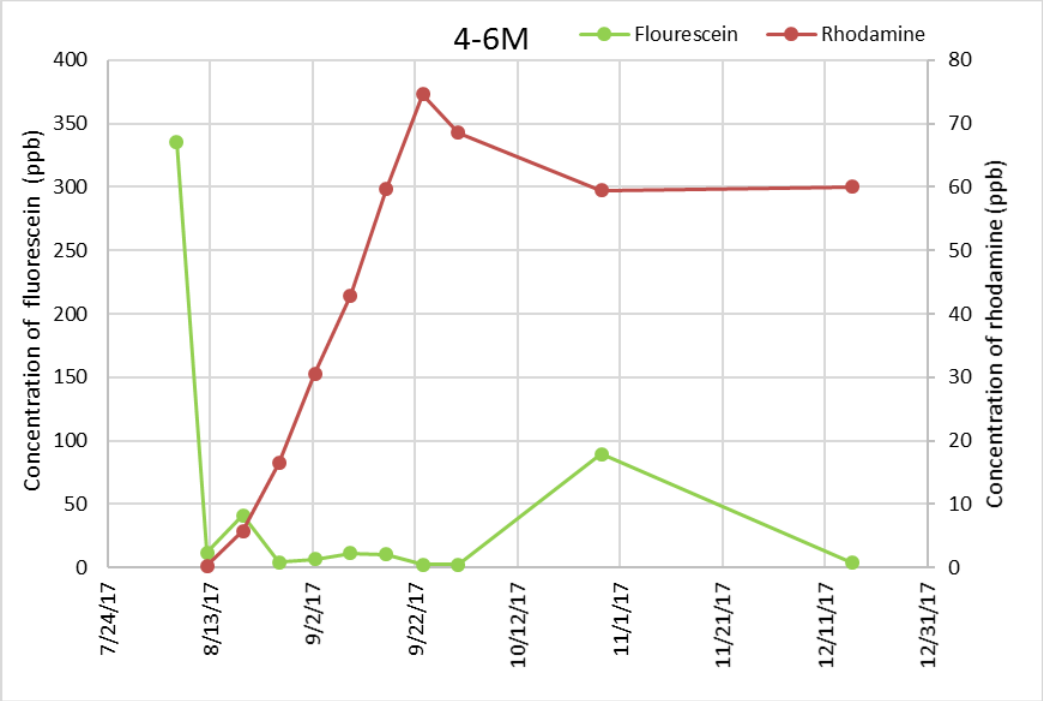


Figure 26: Breakthrough curve for well 4-6M. Rhodamine was injected into well 3-5-1M which is approximately 20 meters from well 4-6M. Fluorescein was injected into well 4-6E2 which is approximately 1.5 meters from well 4-6M.

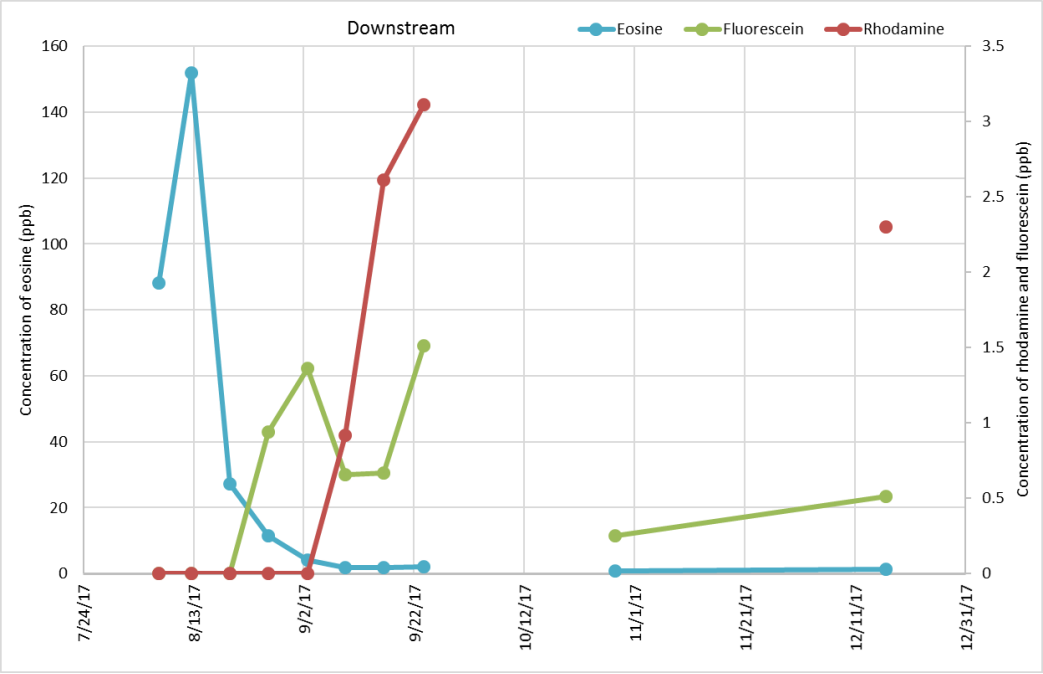


Figure 27: Breakthrough curve for downstream (Cottonwood spring) sampling location. Eosine was injected into well 2-4M, approximately 170 m from the Cottonwood spring. Fluorescein was injected into well 4-6E2, approximately 335 m from the Cottonwood spring. Rhodamine was injected into well 3-5-1M, 315 m from the Cottonwood spring.

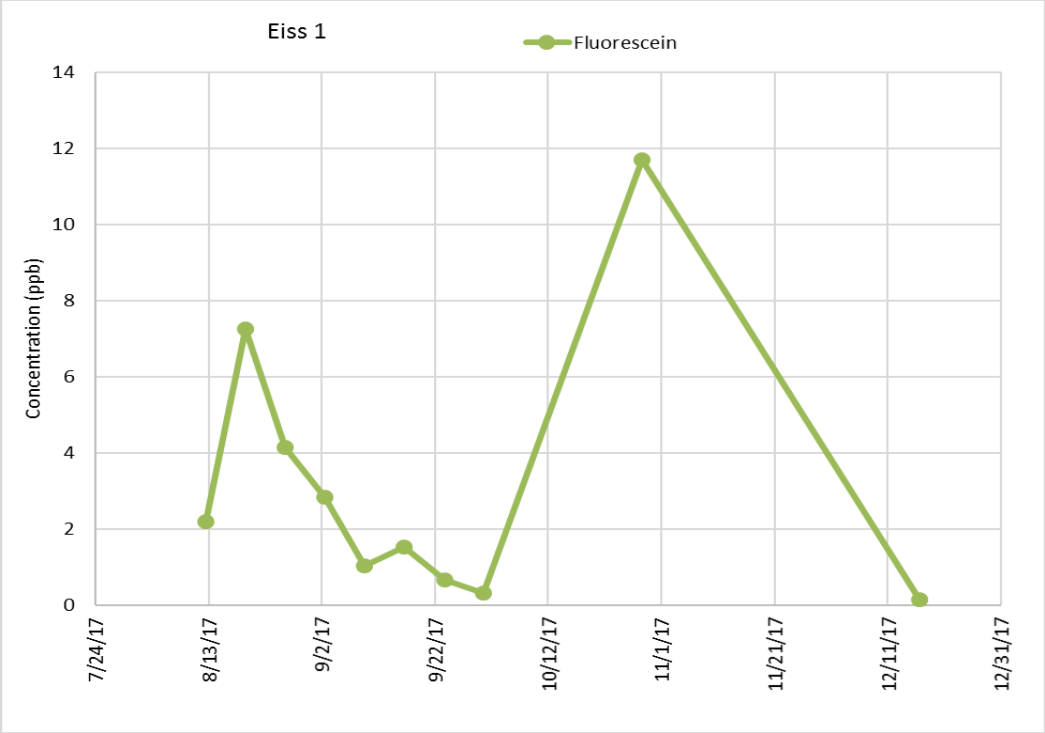


Figure 28: Breakthrough curve for Eiss 1 sampling point, a spring in the stream. Fluorescein was injected into well 4-6E2 approximately 45 m from sampling point Eiss 1.

### 4.7 Estimated travel times

Using the results of the three tracer tests, groundwater velocities were approximated based on the first arrival time of each tracer and the straight-line distance from injection to sampling point (dye-trace velocity; section 4.7). All dye-trace groundwater velocities are approximate and rounded to the nearest week because sample frequency was weekly or longer. All first arrival times occurred within the first two months of the study, in which the sampling period was weekly.

Groundwater velocity was also predicted using Darcy's Law and hydraulic head gradients of the potentiometric surface measured in April 2017, to be consistent with potentiometric surface maps (Darcy-Law velocities). For other parameters required by Darcy's Law, hydraulic conductivity of $10^{-3}$ m $d^{-1}$ (Pomes, 1995) and porosity of 0.2 were used for the

both Morrill and Cottonwood aquifers, although these parameters have not been measured for the Cottonwood at this location. For the Eiss aquifer, a hydraulic conductivity of $10^{-5}$ m $d^{-1}$ and a porosity of 0.2 were used. The largest hydraulic conductivity value was used to predict travel time so that the value would represent the fastest arrival time. Both dye-trace and Darcy's Law velocities are shown in Table 2.

In the Cottonwood aquifer, the dye-trace groundwater velocity was 7 m $d^{-1}$, based on the time elapsed between injection of rhodamine into the Morrill, and detection in the Cottonwood Spring. In the Morrill aquifer, the dye-trace groundwater velocity was 1 m $d^{-1}$, and the Darcy-Law value was also 1 m $d^{-1}$. The Darcy-Law velocity of groundwater in the Eiss was 32 m $d^{-1}$ while the dye-trace velocity was 6 m $d^{-1}$. In some cases, dye was never detected, although Darcy-Law velocities predicted it would be. For example, it was predicted that dye would travel from injection well 2-4M and arrive at well 2-5M in 5 days, and at well 2-1M in 6 days. It was also predicted that dye would travel from injection well 4-6E2 to observation well 2-6E in 11 days. However, no dye arrived in any of these locations during the study period, suggesting no major flow path exists between the injection wells and these observation wells.

| Unit | Injection well to sampling point | Darcy's Law velocity (m d-1) | Actual velocity (m d-1) |
|---|---|---|---|
| Cottonwood | 3-5-1M to downstream | - | 7 |
| Morrill | 3-5-1M to 4-6M | 1 | 1 |
| Eiss | 4-6E2 to Eiss 1 | 32 | 6 |

Table 4: Comparison of Darcy's Law calculations of groundwater velocity and actual groundwater velocity based on tracer arrival.

### 4.8 Cone of impression

The radial distance from the injection well was calculated to determine how far the dye traveled from the well immediately upon injection of dye and flush water, considering the head induced during the injection. The purpose of this was to understand how far away from the well the dye immediately traveled and if the detection of dye was accurate or was a product of the

injection. The radial distance of the fluid front from the well was calculated using equation 1 (shown below) (Green, 1983).

$$r = \sqrt{(\frac{Q}{\pi h \varphi})} \qquad \text{Equation 1}$$

where,

r = radial distance of fluid from well, feet

Q = cumulative volume of fluid injected, cubic feet

Φ= porosity of receiving formation

h= thickness of formation, feet

| Parameter | 2-4M | 3-5-1M | 4-6E2 |
|---|---|---|---|
| Q (ft^3) | 0.3 | 0.5 | 0.4 |
| Φ | 0.2 | 0.2 | 0.2 |
| h (ft) | 1.0 | 6.0 | 3.1 |
| r (ft) | 0.7 | 0.4 | 0.5 |
| r (m) | 0.2 | 0.1 | 0.1 |

Table 5: Input parameters for equation 1 resulting in the radial distance the dye and flush water traveled from the injection well (R).

Using equation 2, we calculated a cone of impression for each injection well (Reeves and Potter, 2011).

$$h_x = \frac{Q}{2\,\pi\,K\,b} \ln\left(\frac{r_w}{x}\right) + h_w \qquad \text{Equation 2}$$

Where,

hx is the hydraulic head [L] at x, the outer boundary of the well [L]

he is the hydraulic head [L] at radius re, the radius of influence of the well [L]

Q is the injection or pumping rate [L3T-1]

K is the hydraulic conductivity of the aquifer or reservoir [LT-1]

b is the thickness of the aquifer or reservoir [L]

| Parameter | 2-4M | 3-5-1M | 4-6E2 |
|---|---|---|---|
| rw (ft) | 0.1 | 0.1 | 0.1 |
| re (ft) | 0.7 | 0.4 | 0.5 |
| Q (ft3/d) | 274.9 | 471.5 | 416.2 |
| k (ft/d) | 0.0 | 0.0 | 0.0 |
| b (ft) | 1.0 | 6.0 | 3.1 |
| hw (ft) | 12.6 | 21.6 | 19.1 |

Table 6: Input parameters for equation 2 resulting in figures 29-31.

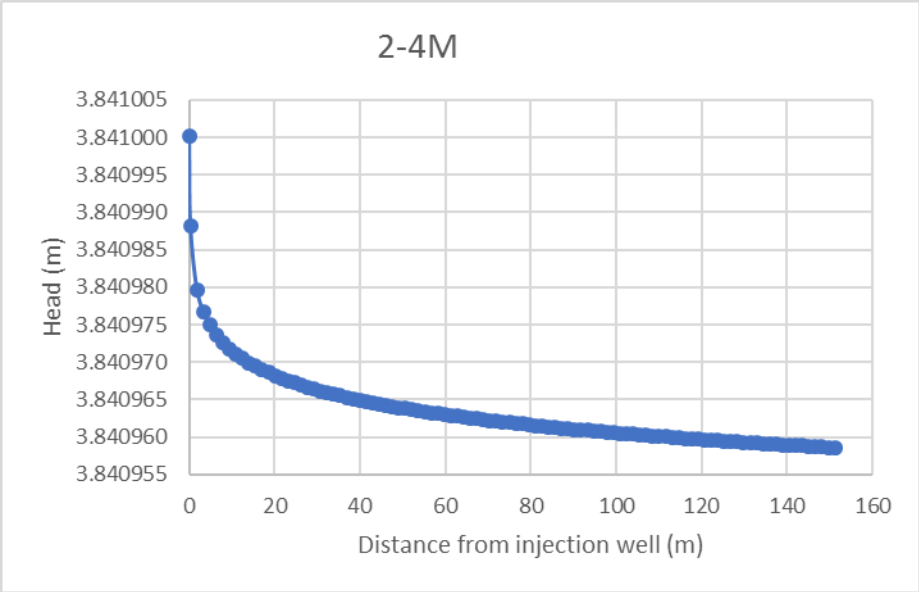


Figure 29: Cone of impression for the injection of eosine into well 2-4M using equation 2.

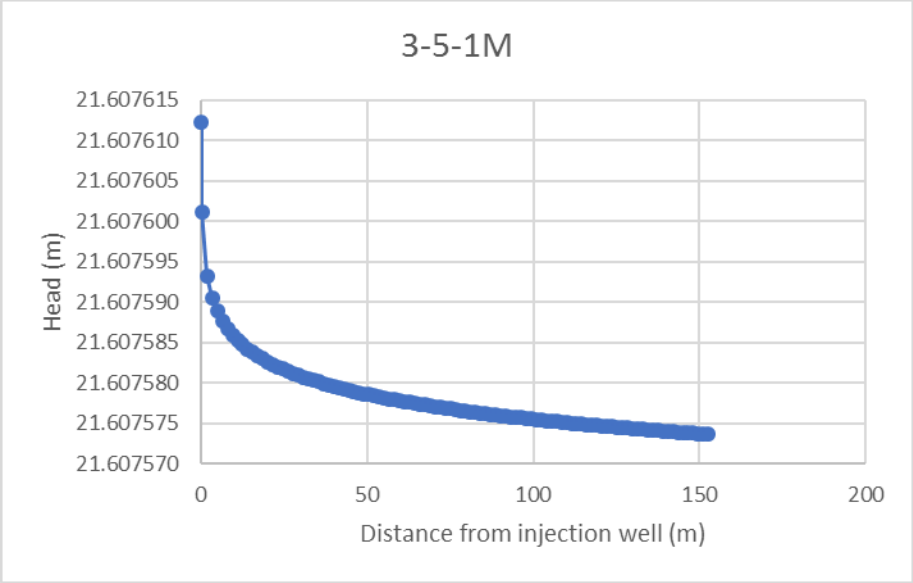


Figure 30: Cone of impression for the injection of rhodamine into well 3-5-1M using equation 2.

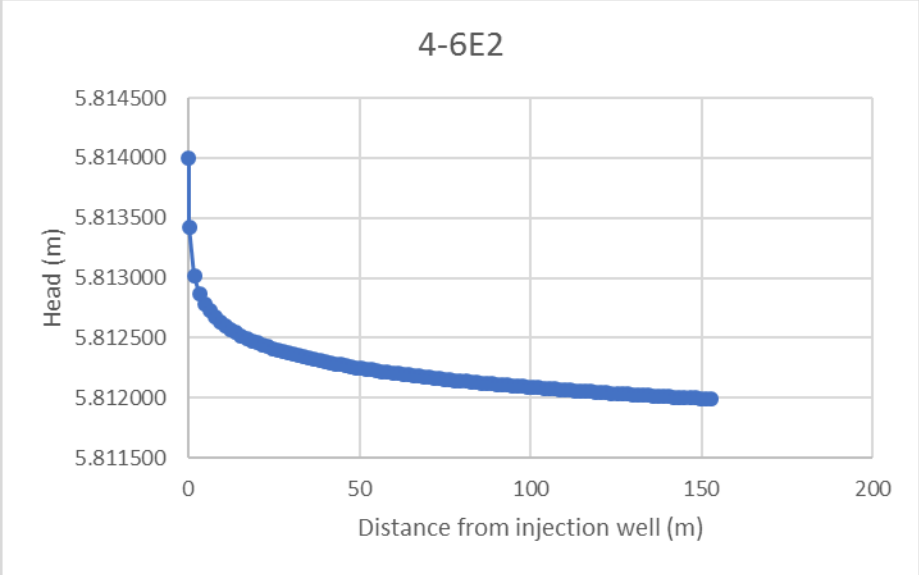


Figure 31: Cone of impression for the injection of fluorescein into well 4-6E2 using equation 2.

The use of equations 1 and 2 create an understanding of the distance the water travelled from the well, and the effect that the pressure from injection had on the aquifer with increasing distance from the well. While the changes in head in Figure 29-31 are small, they demonstrate that pressure still has an influence on the aquifer even though the change in head is less than 5cm.

## 5. Discussion

Results of tracer tests confirmed where groundwater is flowing at Konza. In general, the results of the dye trace correspond with the results of the potentiometric surface maps. The fluorescein dye trace in the Eiss Limestone aquifer as reported in Section 4.7.2 show groundwater flowing north to the stream, which is consistent with the potentiometric surface map (Figure 21). The breakthrough curves in this study exhibited a long tail which is common in low flow tests (Barbera *et al*., 2018). Similar to other karst settings, groundwater in this aquifer flows towards a spring or a stream discharge point.

The rhodamine dye tracing study reported in Section 4.7.3, show groundwater flowing southward in the Morrill, confirming the potentiometric surface map (Figure 20). Therefore, dyes showed flow was in opposite directions in these vertically stacked aquifers. Though it is it common to see multidirectional flow in karst aquifers (Gouzie *et al*., 2015), the flow paths are generally not directly opposed as the ones seen in this study.

The absence of visible dye in the stream suggests this diffuse karst system causes water to flow more slowly, transporting smaller concentrations of dye. It was expected that there would be a flow path from well 2-4M to the stream and that dye would be detected at the Morrill 1 sampling point, based on the background test, where rhodamine previously injected into the stream was detected in well 2-4M likely when stream discharge was much higher. The presence of eosine in roots indicates that there was some movement of eosine from well 2-4M toward the stream or that there were roots intercepting and transmitting the eosine through a root system of some kind. Absence of eosine in the Morrill 1 pool may demonstrate that the amount of eosine moving toward the stream was small and completely sorbed by the roots and that there may be another path or paths that the majority of the eosine followed. Several contributing factors

caused absence of eosine detection in the Morrill 1 pool during the tracer test. First, the potential for groundwater to flow is southward in the Morrill, away from the outcrop which forms the nickpoint above the pool in which the Morrill 1 sampling point is located. Secondly, the stream was losing where the Morrill outcrop is located, so that during the tracer test, water was not flowing into the stream from the Morrill. Finally, the background test was conducted in the spring, when there was more water in the stream and the head was higher in the stream than in well 2-4M. This head change is the driving force for this flow direction. The tracer test on the other hand, was conducted during a dry period in the summer and fall when the stream had much less water flowing. The flow conditions of an aquifer are dependent on how much water is available in the system (Barbera *et al*., 2018). These factors explain the lack of eosine in the stream and the connection of the stream to well 2-4M.

The dye trace results showed a vertical connection between aquifers. The results discussed in Section 4.7.2 demonstrate that the upper and lower Eiss units are connected. The presence of fluorescein in well 4-6M supports that the Morrill and Eiss are connected as well. In contrast, the groundwater chemistry in each aquifer varies, which suggests that they are separate aquifers (Macpherson, 1996). It is possible that the wells, which are partially drilled into the shale underlying the limestone, along with the closeness of these nested wells and the induced head created by dye injection, caused an artificial connection between the wells at this location (Figure 32). To investigate this possibility, I calculated cones of impression based on the tracer test conditions, discussed next.

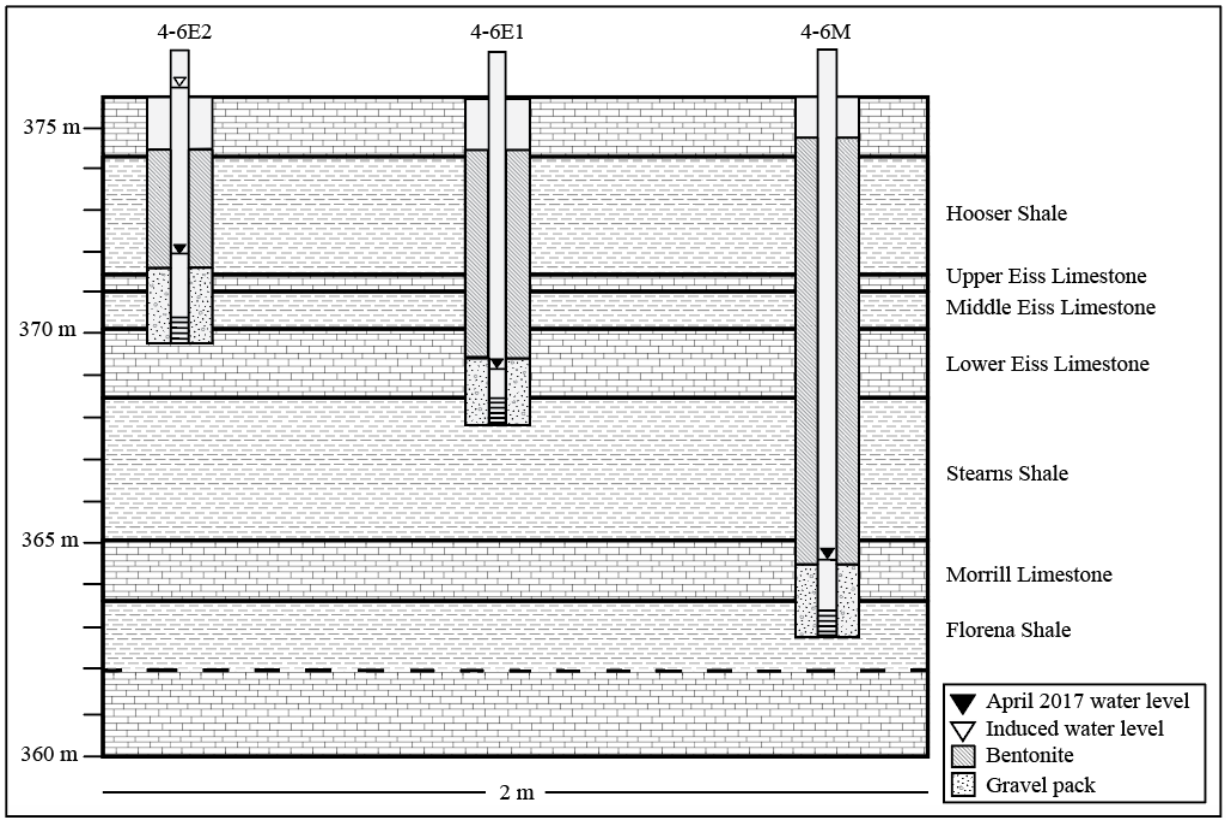


Figure 32: Diagram illustrating the closeness of the 4-6 wells and the induced head from the tracer test compared to the water level from April 2017. Note the construction of the wells screened in multiple units and the overlapping gravel packs of well 4-6E2 and 4-6E1 within the Lower Eiss Limestone.

Cone of impression calculations (Section 4.8) show that the inverted cones are very steep and the amount of induced head near the well is very small. This suggests that the detection of dye in each well was not created by the hydraulic head created during dye injection. Rather, the detection of dye was caused by groundwater flow.

The complexity of these aquifers was further revealed by the discovery of a connection between the Cottonwood and the upper units. During and shortly after the stream was flowing, it seemed obvious that the fluorescein detected downstream would come from the Eiss 1 sampling point located upstream. However, when continuous streamflow ceased, fluorescein was still detected at the Cottonwood spring. This suggests either the pre-existing fluorescein from previous weeks remains, or the possibility that the dye took a flow path outside the Eiss

Limestone. It is likely that the dye sank into the Morrill, and then into the Cottonwood, and traveled to the downstream spring via a flow path in the Cottonwood. This implies that some groundwater in the Eiss flows northeast towards the stream, which agrees with the potentiometric surface map. However, some groundwater from the Eiss flows downward vertically to 4-6M, flows southward in the Morrill and then northward to the Cottonwood spring.

The results of the tracer test suggest that these aquifers are semi-confined, and that the shales in between them act as leaky aquitards. Eosine was detected in the downstream spring coming out of the Cottonwood, but not at any sampling locations in the Morrill, despite being injected into the Morrill. Rhodamine was also detected in a downstream spring coming out of the Cottonwood aquifer, even though it was injected into the Morrill, and was also detected to the south of the injection well within the Morrill Limestone. Detecting dyes in different units than they were injected into shows that the water in these aquifers is not restricted specifically to these units. Although horizontal flow dominates in these aquifers (Macpherson, 1996), tracer data indicates that vertical flow is also occurring. The rhodamine plume splitting and travelling through different aquifers shows a direct connection between these aquifers that allows water to seep down from one aquifer into the one below it (Figure 33). This may be because the unit between the Upper and Lower Eiss is thinner than the limestones. There is also uncertainty about the well completions. These factors may influence the connection between these aquifers.

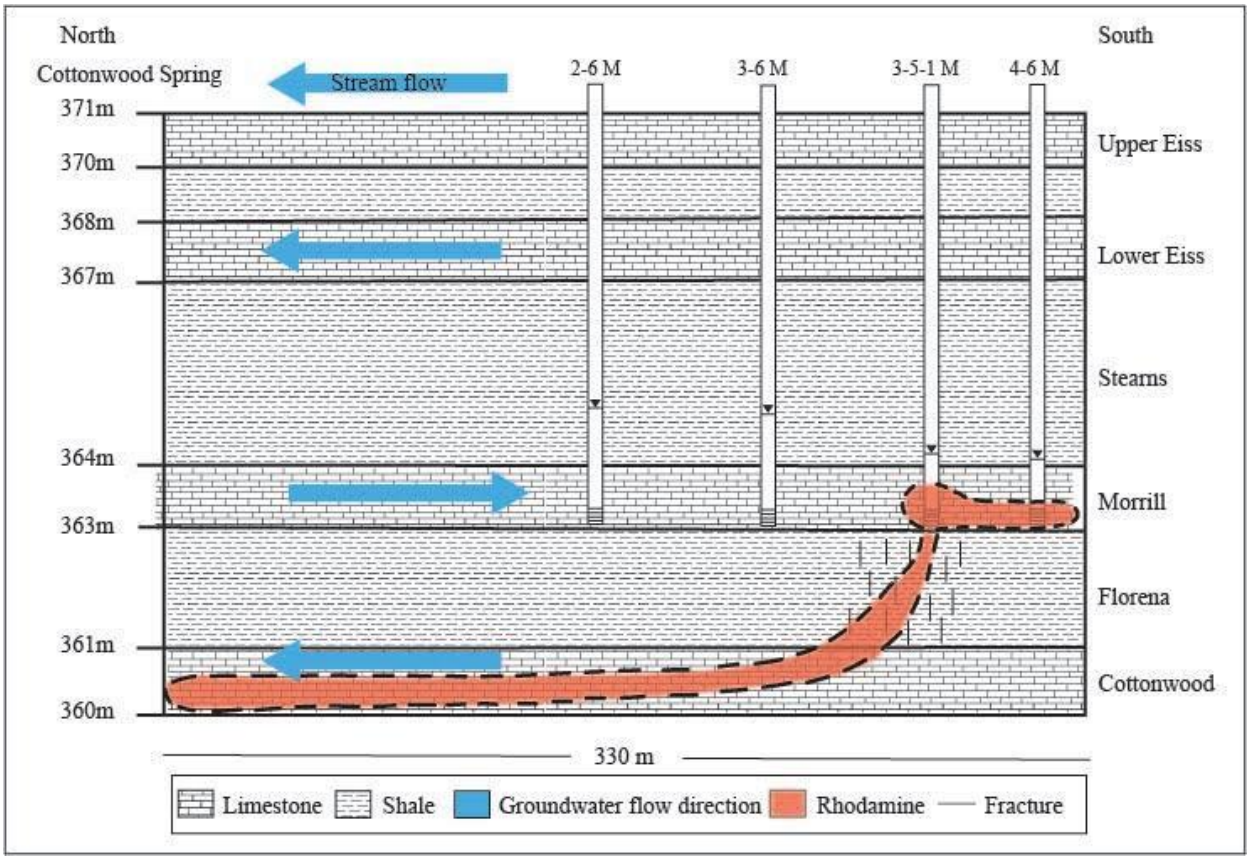


Figure 33: Conceptual diagram showing the estimated movement of the rhodamine plume and estimated location of fractures. Plume not to scale.

Groundwater velocity approximations are reported in section 4.6. The Morrill Darcy-predicted velocity agreed with the dye-trace velocity, while the dye trace velocity in the Eiss was much faster than Darcy-predicted. The velocity results of this study vary from other karst aquifers. As expected, the groundwater velocity in these aquifers moved slower than (m $d^{-1}$) typical velocities measured in well-developed karst aquifers (km $d^{-1}$), at 1 to 32m $d^{-1}$. Flow velocities in karst aquifers typically range from hundreds to thousands of meters per day (Mull *et al*., 1988). Velocities reported from tracer tests in epikarst are on the scale of m $hr^{-1}$ (Williams, 2008). The velocities measured in this study are consistent with the characterization of a diffuse flow system.

The amount of precipitation Konza received in 2017 directly impacted groundwater velocity. In a previous study by Brookfield *et al*. (2017), groundwater demonstrated a rapid response time to precipitation at Konza. The Morrill and Eiss aquifers respond differently to precipitation. In a wet year (2016), the water level in the Upper Eiss rose faster after precipitation than the other aquifers, while the Morrill wells responded second and the Lower Eiss had the slowest response (Table 2). The aquifers at Konza show similar groundwater response times (Figure 19) as epikarst aquifers, where recharge to the aquifer is rapid, indicating that the aquifers at Konza may share similar properties with epikarst aquifers (Williams, 2008). The Upper Eiss is the youngest unit, so it having the largest and first response is reasonable because it is overlies the other units. Geophysical data from this site indicates that these epikarst like features exist at Konza and may aid rapid vertical recharge (Zhang, unpublished data, 2017). The order of Morrill wells responding in 2016 (Table 2) to a precipitation event indicates that recharge into the Morrill is a likely a combination of water from the stream feeding groundwater and vertical recharge from the overlying Eiss Limestone. Though 4-6M reaches its peak water level in response to precipitation 9 hours before 3-5-1M does, the head in 4-6M does not exceed the head in 3-5-1M so flow directions remain consistent with potentiometric surface maps (Figure 20). After its initial peak, 4-6M declines then has a small peak 12 hours later, indicating that initial recharge is from the above Upper Eiss followed by a secondary recharge that comes from the stream. In 2017 however, a dry year, recharge into the Morrill appears to come mostly from the stream, demonstrated by 3-5-1M reaching a peak before 4-6M does. This flow direction is consistent with potentiometric surface maps (Figure 20). The Lower Eiss responding last indicates a slower infiltration time from the Upper Eiss Limestone through a lower permeability layer that separates the upper and lower parts of the Eiss. The Lower Eiss also has a lower

hydraulic conductivity. This also means that travel time in the Lower Eiss would be several days slower than in the Morrill or Upper Eiss.

The water level responds differently to precipitation during wet years (Table 2) and dry years (Table 3). The wet year shows a slower response to precipitation, which is likely because vegetation is more active in wet years and slows down infiltration. Soil conditions are also different during wet and dry years which leads to differences in the connectivity between the surface and bedrock systems. However, the wet year also shows a more dramatic rise in the water level. Graphs that show similar shapes like 3-5-1M, and 4-6M in 2017 (Figure 19 D,H), indicates that water is moving similarly through this unit. The groundwater response time to precipitation is generally slower in years where there is less precipitation (Brookfield *et al*., 2016). The measured velocity is most likely a low approximation due to below-average precipitation (Figure 6), which caused low flow conditions during the study period. Because there was less water in the system, there was less recharge to flush the system, creating a slower travel time of groundwater than during a wet period.

The results of this study show that in the Eiss and the Cottonwood aquifers, groundwater flows north and in the Morrill limestone, groundwater flows south. Figure 34 shows a generalized conceptual cross section of groundwater flow in this watershed. Connections between the limestone units are likely at multiple locations where the shale is either fractured or thickness reduced by physical weathering. Both rhodamine and eosine, which were injected into the Morrill at different points, were detected in the underlying Cottonwood, suggesting multiple connections. In this study, the main connection appears somewhere between well 3-5-1M and 4-6M. The results of this study and a review of the driller's logs show that the connection between these aquifers is likely at the proposed collapse feature discussed in section 4.1. Another

connection occurs surrounding well 2-4M. I propose that the connection between the Morrill and Cottonwood aquifers, demonstrated by the eosine test, is likely very close to well 2-4M because eosine was not detected elsewhere.

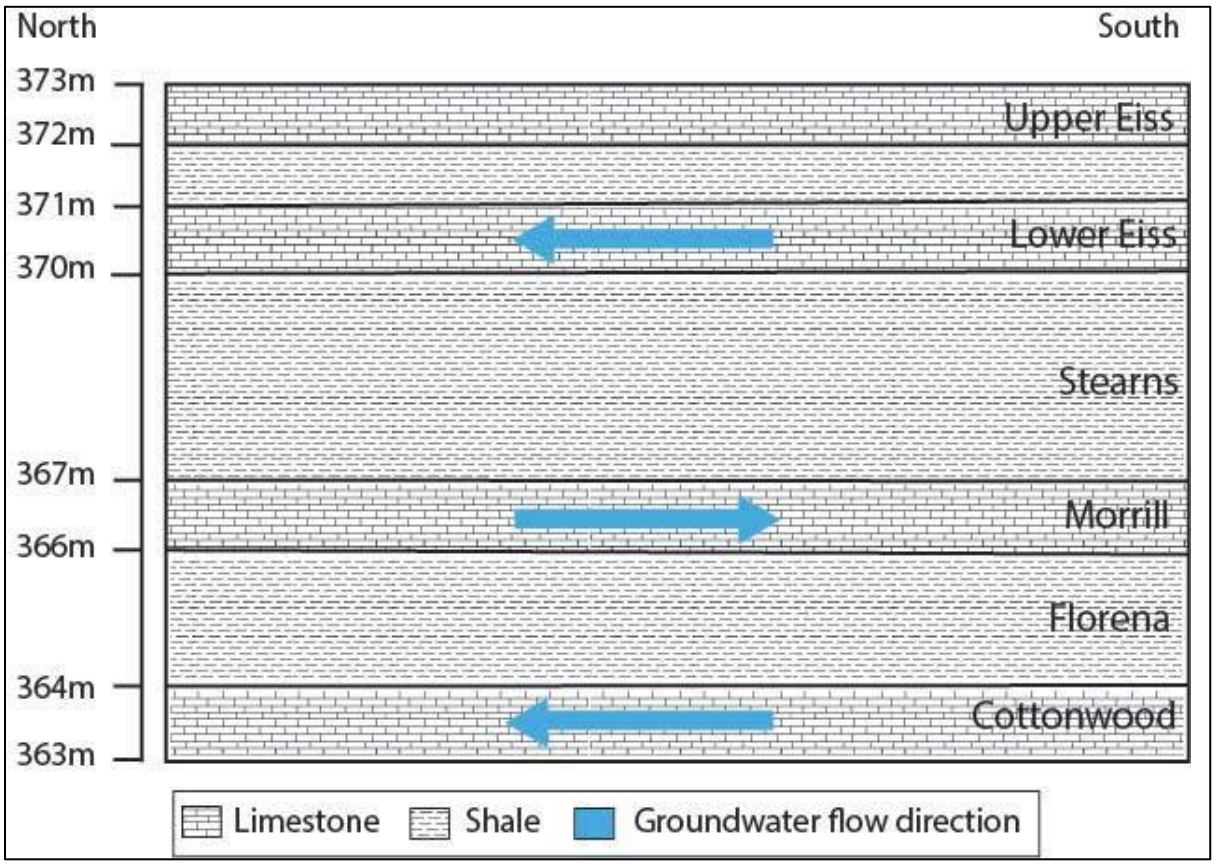


Figure 34: Conceptual model showing groundwater flow direction at Konza.

Highly variable hydraulic conductivity (Pomes, 1995), rapid response time of wells to precipitation (Brookfield *et al*., 2016), geophysical data (unpublished), and rapid ground water velocity (as seen in this study) support the idea that there are solution-enlarged fractures in these aquifers, and that there is a geologic influence on groundwater flow. Other groundwater tracer tests have proved that groundwater flow in karst is significantly influenced by structural trends (Hunt *et al*., 2005). The fractures at Konza influence groundwater flow direction. The dominant fracture set in the Morrill Limestone is oriented northwest-southeast, which controls the southward direction of groundwater flow discussed in section 4.6.3. In the Eiss Limestone, the

dominant fracture set is oriented generally northeast-southwest, which is consistent with the results of the fluorescein trace (section 4.6.2).

The changes in unit thicknesses taken from well log data of many of the wells within N04d as previously discussed demonstrates that the thickness of each unit is variable within the watershed. Our data indicate groundwater in the Morrill and Eiss appears to be flowing towards where these units are thicker. This likely means that the structure of these units has an influence on the direction of groundwater flow on a regional scale. The dip of the regional strata is 0.19° to the northwest. Because these units are nearly horizontal, differences in unit thickness due to variable erosion or differential deposition of sediments will significantly influence the dip of that unit (Smith, 1991). Local erosional or depositional variation is possibly causing the Morrill limestone to dip 0.3° slightly to the south, causing groundwater to follow the unit's slight dip and flow south-southwest.

Contour maps of the base of both the Morrill (Figure 10) and Eiss (Figure 11) show that both units locally dip to the south-southwest. The Morrill, in particular, shows a circular shaped depression surrounding well 3-5-1M. In cross section view, the base of the units form a "V" shape (Figure 12a) which represents a collapse feature in the units at this point. This collapse feature occurs in both the Morrill and Eiss limestones and based on the tracer test results, it is likely a controlling factor in alternating groundwater flow paths. This collapse feature may indicate the presence of a small sink hole or a series of small coalescing sinkholes, like those discussed in Panno *et al*. (2011), in which the topographic depression may have since been filled in with alluvium. This collapse feature is characteristic of karst settings. I hypothesize that this collapse feature is a sinkhole that may be located in the Cottonwood Limestone and may have caused the units above it to collapse on top of it. Wells that are closer to the stream have higher

hydraulic conductivity and appear to be strongly connected to the stream, causing the enhancement of karst features such as solution-enlarged fractures and vugs. If the same is true of the Cottonwood Limestone, the possibility of a sinkhole in this unit is likely. The thickness of the Cottonwood Limestone (2m) is large enough that it would cause the units above to collapse (Figure 10,11,12a). The Eiss limestone has springs that drain it and a higher hydraulic head to the south, causing the water in this units to flow north. The Morrill, however, does not have a spring that discharges in this watershed because the stream segment across the Morrill is losing. The presence of rhodamine in well 4-6M proved that groundwater flows south in the Morrill (Figure 33). I propose that the hypothesized collapse feature is acting as a drain for the Morrill. Because the Cottonwood and Eiss have springs that discharge to the stream, they are not as affected by the collapse feature as the Morrill is, so groundwater flows north in these aquifers.

The results of this study likely have implications to other merokarst areas. It is probable that collapse features or sinkholes also occur outside of Konza. As discussed in section 2.1, karstification was observed in a core approximately 40 km from N04d, and therefore karstification of merokarst occurs elsewhere. Since the karstification of merokarst is occurring elsewhere, the results of this study may be observable in other areas with merokarst. Several characteristics of the landscape of N04d might be indicators of the presence of alternating groundwater flow. Springs are an obvious indicator of where groundwater is flowing within that particular unit. If springs occur in some units but not others, there could be alternating groundwater flow in these units as well. For example, both the Eiss and the Cottonwood have springs that discharge them, but the Morrill does not in N04d even though it outcrops in N04d. Characteristics that may indicate the presence of collapse features may be a meandering stream and an asymmetric stream valley. The meandering of the stream may indicate that the stream is

attempting to make up for the change in slope that is caused by the creation of this collapse feature. An asymmetric stream valley could be indicating the collapse of one side of the valley, but not the other, and thus could mark the presence of a collapse feature. Finally, if field reconnaissance is possible, the presence of a stream that alternates between gaining and losing in merokarst could be the most likely indicator for alternating groundwater flow.

To summarize, several factors control groundwater flow in merokarst aquifers during the dry season. This study shows that the groundwater flow through this system is complex. This complexity was observed through directly opposed flow directions and vertical connections between aquifers. The aquifers behave in a way similar to other karst aquifers. The main controls in this merokarst terrain are spring discharge, solution enlarged fractures and hydraulic gradient within the aquifer.

## 6. Conclusions

This study used the results of three tracer tests to provide greater understanding of how groundwater flows through three merokarst aquifers at the Konza Prairie Long-Term Ecological Research Site in Northeastern Kansas. The results of this study lend insight into the understanding of how groundwater flows through thin limestones, and may be applicable to massive limestones since the aquifers at this site showed characteristics similar to those of massive karst aquifers. The findings from this tracer test can be applicable to contaminant transport and should be considered during the remediation process of merokarst aquifers.

Groundwater at Konza flows in various directions in three vertically stacked karst aquifers, as determined by fluorescent dye tracers and potentiometric surface maps. In the lowest stratigraphic unit, the Cottonwood Limestone member of the Beattie Limestone Formation, groundwater generally flows north. In the Morrill Limestone member of the Beattie Limestone

Formation, groundwater generally flows south. In the highest stratigraphic unit, the Eiss Limestone member of the Bader Formation, groundwater generally flows north and discharges into a spring in the stream. The presence of dye in aquifers without a dye injection suggests these aquifers, although separated by shales thicker than the limestones, are connected via leaky aquitards. Groundwater velocity measurements showed the karst aquifers had velocities that range from 1 meters per day in the Morrill to 6 m $d^{-1}$ in the Eiss to 7 m $d^{-1}$ in the Cottonwood. The velocity of groundwater in these aquifers as well as their other characteristics classifies them as diffuse flow karst aquifers.

I hypothesize that a collapse feature in the Morrill, Stearns, and Eiss or the underlying units, the thickening of the structure, and solution-enlarged fractures which cause preferential flow paths, causes groundwater in the Morrill to flow south. A direct flow path between the injection well 3-5-1M and 4-6M was discovered from this study. I propose that the regional dip of the strata, springs, and the hydraulic gradient of the Cottonwood and the Eiss aquifers causes water in these aquifers to flow north. Groundwater flow directions in this area follow trends in the fractures. The results of this study show that there are many contributing factors to groundwater flow and that the results of a dye trace done in merokarst are comparable to those done in holokarst.

**References**


Aley, Thomas. "Groundwater tracing handbook." *Ozark Underground Labs* (2002).

Aley, Thomas J.. 2016. Using activated carbon samplers to improve detection of fluorescent tracer dyes in groundwater remediation studies**.** Tenth International Conference on Remediation of Chlorinated and Recalcitrant Compounds, Palm Springs, CA. ISBN 978-0-9964071-1-3, Battelle Memorial Institute. Paper A-056 10p.

Aley, T. (2017). Improving the detection of fluorescent tracer dyes in groundwater investigations. *Remediation Journal*, *27*(4), 39-46.

Barberá, J. A., Mudarra, M., Andreo, B., & De la Torre, B. (2018). Regional-scale analysis of karst underground flow deduced from tracing experiments: examples from carbonate aquifers in Malaga province, southern Spain. *Hydrogeology Journal*, *26*(1), 23-40.

Benson, R. C., & Yuhr, L. B. (2015). *Site Characterization in Karst and Pseudokarst Terraines: Practical Strategies and Technology for Practicing Engineers, Hydrologists and Geologists*. Springer.

Brookfield, A. E., Macpherson, G. L., & Covington, M. D. (2017). Effects of changing meteoric precipitation patterns on groundwater temperature in karst environments. *Groundwater*, *55*(2), 227-236.

Chelikowsky, J. R. (1972). *Structural geology of the Manhattan, Kansas, area*. University of Kansas Publ..

Chen, Z., Auler, A. S., Bakalowicz, M., Drew, D., Griger, F., Hartmann, J., ... & Veni, G. (2017). The World Karst Aquifer Mapping project: concept, mapping procedure and map of Europe. *Hydrogeology Journal*, *25*(3), 771-785.

Climate and Hydrology Database Projects (CLIMDB/HYDRODB). (n.d.). Retrieved February 26, 2018, from https://climhy.lternet.edu/

Field, M. S., Wilhelm, R. G., Quinlan, J. F., & Aley, T. J. (1995). An assessment of the potential adverse properties of fluorescent tracer dyes used for groundwater tracing. *Environmental Monitoring and Assessment*, *38*(1), 75-96.

Friederich, H., & Smart, P. L. (1981). Dye tracer studies of the unsaturated zone: recharge of the Carboniferous Limestone aquifer of the Mendip Hills, England. In *Proceedings of the 8th International Congress of Speleology* (Vol. 1, pp. 283-6). Kentucky USA.

Ford, D., & Williams, P. (2007). Introduction to Karst. *Karst Hydrogeology and Geomorphology*, 1-8.

Gouzie, D., Berglund, J., & Mickus, K. L. (2015). The application of quantitative fluorescent dye tracing to evaluate karst hydrogeologic response to varying recharge conditions in an urban area. *Environmental Earth Sciences*, *74*(4), 3099-3111.

Green, R. T., Painter, S. L., Sun, A., & Worthington, S. R. (2006). Groundwater contamination in karst terranes. *Water, Air, & Soil Pollution: Focus*, *6*(1-2), 157-170.

Greene, C. J. (1983). *Underground injection-control technical assistance manual: subsurface disposal and solution mining* (No. PB-85-176477/XAB; TDWR/R-274). Texas Dept. of Water Resources, Austin (USA).

Hauwert, N. M., Johns, D. A., Sansom, J. W., & Aley, T. J. (2002). Groundwater tracing of the Barton Springs Edwards Aquifer, Travis and Hays Counties, Texas.

Hvorslev, M. J. (1951). Time lag and soil permeability in ground-water observations.

Jewett, J.M., 1941, The geology of Riley and Geary counties, Kansas: Kansas Geological Survey, Bulletin, no. 39, 164 p.,http://www.kgs.ku.edu/General/Geology/Riley/strat01.html, accessed Jan. 2018

Macfarlane, P.A., (2003). The hydrogeology of Crystal Spring with and delineation of its source water assessment area: Kansas Geological Survey, Open-file Report no. 2003-35, 156 p.

Macpherson, G. L. (1996). Hydrogeology of thin limestones: the Konza Prairie long-term ecological research site, Northeastern Kansas. *Journal of Hydrology*, *186*(1-4), 191-228.

Monroe, W. H. (1970). *A glossary of karst terminology* (No. 1899-K). US Govt. Print. Off.,.

Mull, D. S., Liebermann, T. D., Smoot, J. L., & Woosley, L. H. (1988). *Application of dye-tracing techniques for determining solute-transport characteristics of ground water in karst terranes* (No. PB-92-231356/XAB; EPA--904/6-88/001). Environmental Protection Agency, Atlanta, GA (United States). Region IV.

Mull, D. S. (1993). *Use of dye tracing to determine the direction of ground-water flow in karst terrane at the Kentucky State University Research Farm near Frankfort, Kentucky*. US Department of the Interior, US Geological Survey.

Panno, S. V., Hackley, K. C., Kelly, W. R., & Luman, D. E. (2011). Illinois' sinkhole plain, classic karst terrain of the Midwestern United States: geological field trip guidebook for the 12th Multidisciplinary Conference on Sinkholes and the Engineering & Environmental Impacts of Karst, January 10-14, 2011, St. Louis, Missouri, USA. *Guidebook no. 039*.

Pomes, M. L. (1996). A study of the aquatic humic substances and hydrogeology in a prairie watershed: Use of humic material as a tracer of recharge through soils.

Quinlan, J. F., & Ewers, R. O. (1989). Subsurface drainage in the Mammoth Cave area. In *Karst Hydrology* (pp. 65-103). Springer, Boston, MA.

Reeves, M., & Potter. G. (2011). Preliminary Design and Assessment of Injection Well Array For Fortune Minerals Limited Saskatchewan Metals Processing Plant. *MDH Engineered Solutions*. Retrieved April 01,2018.

Shuster, E. T., & White, W. B. (1971). Seasonal fluctuations in the chemistry of lime-stone springs: A possible means for characterizing carbonate aquifers. *Journal of Hydrology*, *14*(2), 93-128.

Smith, B. A., Hunt, B. B., & Schindel, G. M. (2005). Groundwater flow in the Edwards Aquifer: comparison of groundwater modeling and dye trace results. In *Sinkholes and the Engineering and Environmental Impacts of Karst* (pp. 131-141).

Smith, G. N. (1991). *Geomorphology and geomorphic history of the Konza prairie research natural area, Riley and Geary Counties, Kansas* (Doctoral dissertation, Kansas State University).

Tóth, J. (1962). A theory of groundwater motion in small drainage basins in central Alberta, Canada. *Journal of Geophysical Research*, *67*(11), 4375-4388.

Twiss, P. C. (1991). Chase Group from the near-surface Amoco No. 1 Hargrave core, Riley County, Kansas. In *Midcontinent Core Workshop: Integrated Studies of Petroleum Reservoirs in the Midcontinent: American Association of Petroleum Geologists, Midcontinent Section Meeting, Wichita, Kansas* (pp. 123-141).

Weary, D. J., & Doctor, D. H. (2014). *Karst in the United States: A digital map compilation and database*. US Department of the Interior, US Geological Survey.

Williams, P. W. (2008). The role of the epikarst in karst and cave hydrogeology: a review. *International Journal of Speleology*, *37*(1), 1.

Worthington, S. R. H., Smart, C. C., & Ruland, W. W. (2002). Assessment of groundwater velocities to the municipal wells at Walkerton. *Ground and Water: Theory to Practice*, 1081-1086.

Zeller, D. E. (1968). Stratigraphic succession in Kansas.

## Chapter 3: Future Work

Konza is a well-researched site; however, in general, a lack of research exists in thin limestones (a feature of Konza's geology). Aqueous geochemistry and water level measurement datasets spanning nearly 30 years provided important insight into this study. To more fully understand flow dynamics in thin karst aquifers, future studies should be conducted in aquifers similar to those at Konza. While this study provided understanding into groundwater flow through N04d, there were several questions that were raised from the results of this tracer test.

The findings of this study have direct implications for groundwater remediation. Learning that groundwater can flow in different directions in different aquifers within the same system could be crucial to designing remediation solutions for future environmental contamination in thin limestones. While this study has revealed an important aspect of karst aquifer systems, the dataset is preliminary. A more detailed set of tracer data during a different time of year would help provide a clearer picture of the Konza's aquifer system. Additionally, this study was conducted during the dry season of a dry year in the dry season. In karst aquifers, flow can be different depending how much water is in the aquifer. Tracer tests during a year with greater rain fall would be beneficial to understanding groundwater flow in these aquifers and could potentially provide insight into different flow paths from those discovered in this study.

The results of this study showed that groundwater is leaking through the shales. It would be beneficial to develop methods of determining where shales acting as leaky aquitards and where they act as confining units. Additionally, further study of the causes of leaky shale beds could be important to understand how water or contaminants flow through them.

A consequence of this study being conducted on a diffuse karst system during low flow conditions is that most of the dye still resides in the wells. Some of the dye traveled with the

groundwater, however a great amount of it did not leave the wells. It is unclear how long the dye will linger in the wells and future studies at this site may be impacted by this. Tests should be conducted to determine how long it will take to degrade, or attempt to remove the dye from the wells.

Another very important finding in this study is that groundwater flows north in the Cottonwood limestone. This is only known because a spring that comes out of the Cottonwood contained dye that came from the Morrill and the Eiss limestones. Wells installed in the Cottonwood limestone would help confirm that groundwater actually does flow north in the Cottonwood limestone. Additionally, if these wells were cored, the location of the sinkhole in the Cottonwood could be confirmed.

The majority of the wells used in this project were drilled using air rotary. This methods of well construction does not result in accurate elevation measurements of the rock units that are drilled. Evidence of the error in these measurements was found through the presence of rhodamine in well 4-6M even though the elevation of well 4-6M is higher than well 3-5-1M (injection well). If the elevation of 4-6M were actually higher than 3-5-1M, the dye would not have travelled from 3-5-1M to 4-6M. Though there have been several geophysical studies conducted at this site (unpublished data), it would be valuable to use more geophysical methods to better characterize the fractures and strata at this site. After this study was conducted, some of the geophysical methods that have been used are GPR, NMR, ERT, and borehole NMR. It would be very useful in understanding exact locations of the limestones to conduct a borehole GPR survey that would result in the exact elevation of the limestones being determined. Combining the geophysical data with the tracer data would prove useful in understanding the exact limestone

elevations. These various methods would provide necessary insight to solve unanswered questions from this project.

**Appendix**

Table of contents

Table 1: Charcoal packet results from Ozark Underground Laboratory

| OUL | Station | Station | Date/Time | Date/Time | Fluorescein | | Eosine | | RWT | |
|---|---|---|---|---|---|---|---|---|---|---|
| Number | Number | Name | Placed | Collected | Peak (nm) | Conc (ppb) | Peak (nm) | Conc (ppb) | Peak (nm) | Conc (ppb) |
| C5152 | 1 | 2-1M | 7/28/17 1336 | 8/6/17 1218 | ND | | ND | | ND | |
| C5173 | 1 | 2-1M | 8/6/17 1218 | 8/12/17 1202 | ND | | ND | | ND | |
| C5194 | 1 | 2-1M | 8/12/17 1202 | 8/19/17 1230 | ND | | ND | | ND | |
| C5216 | 1 | 2-1M | 8/19/17 1230 | 8/26/17 1137 | ND | | ND | | ND | |
| C4959 | 1 | 2-1M | 8/26/17 1137 | 9/2/17 1232 | ND | | ND | | ND | |
| C5238 | 1 | 2-1M | 9/2/17 1232 | 9/9/17 1112 | ND | | ND | | ND | |
| C5259 | 1 | 2-1M | 9/9/17 1112 | 9/16/17 1054 | ND | | ND | | ND | |
| C5595 | 1 | 2-1M | 9/16/17 1054 | 9/23/17 1436 | ND | | ND | | ND | |
| C7694 | 1 | 2-1M | 9/23/17 1436 | 9/30/17 1148 | ND | | ND | | ND | |
| C7674 | 1 | 2-1M | 9/30/17 1148 | 10/28/17 1136 | ND | | ND | | ND | |
| C7654 | 1 | 2-1M | 10/28/17 1136 | 12/16/17 1145 | ND | | ND | | ND | |
| C5153 | 2 | 2-5M | 7/28/17 1105 | 8/6/17 0914 | ND | | ND | | ND | |
| C5174 | 2 | 2-5M | 8/6/17 0914 | 8/12/17 0913 | ND | | ND | | ND | |
| C5195 | 2 | 2-5M | 8/12/17 0913 | 8/19/17 0940 | ND | | ND | | ND | |
| C5217 | 2 | 2-5M | 8/19/17 0940 | 8/26/17 0915 | ND | | ND | | ND | |
| C4961 | 2 | 2-5M | 8/26/17 0915 | 9/2/17 0938 | ND | | ND | | ND | |
| C5239 | 2 | 2-5M | 9/2/17 0938 | 9/9/17 0909 | ND | | ND | | ND | |
| C5261 | 2 | 2-5M | 9/9/17 0909 | 9/16/17 0929 | ND | | ND | | ND | |
| C5596 | 2 | 2-5M | 9/16/17 0929 | 9/23/17 1306 | ND | | ND | | ND | |
| C7695 | 2 | 2-5M | 9/23/17 1306 | 9/30/17 0935 | ND | | ND | | ND | |
| C7675 | 2 | 2-5M | 9/30/17 0935 | 10/28/17 0904 | ND | | ND | | ND | |
| C7655 | 2 | 2-5M | 10/28/17 0904 | 12/16/17 1037 | ND | | ND | | ND | |

| | | | | | | | | | | |
|---|---|---|---|---|---|---|---|---|---|---|
| C5154 | 3 | 2-6M | 7/28/17 1130 | 8/6/17 0939 | ND | | ND | | ND | |
| C5175 | 3 | 2-6M | 8/6/17 0935 | 8/12/17 0927 | ND | | ND | | ND | |
| C5196 | 3 | 2-6M | 8/12/17 0927 | 8/19/17 0953 | ND | | ND | | ND | |
| C5218 | 3 | 2-6M | 8/19/17 0953 | 8/26/17 0924 | ND | | ND | | ND | |
| C4962 | 3 | 2-6M | 8/26/17 0924 | 9/2/17 0950 | ND | | ND | | ND | |
| C5241 | 3 | 2-6M | 9/2/17 0950 | 9/9/17 0919 | ND | | ND | | ND | |
| C5262 | 3 | 2-6M | 9/9/17 0919 | 9/16/17 0940 | ND | | ND | | ND | |
| C5597 | 3 | 2-6M | 9/16/17 0940 | 9/23/17 1313 | ND | | ND | | ND | |
| C7696 | 3 | 2-6M | 9/23/17 1313 | 9/30/17 0940 | ND | | ND | | ND | |
| C7676 | 3 | 2-6M | 9/30/17 0940 | 10/28/17 0921 | ND | | ND | | ND | |
| C7656 | 3 | 2-6M | 10/28/17 0921 | 12/16/17 1044 | ND | | ND | | ND | |
| C5155 | 4 | 2-6E | 7/28/17 1125 | 8/6/17 0935 | ND | | ND | | ND | |
| C5176 | 4 | 2-6E | 8/6/17 0935 | 8/12/17 0936 | ND | | ND | | ND | |
| C5197 | 4 | 2-6E | 8/12/17 0936 | 8/19/17 1001 | ND | | ND | | ND | |
| C5219 | 4 | 2-6E | 8/19/17 1001 | 8/26/17 0936 | ND | | ND | | ND | |
| C4963 | 4 | 2-6E | 8/26/17 0936 | 9/2/17 1002 | ND | | ND | | ND | |
| C5242 | 4 | 2-6E | 9/2/17 1002 | 9/9/17 0927 | ND | | ND | | ND | |
| C5263 | 4 | 2-6E | 9/9/17 0927 | 9/16/17 0937 | ND | | ND | | ND | |
| C5598 | 4 | 2-6E | 9/16/17 0937 | 9/23/17 1321 | ND | | ND | | ND | |
| C7697 | 4 | 2-6E | 9/23/17 1321 | 9/30/17 0947 | ND | | ND | | ND | |
| C7677 | 4 | 2-6E | 9/30/17 0947 | 10/28/17 0930 | ND | | ND | | ND | |
| C5156 | 5 | 3-2M | 7/28/17 1320 | 8/6/17 1238 | ND | | ND | | ND | |
| C5177 | 5 | 3-2M | 8/6/17 1238 | 8/12/17 1219 | ND | | ND | | ND | |
| C5198 | 5 | 3-2M | 8/12/17 1219 | 8/19/17 1243 | ND | | ND | | ND | |
| C5221 | 5 | 3-2M | 8/19/17 1243 | 8/26/17 1149 | ND | | ND | | ND | |

| | | | | | | | | | | |
|---|---|---|---|---|---|---|---|---|---|---|
| C4964 | 5 | 3-2M | 8/26/17 1149 | 9/2/17 1250 | ND | | ND | | ND | |
| C5243 | 5 | 3-2M | 9/2/17 1250 | 9/9/17 1129 | ND | | ND | | ND | |
| C5264 | 5 | 3-2M | 9/9/17 1129 | 9/16/17 1101 | ND | | ND | | ND | |
| C5599 | 5 | 3-2M | 9/16/17 1101 | 9/23/17 1445 | ND | | ND | | ND | |
| C7698 | 5 | 3-2M | 9/23/17 1445 | 9/30/17 1156 | ND | | ND | | ND | |
| C7678 | 5 | 3-2M | 9/30/17 1156 | 10/28/17 1144 | ND | | ND | | ND | |
| C7657 | 5 | 3-2M | 10/28/17 1144 | 12/16/17 1154 | ND | | ND | | ND | |
| C5157 | 6 | 3-2E | 7/28/17 1325 | 8/6/17 1230 | ND | | ND | | ND | |
| C5178 | 6 | 3-2E | 8/6/17 1230 | 8/12/17 1228 | ND | | ND | | ND | |
| C5199 | 6 | 3-2E | 8/12/17 1228 | 8/19/17 1248 | ND | | ND | | ND | |
| C5222 | 6 | 3-2E | 8/19/17 1248 | 8/26/17 1156 | ND | | ND | | ND | |
| C4965 | 6 | 3-2E | 8/26/17 1156 | 9/2/17 1305 | ND | | ND | | ND | |
| C5244 | 6 | 3-2E | 9/2/17 1305 | 9/9/17 1138 | ND | | ND | | ND | |
| C5265 | 6 | 3-2E | 9/9/17 1138 | 9/16/17 1104 | ND | | ND | | ND | |
| C5601 | 6 | 3-2E | 9/16/17 1104 | 9/23/17 1450 | ND | | ND | | ND | |
| C7699 | 6 | 3-2E | 9/23/17 1450 | 9/30/17 1202 | ND | | ND | | ND | |
| C7679 | 6 | 3-2E | 9/30/17 1202 | 10/28/17 1150 | ND | | ND | | ND | |
| C7658 | 6 | 3-2E | 10/28/17 1150 | 12/16/17 1157 | ND | | ND | | ND | |
| C5158 | 7 | 3-5M | 7/28/17 1145 | 8/6/17 1025 | ND | | ND | | ND | |
| C5179 | 7 | 3-5M | 8/6/17 1025 | 8/12/17 0948 | ND | | ND | | ND | |
| C5201 | 7 | 3-5M | 8/12/17 0948 | 8/19/17 1012 | ND | | ND | | ND | |
| C5223 | 7 | 3-5M | 8/19/17 1012 | 8/26/17 0943 | ND | | ND | | ND | |
| C4966 | 7 | 3-5M | 8/26/17 0943 | 9/2/17 1012 | ND | | ND | | ND | |
| C5245 | 7 | 3-5M | 9/2/17 1012 | 9/9/17 0935 | ND | | ND | | ND | |
| C5266 | 7 | 3-5M | 9/9/17 0935 | 9/16/17 0957 | ND | | ND | | ND | |

| | | | | | | | | | | |
|---|---|---|---|---|---|---|---|---|---|---|
| C5602 | 7 | 3-5M | 9/16/17 0957 | 9/23/17 1350 | ND | | ND | | ND | |
| C7701 | 7 | 3-5M | 9/23/17 1350 | 9/30/17 0956 | ND | | ND | | ND | |
| C7681 | 7 | 3-5M | 9/30/17 0956 | 10/28/17 0940 | ND | | ND | | ND | |
| C7659 | 7 | 3-5M | 10/28/17 0940 | 12/16/17 1059 | ND | | ND | | ND | |
| C5159 | 8 | 3-6M | 7/28/17 1200 | 8/6/17 1005 | ND | | ND | | ND | |
| C5181 | 8 | 3-6M | 8/6/16 1010 | 8/12/17 1001 | ND | | ND | | ND | |
| C5202 | 8 | 3-6M | 8/12/17 1001 | 8/19/17 1024 | ND | | ND | | ND | |
| C5224 | 8 | 3-6M | 8/19/17 1024 | 8/26/17 0952 | ND | | ND | | ND | |
| C4967 | 8 | 3-6M | 8/26/17 0952 | 9/2/17 1025 | ND | | ND | | ND | |
| C5246 | 8 | 3-6M | 9/2/17 1025 | 9/9/17 0946 | ND | | ND | | ND | |
| C5267 | 8 | 3-6M | 9/9/17 0946 | 9/16/17 1012 | ND | | ND | | ND | |
| C5603 | 8 | 3-6M | 9/16/17 1012 | 9/23/17 1329 | ND | | ND | | ND | |
| C7702 | 8 | 3-6M | 9/23/17 1329 | 9/30/17 1006 | ND | | ND | | ND | |
| C7682 | 8 | 3-6M | 9/30/17 1006 | 10/28/17 0952 | ND | | ND | | ND | |
| C7661 | 8 | 3-6M | 10/28/17 0952 | 12/16/17 1108 | ND | | ND | | ND | |
| C5161 | 9 | 3-6E | 7/28/17 1205 | 8/6/17 1000 | ND | | ND | | ND | |
| C5182 | 9 | 3-6E | 8/6/16 1000 | 8/12/17 1022 | ND | | ND | | ND | |
| C5203 | 9 | 3-6E | 8/12/17 1022 | 8/19/17 1032 | ND | | ND | | ND | |
| C5225 | 9 | 3-6E | 8/19/17 1032 | 8/26/17 1001 | ND | | ND | | ND | |
| C4968 | 9 | 3-6E | 8/26/17 1001 | 9/2/17 1034 | ND | | ND | | ND | |
| C5247 | 9 | 3-6E | 9/2/17 1034 | 9/9/17 0950 | ND | | ND | | ND | |
| C5268 | 9 | 3-6E | 9/9/17 0950 | 9/16/17 1015 | ND | | ND | | ND | |
| C5604 | 9 | 3-6E | 9/16/17 1015 | 9/23/17 1334 | ND | | ND | | ND | |
| C7703 | 9 | 3-6E | 9/23/17 1334 | 9/30/17 1009 | ND | | ND | | ND | |
| C7683 | 9 | 3-6E | 9/30/17 1009 | 10/28/17 0954 | ND | | ND | | ND | |

| | | | | | | | | | | |
|---|---|---|---|---|---|---|---|---|---|---|
| C7662 | 9 | 3-6E | 10/28/17 0954 | 12/16/17 1110 | ND | | ND | | ND | |
| C5162 | 10 | 4-2M | 7/28/17 1300 | 8/6/17 1314 | ND | | ND | | ND | |
| C5183 | 10 | 4-2M | 8/6/16 1314 | 8/12/17 1240 | ND | | ND | | ND | |
| C5204 | 10 | 4-2M | 8/12/17 1240 | 8/19/17 1255 | ND | | ND | | ND | |
| C5226 | 10 | 4-2M | 8/19/17 1255 | 8/26/17 1205 | ND | | ND | | ND | |
| C4969 | 10 | 4-2M | 8/26/17 1205 | 9/2/17 1316 | ND | | ND | | ND | |
| C5248 | 10 | 4-2M | 9/2/17 1316 | 9/9/17 1145 | ND | | ND | | ND | |
| C5269 | 10 | 4-2M | 9/9/17 1145 | 9/16/17 1111 | ND | | ND | | ND | |
| C5605 | 10 | 4-2M | 9/16/17 1111 | 9/23/17 1458 | ND | | ND | | ND | |
| C7704 | 10 | 4-2M | 9/23/17 1458 | 9/30/17 1207 | ND | | ND | | ND | |
| C7684 | 10 | 4-2M | 9/30/17 1207 | 10/28/17 1155 | ND | | ND | | ND | |
| C7663 | 10 | 4-2M | 10/28/17 1155 | 12/16/17 1203 | ND | | ND | | ND | |
| C5163 | 11 | 4-2E2 | 7/28/17 1310 | 8/6/17 1326 | ND | | ND | | ND | |
| C5184 | 11 | 4-2E2 | 8/6/16 1326 | 8/12/17 1256 | ND | | ND | | ND | |
| C5205 | 11 | 4-2E2 | 8/12/17 1256 | 8/19/17 1256 | ND | | ND | | ND | |
| C5227 | 11 | 4-2E2 | 8/19/17 1256 | 8/26/17 1216 | ND | | ND | | ND | |
| C4970 | 11 | 4-2E2 | 8/26/17 1216 | 9/2/17 1327 | ND | | ND | | ND | |
| C5249 | 11 | 4-2E2 | 9/2/17 1327 | 9/9/17 1154 | ND | | ND | | ND | |
| C5270 | 11 | 4-2E2 | 9/9/17 1000 | 9/16/17 1114 | ND | | ND | | ND | |
| C5606 | 11 | 4-2E2 | 9/16/17 1114 | 9/23/17 1507 | ND | | ND | | ND | |
| C7705 | 11 | 4-2E2 | 9/23/17 1507 | 9/30/17 1215 | ND | | ND | | ND | |
| C7685 | 11 | 4-2E2 | 9/30/17 1215 | 10/28/17 1200 | ND | | ND | | ND | |
| C7664 | 11 | 4-2E2 | 10/28/17 1200 | 12/16/17 1207 | ND | | ND | | ND | |
| C5164 | 12 | 4-6M | 7/28/17 1215 | 8/6/17 1042 | 516.2 | 550 | ND | | ND | |
| C5185 | 12 | 4-6M | 8/6/16 1042 | 8/12/17 1034 | 515.2 | 127 | ND | | ND | |

| | | | | | | | | | | |
|---|---|---|---|---|---|---|---|---|---|---|
| C5206 | 12 | 4-6M | 8/12/17 1034 | 8/19/17 1055 | 516.3 | 282,000 | ND | | ND | |
| C5228 | 12 | 4-6M | 8/19/17 1055 | 8/26/17 1008 | 516.5 | 33,600 | ND | | ND | |
| C4971 | 12 | 4-6M | 8/26/17 1008 | 9/2/17 1051 | 516.5 | 17,700 | ND | | ND | |
| C5250 | 12 | 4-6M | 9/2/17 1051 | 9/9/17 1000 | 516.5 | 59,500 | ND | | ND | |
| C5271 | 12 | 4-6M | 9/9/17 1007 | 9/16/17 1025 | 516.4 | 37,300 | ND | | ND | |
| C5607 | 12 | 4-6M | 9/16/17 1025 | 9/23/17 1402 | 516.2 | 2,600 | ND | | 568.0 ** | 4.43 |
| C7706 | 12 | 4-6M | 9/23/17 1402 | 9/30/17 1019 | 516.3 | 3,700 | ND | | ND | |
| C7686 | 12 | 4-6M | 9/30/17 1019 | 10/28/17 1001 | 516.0 | 2,380 | ND | | 567.2 | 165 |
| C7665 | 12 | 4-6M | 10/28/17 1001 | 12/16/17 1119 | 516.2 | 5,540 | ND | | 566.6 | 1,010 |
| C5207 | 13 | 4-6E1 | 8/12/17 1044 | 8/19/17 1105 | 514.9 | 1.01 | ND | | ND | |
| C5229 | 13 | 4-6E1 | 8/19/17 1105 | 8/26/17 1016 | 515.3 | 0.501 | ND | | ND | |
| C4972 | 13 | 4-6E1 | 8/26/17 1016 | 9/2/17 1103 | ND | 0 | ND | | ND | |
| C5251 | 13 | 4-6E1 | 9/2/17 1103 | 9/9/17 1007 | 515.0 | 0.256 | ND | | ND | |
| C5272 | 13 | 4-6E1 | 9/9/17 1246 | 9/16/17 1033 | 515.6 | 0.488 | ND | | ND | |
| C5608 | 13 | 4-6E1 | 9/16/17 1033 | 9/23/17 1412 | 515.8 | 7.93 | ND | | ND | |
| C7707 | 13 | 4-6E1 | 9/23/17 1412 | 9/30/17 1025 | 515.9 | 20.3 | ND | | ND | |
| C7687 | 13 | 4-6E1 | 9/30/17 1025 | 10/28/17 1013 | 515.9 | 343 | ND | | ND | |
| C7666 | 13 | 4-6E1 | 10/28/17 1013 | 12/16/17 1126 | 516.2 | 969 | ND | | ND | |
| C5165 | 14 | Morrill 1 | 7/28/17 0900 | 8/6/17 1455 | 515.2 | 2.14 | ND | | ND | |
| C5186 | 14 | Morrill 1 | 8/6/16 1455 | 8/12/17 1405 | 515.7 | 37.9 | ND | | ND | |
| C5208 | 14 | Morrill 1 | 8/12/17 1405 | 8/19/17 1414 | 515.4 | 45.0 | ND | | ND | |
| C5230 | 14 | Morrill 1 | 8/19/17 1414 | 8/26/17 1308 | 515.3 | 42.2 | ND | | ND | |
| C4973 | 14 | Morrill 1 | 8/26/17 1308 | 9/2/17 1435 | 515.8 | 17.9 | ND | | ND | |
| C5252 | 14 | Morrill 1 | 9/2/17 1435 | 9/9/17 1246 | 515.5 | 1.84 | ND | | ND | |
| C5273 | 14 | Morrill 1 | 9/9/17 1242 | 9/16/17 1155 | ND | 0 | ND | | ND | |

| | | | | | | | | | | |
|---|---|---|---|---|---|---|---|---|---|---|
| C5609 | 14 | Morrill 1 | 9/16/17 1155 | 9/23/17 1610 | ND | 0 | ND | | ND | |
| C7708 | 14 | Morrill 1 | 9/23/17 1610 | 9/30/17 1254 | ND | 0 | ND | | ND | |
| C7688 | 14 | Morrill 1 | 9/30/17 1254 | 10/28/17 1235 | 515.4 | 1.03 | ND | | ND | |
| C7667 | 14 | Morrill 1 | 10/28/17 1235 | 12/16/17 1237 | ND | 0 | ND | | ND | |
| C5166 | 15 | Morrill 2 | 7/28/17 0907 | 8/6/17 1439 | 515.4 | 2.77 | ND | | ND | |
| C5187 | 15 | Morrill 2 | 8/6/16 1439 | 8/12/17 1358 | 515.4 | 55.7 | ND | | ND | |
| C5209 | 15 | Morrill 2 | 8/12/17 1358 | 8/19/17 1406 | 515.4 | 73.3 | ND | | ND | |
| C5231 | 15 | Morrill 2 | 8/19/17 1406 | 8/26/17 1304 | 515.3 | 59.1 | ND | | ND | |
| C4974 | 15 | Morrill 2 | 8/26/17 1304 | 9/2/17 1424 | 515.6 | 29.0 | ND | | ND | |
| C5253 | 15 | Morrill 2 | 9/2/17 1424 | 9/9/17 1242 | 515.4 | 5.98 | ND | | ND | |
| C5274 | 15 | Morrill 2 | 9/9/17 1242 | 9/16/17 1153 | ND | 0 | ND | | ND | |
| C5610 | 15 | Morrill 2 | 9/16/17 1153 | 9/23/17 1606 | ND | 0 | ND | | ND | |
| C7709 | 15 | Morrill 2 | 9/23/17 1606 | 9/30/17 1251 | ND | 0 | ND | | ND | |
| C7668 | 15 | Morrill 2 | 10/28/17 1233 | 12/16/17 1235 | ND | 0 | ND | | ND | |
| C5167 | 16 | Morrill 3 | 7/28/17 0912 | 8/6/17 1433 | 515.8 | 9.02 | ND | | ND | |
| C5188 | 16 | Morrill 3 | 8/6/16 1433 | 8/12/17 1350 | 515.8 | 101 | ND | | ND | |
| C5210 | 16 | Morrill 3 | 8/12/17 1350 | 8/19/17 1404 | 515.2 | 238 | ND | | ND | |
| C5232 | 16 | Morrill 3 | 8/19/17 1404 | 8/26/17 1258 | 515.4 | 163 | ND | | ND | |
| C4975 | 16 | Morrill 3 | 8/26/17 1258 | 9/2/17 1417 | 515.8 | 173 | ND | | ND | |
| C5254 | 16 | Morrill 3 | 9/2/17 1417 | 9/9/17 1238 | 515.5 | 26.5 | ND | | ND | |
| C5275 | 16 | Morrill 3 | 9/9/17 1238 | 9/16/17 1151 | ND | 0 | ND | | ND | |
| C5611 | 16 | Morrill 3 | 9/16/17 1151 | 9/23/17 1602 | ND | 0 | ND | | ND | |
| C7710 | 16 | Morrill 3 | 9/23/17 1602 | 9/30/17 1248 | ND | 0 | ND | | ND | |
| C7689 | 16 | Morrill 3 | 9/30/17 1248 | 10/28/17 1230 | 515.6 | 3.23 | ND | | ND | |
| C7669 | 16 | Morrill 3 | 10/28/17 1230 | 12/16/17 1233 | ND | 0 | ND | | ND | |

| | | | | | | | | | | |
|---|---|---|---|---|---|---|---|---|---|---|
| | | Eiss 1 | | 7/28/17 0000 | 0 | 0 | | | | |
| C5168 | 17 | Eiss 1 | 7/28/17 0925 | 8/6/17 1412 | 515.7 | 86.9 | ND | | ND | |
| C5189 | 17 | Eiss 1 | 8/6/17 1412 | 8/12/17 1337 | 515.5 | 205 | ND | | ND | |
| C5211 | 17 | Eiss 1 | 8/12/17 1337 | 8/19/17 1353 | 516.2 | 678 | ND | | ND | |
| C5233 | 17 | Eiss 1 | 8/19/17 1353 | 8/26/17 1250 | 516.5 | 1,080 | ND | | ND | |
| C4976 | 17 | Eiss 1 | 8/26/17 1250 | 9/2/17 1408 | 516.4 | 520 | ND | | ND | |
| C5255 | 17 | Eiss 1 | 9/2/17 1408 | 9/9/17 1231 | 515.4 | 226 | ND | | ND | |
| C5276 | 17 | Eiss 1 | 9/9/17 1231 | 9/16/17 1145 | 515.0 | 30.2 | ND | | ND | |
| C5612 | 17 | Eiss 1 | 9/16/17 1145 | 9/23/17 1548 | 515.4 | 93.5 | ND | | ND | |
| C7711 | 17 | Eiss 1 | 9/23/17 1548 | 9/30/17 1241 | 515.7 | 9.86 | ND | | ND | |
| C7690 | 17 | Eiss 1 | 9/30/17 1241 | 10/28/17 1225 | 515.6 | 113 | ND | | ND | |
| C7670 | 17 | Eiss 1 | 10/28/17 1225 | 12/16/17 1229 | 515.6 | 114 | ND | | ND | |
| C5169 | 18 | Eiss 2 | 7/28/17 0937 | 8/6/17 1406 | ND | | ND | | ND | |
| C5190 | 18 | Eiss 2 | 8/6/17 1406 | 8/12/17 1328 | ND | | ND | | ND | |
| C5212 | 18 | Eiss 2 | 8/12/17 1328 | 8/19/17 1343 | ND | | ND | | ND | |
| C5234 | 18 | Eiss 2 | 8/19/17 1343 | 8/26/17 1242 | ND | | ND | | ND | |
| C4977 | 18 | Eiss 2 | 8/26/17 1242 | 9/2/17 1402 | ND | | ND | | ND | |
| C5256 | 18 | Eiss 2 | 9/2/17 1402 | 9/9/17 1226 | ND | | ND | | ND | |
| C5277 | 18 | Eiss 2 | 9/9/17 1226 | 9/16/17 1138 | ND | | ND | | ND | |
| C5613 | 18 | Eiss 2 | 9/16/17 1138 | 9/23/17 1540 | ND | | ND | | ND | |
| C7712 | 18 | Eiss 2 | 9/23/17 1540 | 9/30/17 1235 | ND | | ND | | ND | |
| C7691 | 18 | Eiss 2 | 9/30/17 1235 | 10/28/17 1221 | ND | | ND | | ND | |
| C7671 | 18 | Eiss 2 | 10/28/17 1221 | 12/16/17 1223 | ND | | ND | | ND | |
| C5170 | 19 | Eiss 3 | 7/28/17 0943 | 8/6/17 1354 | ND | | ND | | ND | |
| C5191 | 19 | Eiss 3 | 8/6/17 1354 | 8/12/17 1318 | ND | | ND | | ND | |

| | | | | | | | | | | |
|---|---|---|---|---|---|---|---|---|---|---|
| C5213 | 19 | Eiss 3 | 8/12/17 1318 | 8/19/17 1329 | ND | | ND | | ND | |
| C5235 | 19 | Eiss 3 | 8/19/17 1329 | 8/26/17 1235 | ND | | ND | | ND | |
| C4978 | 19 | Eiss 3 | 8/26/17 1235 | 9/2/17 1353 | ND | | ND | | ND | |
| C5257 | 19 | Eiss 3 | 9/2/17 1353 | 9/9/17 1216 | ND | | ND | | ND | |
| C5278 | 19 | Eiss 3 | 9/9/17 1216 | 9/16/17 1132 | ND | | ND | | ND | |
| C5614 | 19 | Eiss 3 | 9/16/17 1132 | 9/23/17 1529 | ND | | ND | | ND | |
| C7713 | 19 | Eiss 3 | 9/23/17 1529 | 9/30/17 1228 | ND | | ND | | ND | |
| C7692 | 19 | Eiss 3 | 9/30/17 1228 | 10/28/17 1214 | ND | | ND | | ND | |
| C7672 | 19 | Eiss 3 | 10/28/17 1214 | 12/16/17 1218 | ND | | ND | | ND | |
| C5171 | 20 | Upstream | 7/28/17 0955 | 8/6/17 1344 | ND | | ND | | ND | |
| C5192 | 20 | Upstream | 8/6/17 1344 | 8/12/17 1311 | ND | | ND | | ND | |
| C5214 | 20 | Upstream | 8/12/17 1311 | 8/19/17 1321 | ND | | ND | | ND | |
| C5236 | 20 | Upstream | 8/19/17 1321 | 8/26/17 1226 | ND | | ND | | ND | |
| C4979 | 20 | Upstream | 8/26/17 1226 | 9/2/17 1342 | ND | | ND | | ND | |
| C5172 | 21 | Downstream | 7/28/17 1015 | 8/6/17 1514 | ND | 0 | 541.2 | 88.2 | ND | 0 |
| C5193 | 21 | Downstream | 8/6/17 1514 | 8/12/17 1417 | ND | 0 | 541.2 | 152 | ND | 0 |
| C5215 | 21 | Downstream | 8/12/17 1417 | 8/19/17 1432 | ND | 0 | 541.4 | 27.2 | ND | 0 |
| C5237 | 21 | Downstream | 8/19/17 1432 | 8/26/17 1320 | 515.2 * | 0.940 | 541.0 | 11.5 | ND | 0 |
| C4981 | 21 | Downstream | 8/26/17 1320 | 9/2/17 1450 | 516.0 | 1.36 | 541.0 | 4.06 | ND | 0 |
| C5258 | 21 | Downstream | 9/2/17 1450 | 9/9/17 1252 | 518.4 | 0.659 | 541.4 | 1.93 | 567.2 * | 0.918 |
| C5279 | 21 | Downstream | 9/9/17 1252 | 9/16/17 1200 | 517.4 | 0.665 | 540.4 | 1.90 | 565.2 | 2.61 |
| C5615 | 21 | Downstream | 9/16/17 1200 | 9/23/17 1621 | 519.2 | 1.51 | 539.4 | 1.95 | 566.0 | 3.11 |

| | | | | | | | | | | |
|---|---|---|---|---|---|---|---|---|---|---|
| C7714 | 21 | Downstream | 9/23/17 1621 | 9/30/17 1258 | ND | | ND | | ND | |
| C7693 | 21 | Downstream | 9/30/17 1258 | 10/28/17 1240 | 518.4 | 0.251 | 541.0 | 0.729 | ND | |
| C7673 | 21 | Downstream | 10/28/17 1240 | 12/16/17 1242 | 519.8 ** | 0.512 | 538.2 | 1.20 | 560.0 * | 2.30 |
| C5616 | | Morrill 1 - Roots | NDT | 9/23/17 NT | ND | | ND | | ND | |

Table 2: Water sample results from Ozark Underground Laboratory

| OUL Number | Station Number | Station Name | Date/Time Collected | Fluorescein | | Eosine | | RWT | |
|---|---|---|---|---|---|---|---|---|---|
| | | | | Peak (nm) | Conc (ppb) | Peak (nm) | Conc (ppb) | Peak (nm) | Conc (ppb) |
| C5383 | 10 | 4-2M | 8/19/17 1255 | ND | | ND | | ND | |
| C5371 | 12 | 4-6M | 8/6/17 1042 | 507.4 | 335 | ND | | ND | 0 |
| C5376 | 12 | 4-6M | 8/12/17 1034 | 508.1 | 11.8 | ND | | 573.8 | 0.325 |
| C5384 | 12 | 4-6M | 8/19/17 1055 | 507.5 | 41.0 | ND | | 573.7 | 5.74 |
| C5392 | 12 | 4-6M | 8/26/17 1008 | 508.0 | 4.43 | ND | | 573.7 | 16.5 |
| C4998 | 12 | 4-6M | 9/2/17 1051 | 508.2 | 6.50 | ND | | 574.0 | 30.6 |
| C5399 | 12 | 4-6M | 9/9/17 1000 | 507.9 | 11.3 | ND | | 573.7 | 42.9 |
| C5404 | 12 | 4-6M | 9/16/17 1025 | 507.8 | 10.2 | ND | | 573.7 | 59.7 |
| C5693 | 12 | 4-6M | 9/23/17 1402 | 507.8 | 2.43 | ND | | 573.6 | 74.6 |
| C7742 | 12 | 4-6M | 9/30/17 1019 | 507.9 | 2.34 | ND | | 573.8 | 68.5 |
| C7736 | 12 | 4-6M | 10/28/17 1001 | 507.5 | 89.4 | ND | | 573.7 | 59.4 |
| C7731 | 12 | 4-6M | 12/16/17 1119 | 508.0 | 3.83 | ND | | 573.7 | 60.0 |
| **C5588** | **13** | **4-6E1** | **8/12/17 1044** | **ND** | | **ND** | | **ND** | |
| C5385 | 13 | 4-6E1 | 8/19/17 1105 | ND | | ND | | ND | |
| C5393 | 13 | 4-6E1 | 8/26/17 1016 | ND | | ND | | ND | |
| C5401 | 13 | 4-6E1 | 9/9/17 1007 | ND | | ND | | ND | |
| C5405 | 13 | 4-6E1 | 9/16/17 1033 | 508.4 | 0.041 | ND | | ND | |
| C5694 | 13 | 4-6E1 | 9/23/17 1412 | 507.8 | 0.307 | ND | | ND | |
| C7775 | 13 | 4-6E1 | **9/30/17 1025** | 507.7 | 2.23 | ND | | ND | |
| C7737 | 13 | 4-6E1 | 10/28/17 1013 | 509.4 | 1.84 | ND | | ND | |
| C7732 | 13 | 4-6E1 | 12/16/17 1126 | 507.5 | 53.8 | ND | | ND | |
| **C5372** | **14** | **Morrill 1** | **8/6/17 1455** | **509.0** | **0.157** | **ND** | | **ND** | |
| C5377 | 14 | Morrill 1 | 8/12/17 1405 | 507.9 | 0.146 | ND | | ND | |

| | | | | | | | | | |
|---|---|---|---|---|---|---|---|---|---|
| C5386 | 14 | Morrill 1 | 8/19/17 1414 | 507.0 | 0.017 | ND | | ND | |
| C5394 | 14 | Morrill 1 | 8/26/17 1308 | 509.6 | 0.174 | ND | | ND | |
| C4999 | 14 | Morrill 1 | 9/2/17 1435 | 507.8 | 0.085 | ND | | ND | |
| **C5373** | **15** | **Morrill 2** | **8/6/17 1439** | **508.0** | **0.179** | **ND** | | **ND** | |
| C5378 | 15 | Morrill 2 | 8/12/17 1358 | 508.2 | 0.220 | ND | | ND | |
| C5387 | 15 | Morrill 2 | 8/19/17 1406 | 507.8 | 0.186 | ND | | ND | |
| C5395 | 15 | Morrill 2 | 8/26/17 1304 | 508.0 | 0.187 | ND | | ND | |
| C5001 | 15 | Morrill 2 | 9/2/17 1424 | 508.2 | 0.114 | ND | | ND | |
| **C5374** | **16** | **Morrill 3** | **8/6/17 1433** | **508.4** | **0.177** | **ND** | | **ND** | |
| C5379 | 16 | Morrill 3 | 8/12/17 1350 | 508.2 | 0.304 | ND | | ND | |
| C5388 | 16 | Morrill 3 | 8/19/17 1404 | 508.2 | 0.370 | ND | | ND | |
| C5396 | 16 | Morrill 3 | 8/26/17 1258 | 508.2 | 0.558 | ND | | ND | |
| C5002 | 16 | Morrill 3 | 9/2/17 1417 | 508.2 | 0.292 | ND | | ND | |
| **C5381** | **17** | **Eiss 1** | **8/12/17 1337** | **508.0** | **2.18** | **ND** | | **ND** | |
| C5389 | 17 | Eiss 1 | 8/19/17 1353 | 508.0 | 7.24 | ND | | ND | |
| C5397 | 17 | Eiss 1 | 8/26/17 1250 | 507.8 | 4.13 | ND | | ND | |
| C5003 | 17 | Eiss 1 | 9/2/17 1408 | 507.7 | 2.84 | ND | | ND | |
| C5402 | 17 | Eiss 1 | 9/9/17 1231 | 508.0 | 1.03 | ND | | ND | |
| C5406 | 17 | Eiss 1 | 9/16/17 1145 | 507.8 | 1.53 | ND | | ND | |
| C5695 | 17 | Eiss 1 | 9/23/17 1548 | 507.4 | 0.658 | ND | | ND | |
| C7743 | 17 | Eiss 1 | 9/30/17 1241 | 508.4 | 0.318 | ND | | ND | |
| C7738 | 17 | Eiss 1 | 10/28/17 1225 | 507.8 | 11.7 | ND | | ND | |
| C7733 | 17 | Eiss 1 | 12/16/17 1229 | 508.6 | 0.147 | ND | | ND | |
| **C5390** | **19** | **Eiss 3** | **8/19/17 1329** | **ND** | | **ND** | | **ND** | |
| **C5696** | **20** | **Upstream** | **9/23/17 1523** | **ND** | | **ND** | | **ND** | |
| C7744 | 20 | Upstream | 9/30/17 1226 | ND | | ND | | ND | |
| C7739 | 20 | Upstream | 10/28/17 1207 | ND | | ND | | ND | |
| C7734 | 20 | Upstream | 12/16/17 1215 | ND | | ND | | ND | |
| **C5375** | **21** | **Downstream** | **8/6/17 1514** | **ND** | | **534.7** | **39.7** | **ND** | |
| C5382 | 21 | Downstream | 8/12/17 1417 | ND | | 534.8 | 0.193 | ND | |
| C5391 | 21 | Downstream | 8/19/17 1432 | 512.2 (1) | 0.009 | 534.0 | 0.057 | ND | |
| C5398 | 21 | Downstream | 8/26/17 1320 | 511.4 * | 0.029 | 531.0 (1) | 0.157 | ND | |
| C5004 | 21 | Downstream | 9/2/17 1450 | 508.8 (1) | 0.013 | ND | | ND | |

| | | | | | | | | | |
|---|---|---|---|---|---|---|---|---|---|
| C5403 | 21 | Downstream | 9/9/17 1252 | ND | | ND | | ND | |
| C5407 | 21 | Downstream | 9/16/17 1200 | 508.2 (1) | 0.019 | ND | | ND | |
| C5697 | 21 | Downstream | 9/23/17 1621 | 506.8 | 0.048 | 534.2 | 0.168 | ND | |
| C7745 | 21 | Downstream | 9/30/17 1258 | ND | | 534.0 | 0.104 | ND | |
| C7741 | 21 | Downstream | 10/28/17 1240 | ND | | ND | | ND | |
| C7735 | 21 | Downstream | 12/16/17 1242 | ND | | ND | | ND | |
| **C5408** | | **Background** | **7/29/17 NT** | **ND** | | **ND** | | **ND** | |

## Dye break through curves

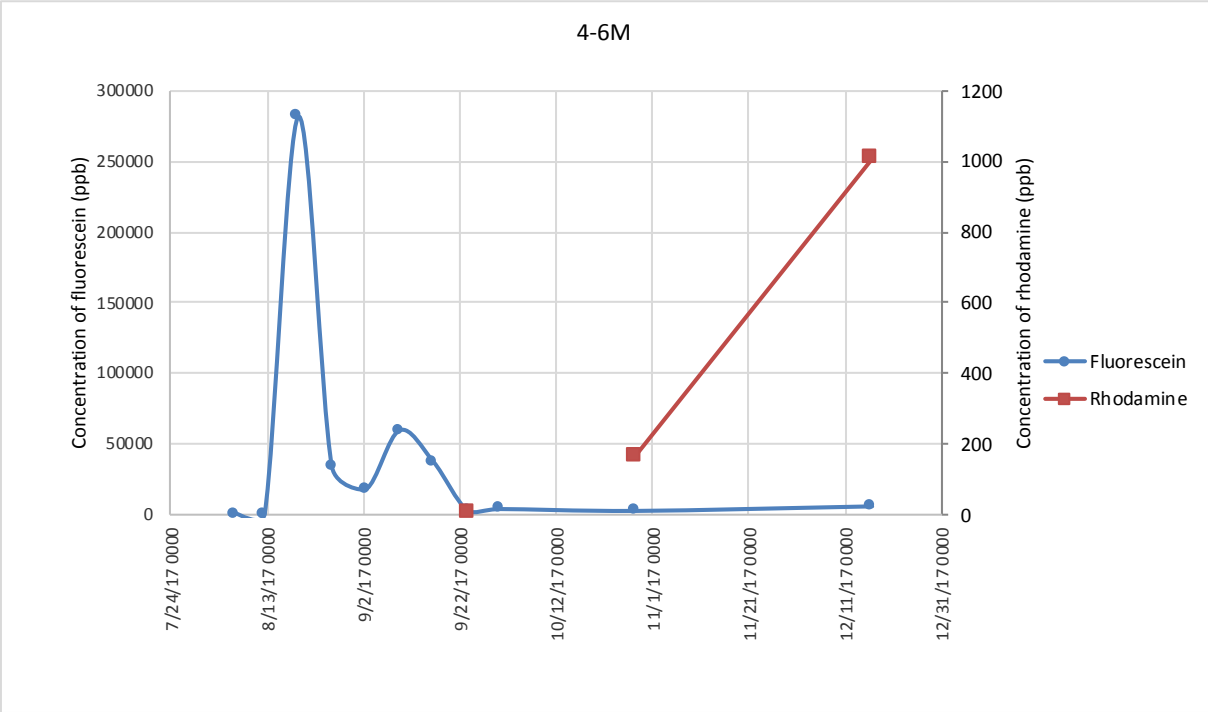


Figure 1 Dye break through curve from well 4-6M

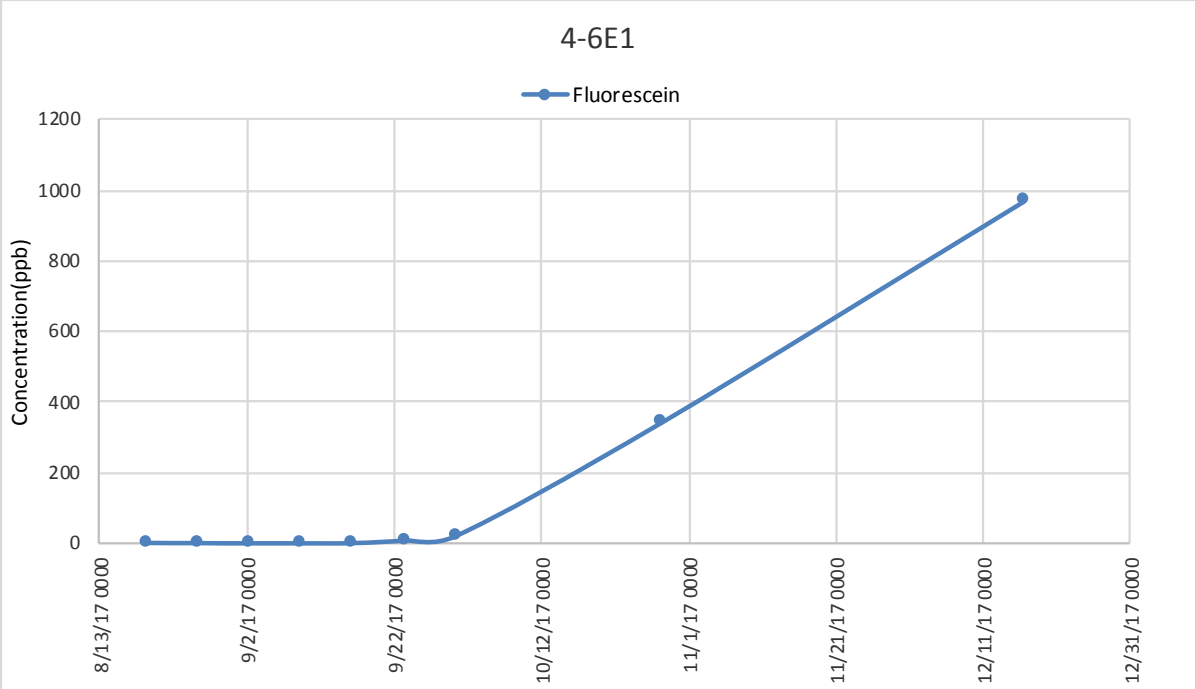


Figure 2 Dye break through curve from well 4-6E1

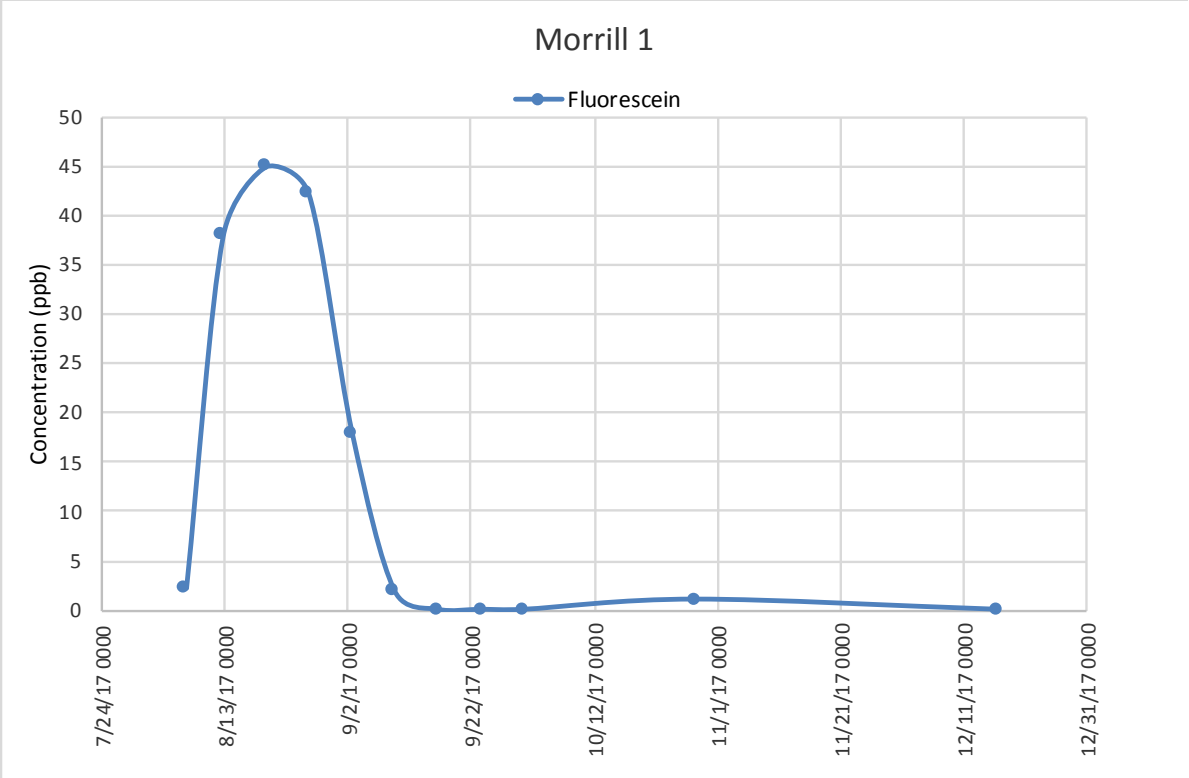


Figure 4 Dye break through curve from stream site Morrill 1

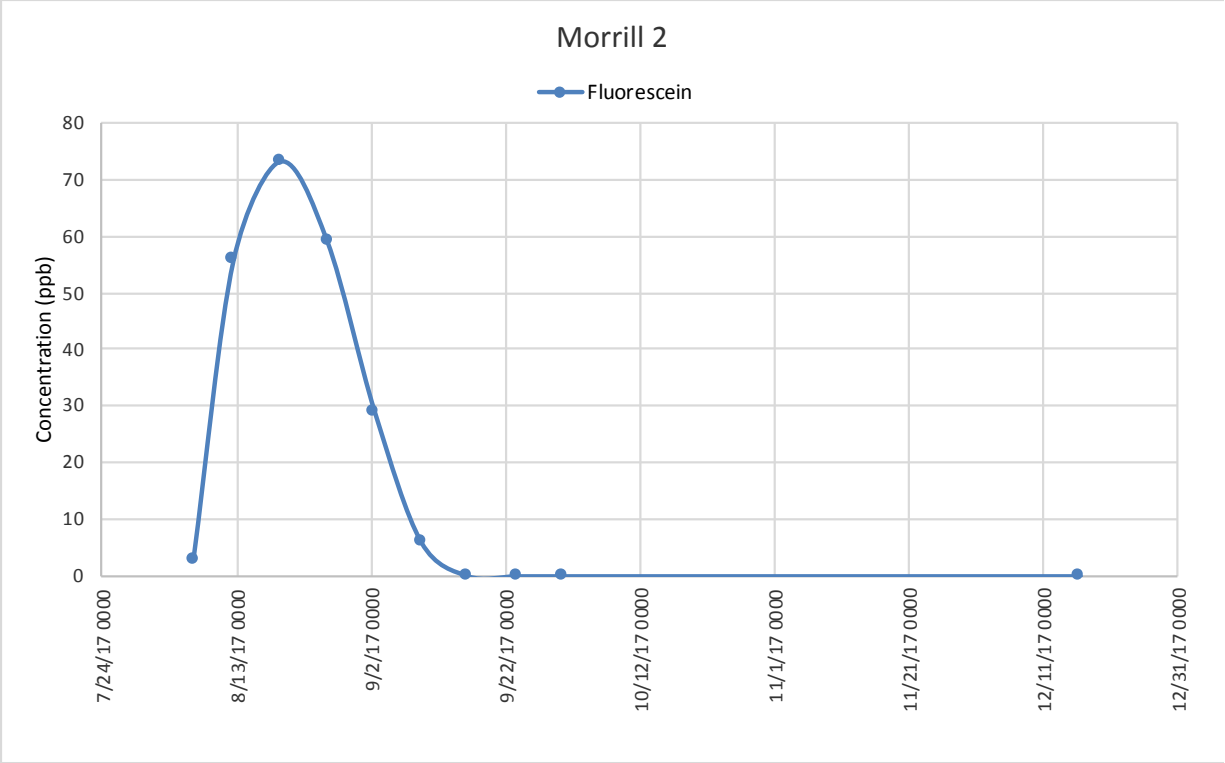


Figure 5 Dye break through curve from stream site Morrill 2


Figure 6 Dye break through curve from stream site Morrill 3

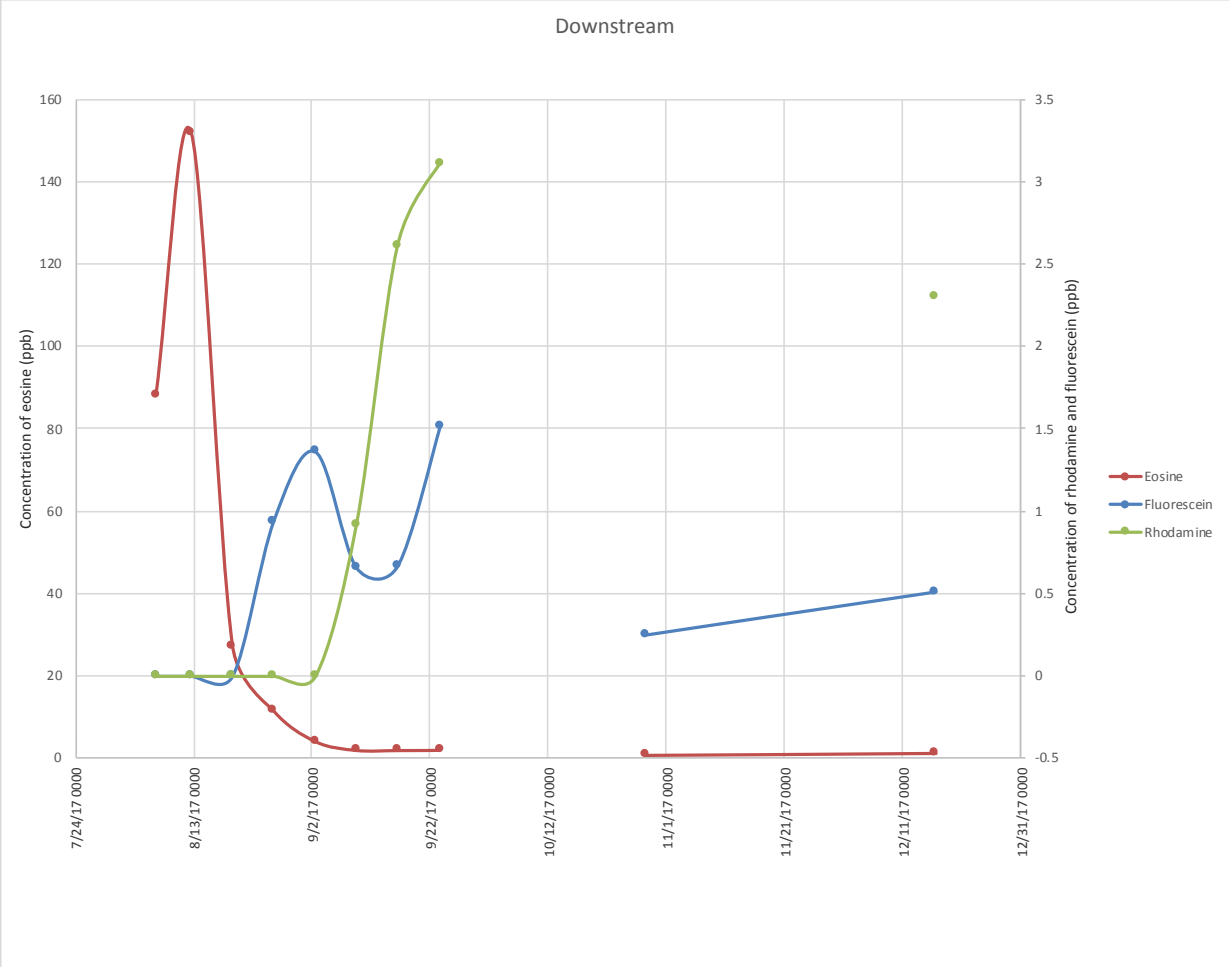


Figure 7 Dye break through curve from stream site “downstream”

## Water sample break through curves

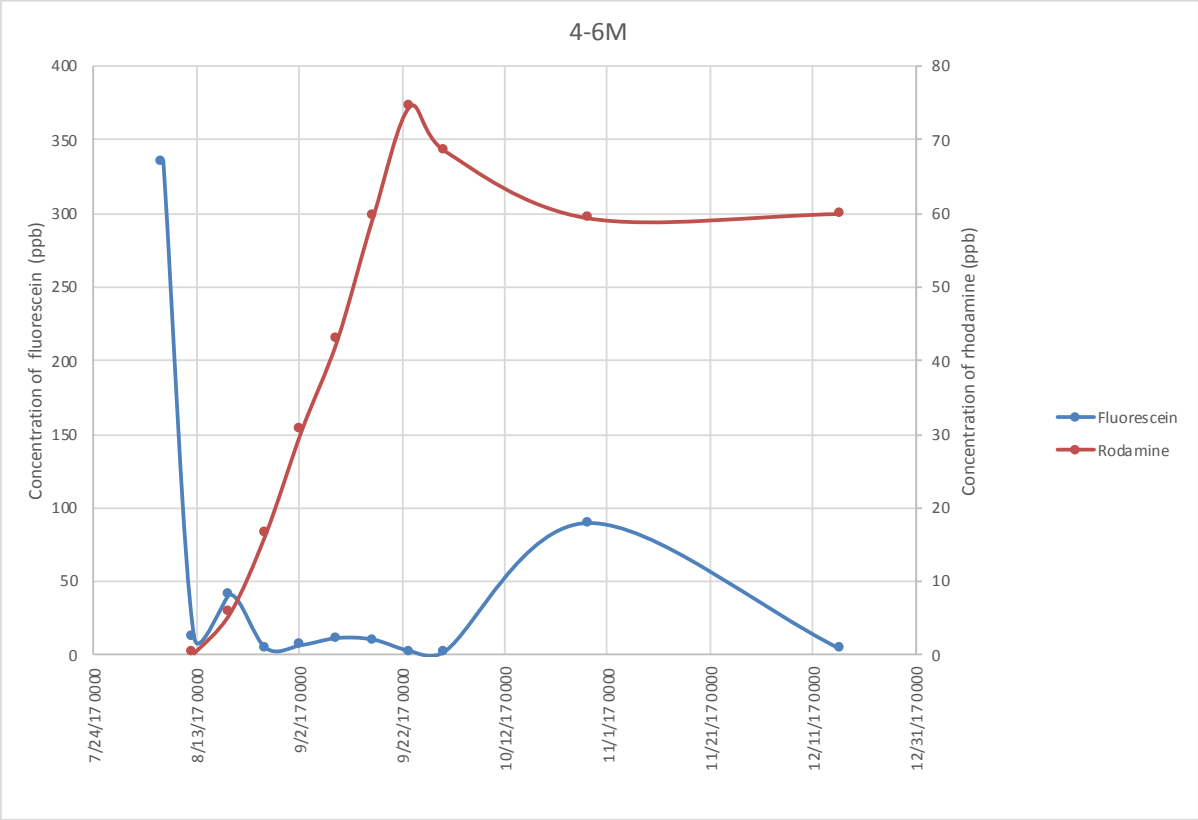


Figure 8 Dye break through curve from well 4-6M

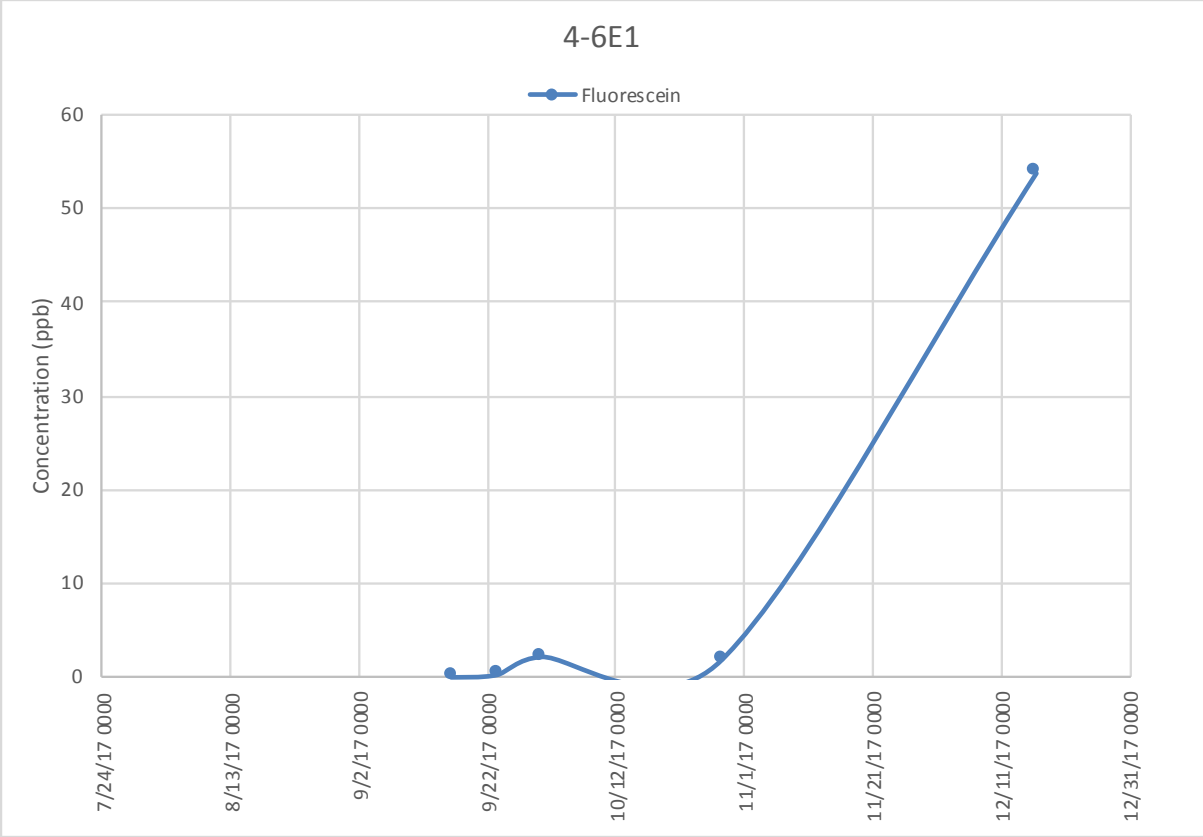


Figure 9 Dye break through curve from well 4-6E1

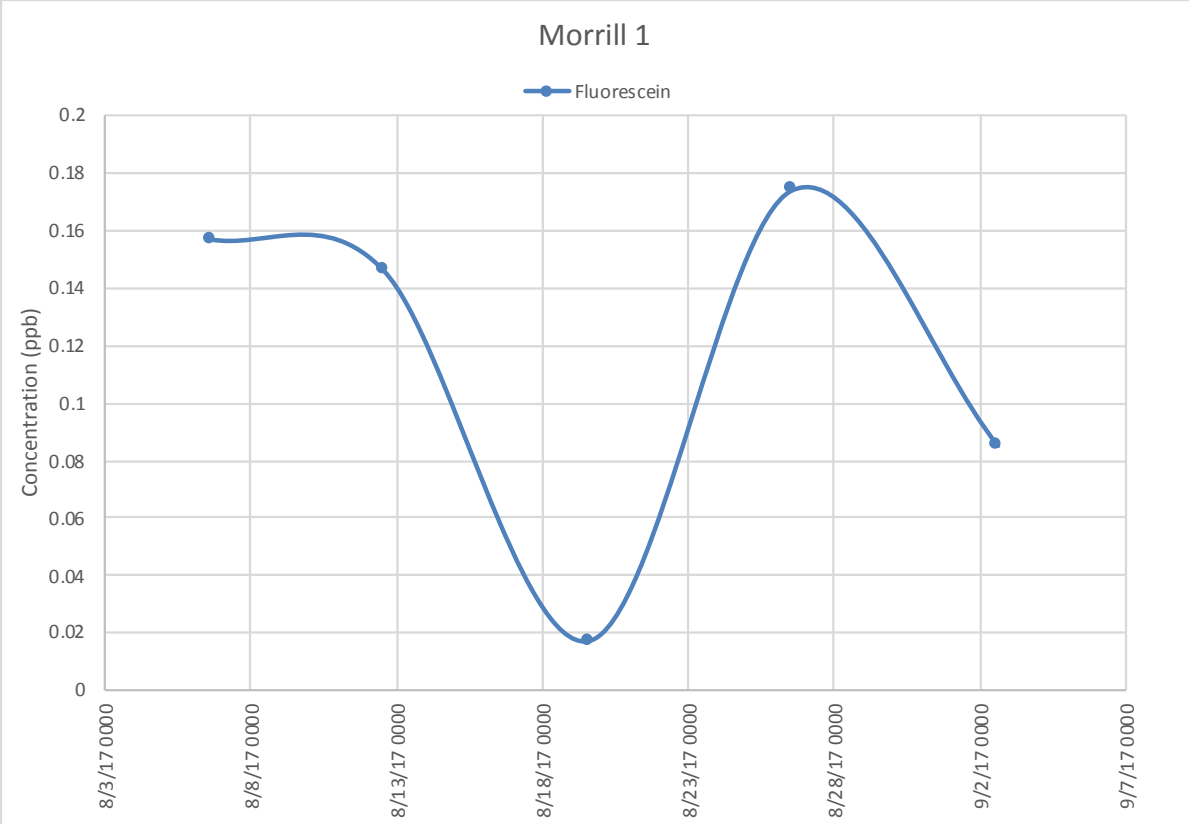


Figure 10 Dye break through curve from stream site Morrill 1

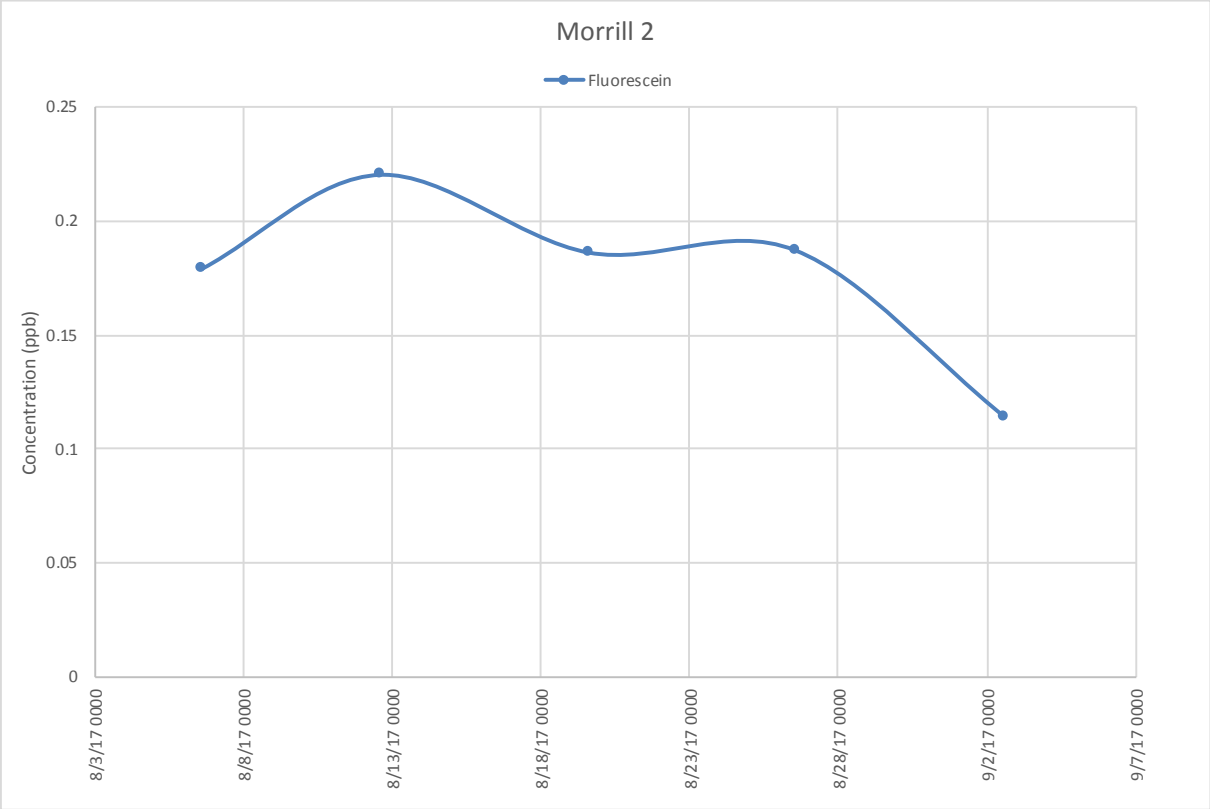


Figure 11 Dye break through curve from stream site Morrill 2

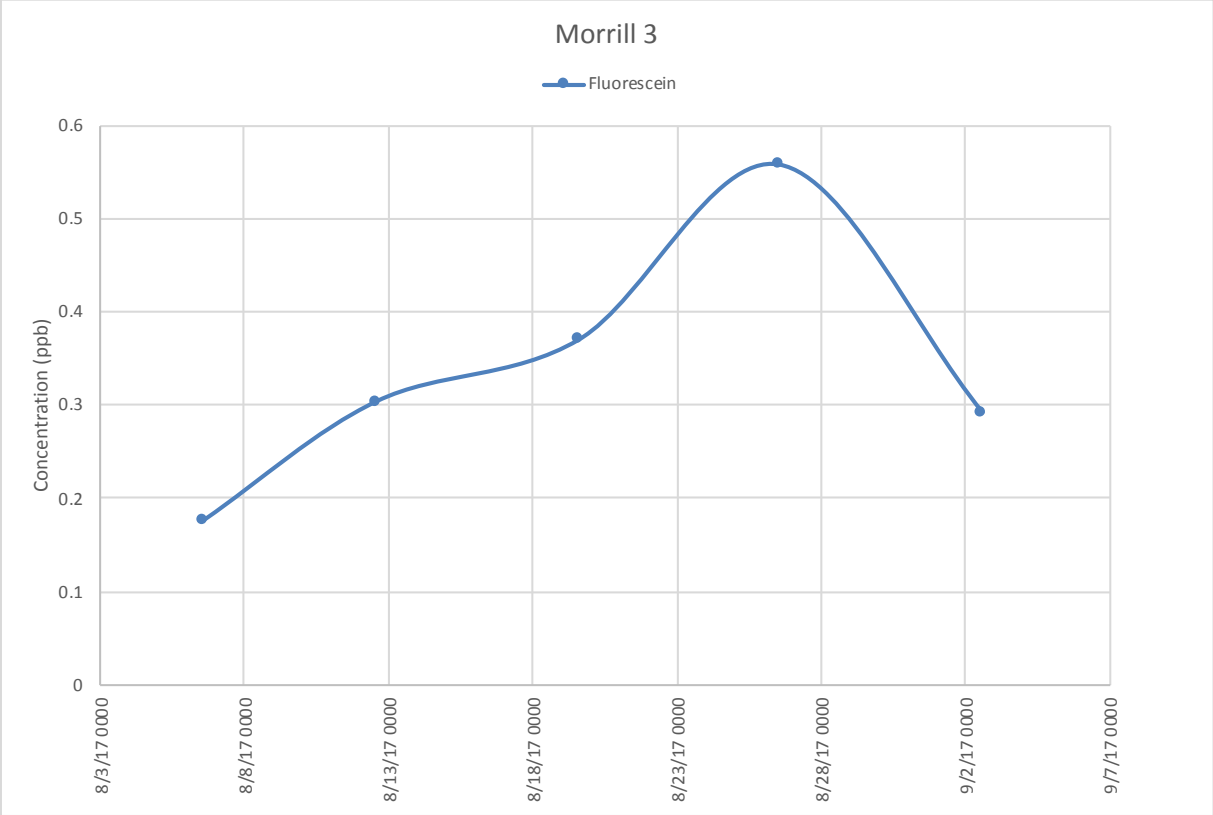


Figure 12 Dye break through curve from stream site Morrill 3

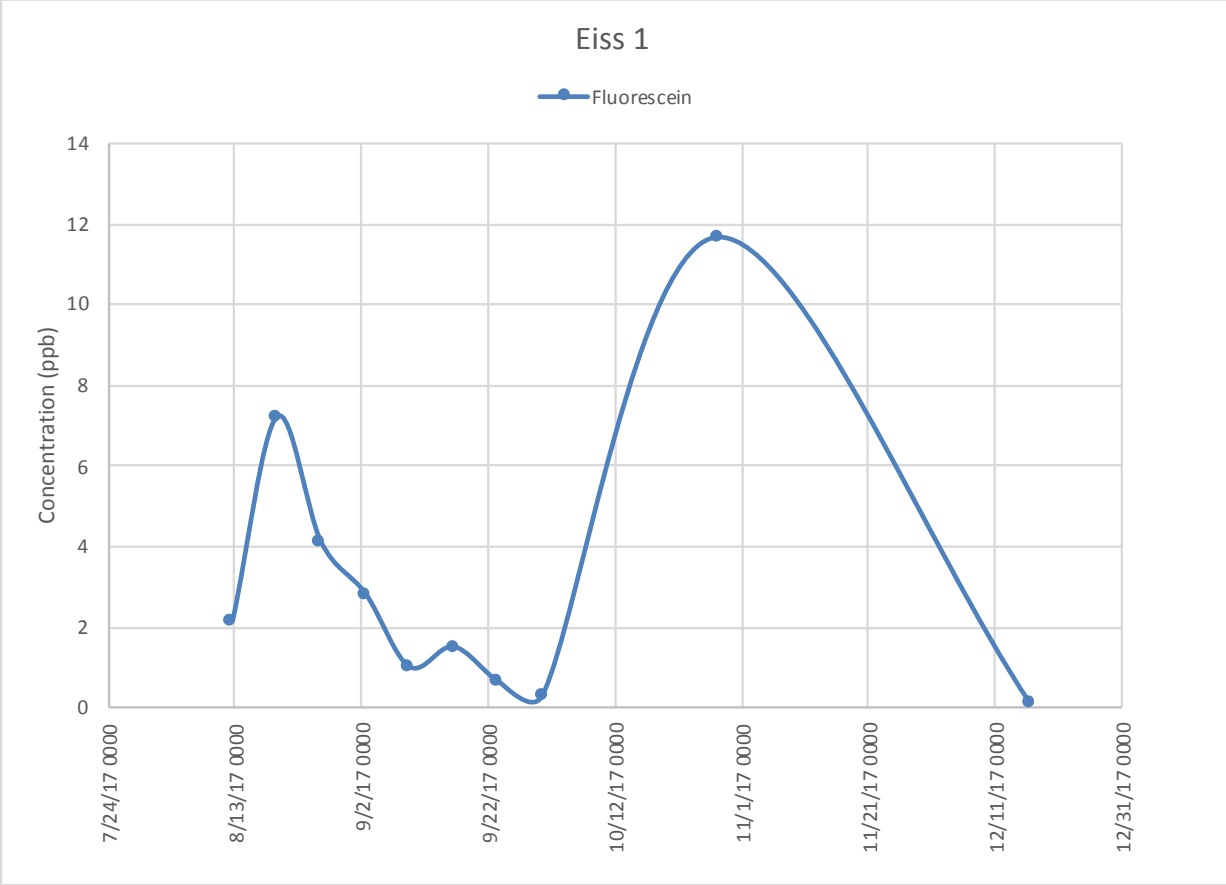


Figure 13 Dye break through curve from stream site Eiss 1

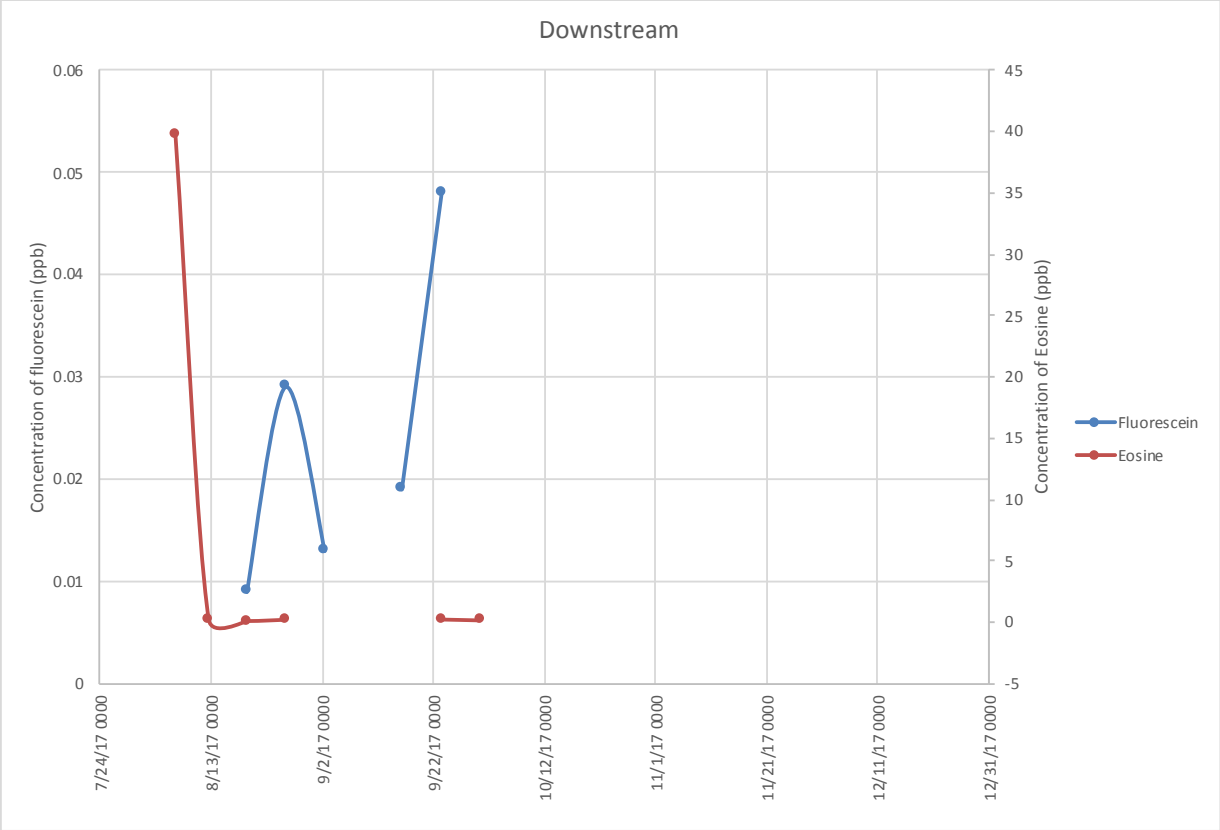


Figure 14 Dye break through curve from stream site “Downstream”

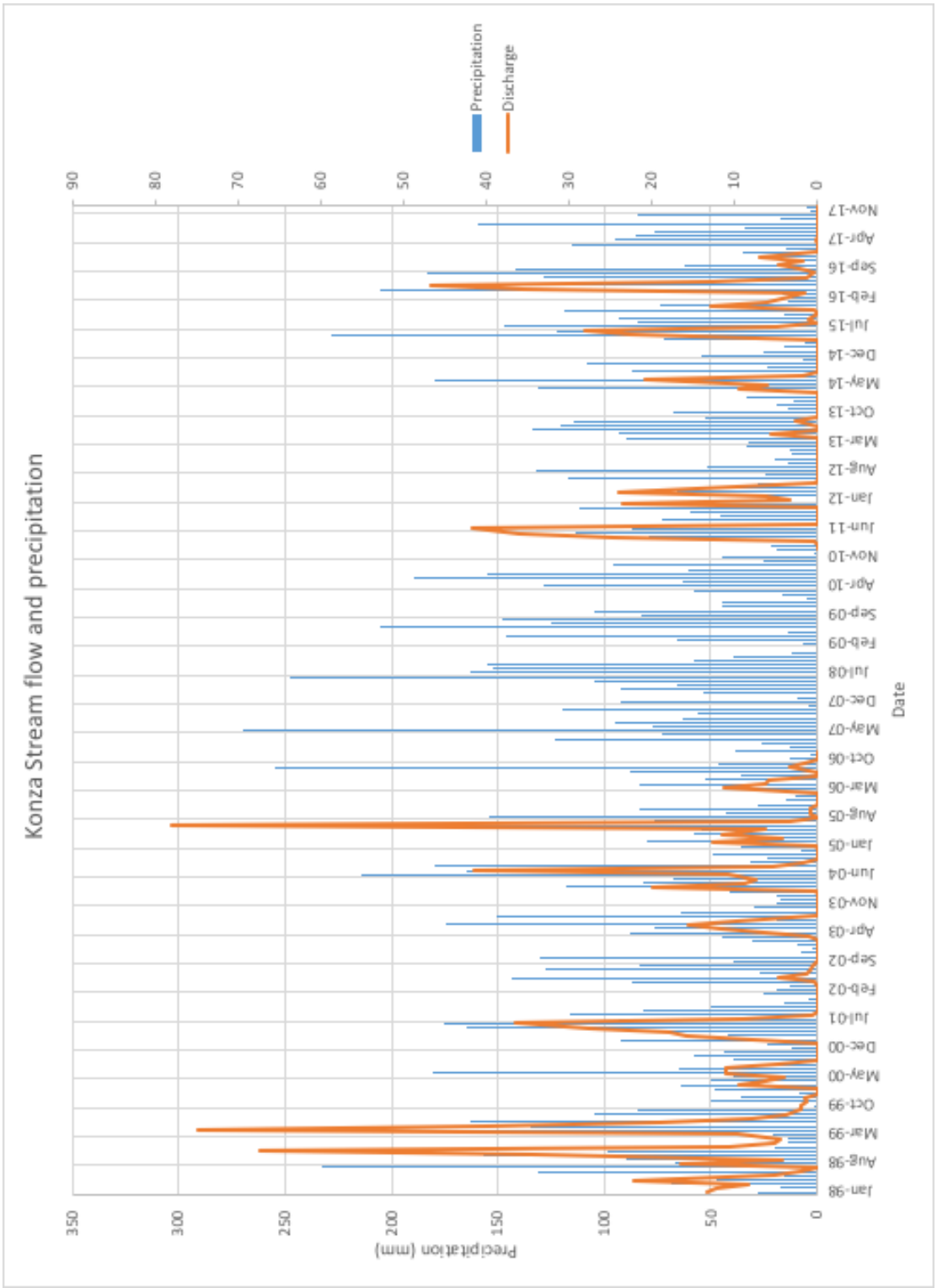


Figure 15 Konza Stream discharge and precipitation from January 1998 to December 2017. Data from ClimDB

| Sampling Period | Date Placed | Date Collected |
|---|---|---|
| 1 | 7/28/17 | 8/6/17 |
| 2 | 8/6/17 | 8/12/17 |
| 3 | 8/12/17 | 8/19/17 |
| 4 | 8/19/17 | 8/26/17 |
| 5 | 8/26/17 | 9/2/17 |
| 6 | 9/2/17 | 9/9/17 |
| 7 | 9/9/17 | 9/16/17 |
| 8 | 9/16/17 | 9/23/17 |
| 9 | 9/23/17 | 9/30/17 |
| 10 | 9/30/17 | 10/28/17 |
| 11 | 10/28/17 | 12/16/17 |

Table 3: Sampling periods and corresponding dates that Charcoal packets and water sample were collected.

| Well | Volume of dye (lb) | Volume of chaser (L) | Induced head (m) | Date of injection | Time of injection |
|---|---|---|---|---|---|
| 2-4M | 1 | 4 | 3.8 | 7/29/2017 | 12:48-12:56 pm |
| 3-5-1M | 3 | 8 | 6.6 | 7/29/2017 | 1:34-1:40 pm |
| 4-6E2 | 1 | 8 | 5.8 | 7/29/2017 | 2:27-2:30 pm |

Table 4: Dye injection volume, chaser water volume, induced head, date and time of injection.

Detailed methods:

Instructions for slug test

- Record and relevant information in field book such as location, date, start time, etc.
- Field note book should be set up prior to starting slug test, with a column for the time and a column for the depth to water.
- Using a water level meter, record the depth to water.
- Drop the slug down the well and record the water level at the following time increments: 0.17, 0.33, 0.5, 0.67, 0.83, 1.0, 1.25, 1.5, 1.75, 2.0, 2.25, 2.5, 2.75, 3.0, 3.5, 4.0, 4.5, 5.0, 5.5, 6.0, 6.5, 7.0, 8.0, 9.0, 10.0, 11.0, 12.0, 14.0, 16.0, 18.0, 20.0, 25.0, 30.0, 35.0, 40.0 minutes or until the water level returns to the initial level.
- Record the time and pull the slug out of the well.
- Record the water level at the following time increments: 0.17, 0.33, 0.5, 0.67, 0.83, 1.0, 1.25, 1.5, 1.75, 2.0, 2.25, 2.5, 2.75, 3.0, 3.5, 4.0, 4.5, 5.0, 5.5, 6.0, 6.5, 7.0, 8.0, 9.0, 10.0, 11.0, 12.0, 14.0, 16.0, 18.0, 20.0, 25.0, 30.0, 35.0, 40.0 minutes or until the water level returns to the initial level.

Instructions for making marble bags

- The intent of a marble bag is to weigh down the charcoal packet when suspended in the well so that it is fully submerged in water. The marble bag does should not be so heavy that it will weigh down the string and cause it to snap.
- Materials needed: Nylon screen (any mesh size is fine as long as the marbles won't fall through), clear marbles, monofilament clear string (any brand is fine), sewing needle, zip tie, 5 marbles per bag
- Using scissors, cut a piece of nylon screen so that it is 3 inches by 5 inches.
- Fold the screen in half, length wise.
- Thread the string through the needle and sew along the bottom of the screen and the side that is left open. Sewing along the bottom and open side twice will enforce the marble pack more. Leave the top of the packet open.
- Place 5 marbles inside the packet.
- Using a zip tie, close the top of the packet.
- Marble bag will be attached to bottom of charcoal pack using the zip tie.

Instructions for making well caps

- Materials needed: PVC well cap that will fit the outside diameter of the well, eye bolt screws, two washers, two hex nuts, one lock washer.
- Drill hole through the center of the well cap with a drill bit that matches the size of the eyebolt screws.
- Put one hex nut and one washer on top of that so that the washer is touching the inside of the well cap.
- Stick the eye bolt screw through the drilled hole so that the length of the screw is inside the well cap and leave part of the screw sticking out through the top of the well cap.

- Place the washer, lock washer, and hex nut on the part of the screw that is sticking out of the top of the well cap.
- Tighten both ends hex nuts so that the hex nuts and washers are tight against the well cap
- Attach a carabiner to the eye bolt screw.
- Sand down the inside of the well cap slightly to prevent sticking to the casing.

Instructions for installing charcoal receptors in a non-well location

- Once at the location where the packet is to be deployed, put on a new pair of powder-free NDex® nitrile gloves.
- Attach white nylon rope/ Nylon coated wire rope (1/8 inch) to tree or rock (rock must be big enough to not get washed away during a storm). Nylon coated wire rope should be used in locations where the security of the charcoal packet is questionable.
- Remove receptor from bag and use Tool City® 4 inch cable tie to attach receptor to rope.
- Place packet in water where it will receive optimal flow.
- Place a marker flag next to the receptor so that it can be found easier when the receptor is changed out.
- Take a GPS waypoint at the location where the receptor is placed.

Instructions for installing charcoal receptors in monitoring wells

- Prior to going to field work, nylon string should be cut to the length of each well for suspending the charcoal packets and placed into a Ziploc bag and labeled with the name of the well. String should be long enough so it will be suspended at the center of the well screen.
- Put on a new pair of powder-free NDex® nitrile gloves.
- Tie nylon string to the carabiner inside the well cap.
- Attach receptor to the end of the string using a Tool City® 4 inch cable tie and attach marble bag (weight) to receptor using Tool City® 4 inch cable tie.
- Lower receptor down the well and place cap on well. Close well protector cap and secure it.
- Record time, day, and any other information about installing receptor in field book.

Instructions for mixing dye

- Mix dye one day prior to injection.
- Lay disposable plastic tarp out on the ground.
- Put mixing bucket, dye box, powder-free NDex® nitrile gloves, Tyvek® suit, mixing water, stirring stick, and any other supplies necessary on the tarp. (Supplies can be bought at most standard hardware stores such as Home Depot).
- Put Tyvek® suit and gloves on.
- Pour mixing water into bucket.

- Open dye box.
- Gently pour dye into water and mix with stick until all powder is dissolved. Powder is very fine so it should be poured into mixing container very carefully out of any wind. Try not to inhale powder while mixing it.
- Once dye is mixed, put lid on dye bucket and make sure the lid is secure.
- Wipe up any powder that got on tarp with paper towels.
- Roll up tarp and place in garbage bag.
- Remove Tyvek® suit and gloves, flipping them inside out as you remove them, and place in garbage bag.
- Place any waste from mixing the dye in a garbage bag and dispose of bag.
- Place dye container in safe place so that it will not be spilled or stolen. Dye should be stored away from charcoal packets and sample vials at all times to avoid cross contamination.

Instructions for dye injection

- Bring all necessary flush water and equipment to each well. Flush water was bailed using a disposable bailer the day prior to injection and stored in 2 liter plastic jugs at the field site. The purpose of bailing the water was to avoid altering the chemistry of the groundwater. Some of the flush water used was distilled water made using a distillate at the University of Kansas, but only if water could not be bailed from the well to use as flush water. The minimum amount of flush water should be 3 times the amount of water in the well prior to injection. This allows the dye to be flushed out of the well and into the aquifer.
- Observers should be assigned to locations in stream and watching for dye entering the stream
- Record the date, time, and location of the dye trace and any other important information
- Put Tyveck® suit and powder-free NDex® nitrile gloves on.
- Place 9 foot by 12 foot 0.7 millimeter thick plastic tarp over well and cut a small hole for the well casing to go through.
- Place bottom of funnel into the opening of the hose and secure the two together using duct tape.
- Feed hose down well.
- Open dye container and pour dye into the funnel.
- Pour flush water into the funnel except for one 2 liter plastic jug.
- Slowly pull hose out of well and place into garbage bag.
- Pour the remaining jug of water down the well so that the inside of the casing is rinsed.
- Record end time of injection.
- Place empty water jugs into garbage bags.
- Wipe up any spilled dye and clean with bleach.
- Dispose of materials used in dye injection.

Instructions for dye receptor exchange at non-well location

- Put on a new pair of powder-free NDex® nitrile gloves.
- Write project name, receptor ID, location name, date and time, and initials of the collector on Nasco Whirl-pak® bag with black (no other color) sharpie.

- Approach receptor from downstream.
- Remove receptor and grab 50 ml plastic sample vial from field bag.
- Attach new receptor to rope without touching the old receptor then remove old receptor.
- Place receptor in Nasco Whirl-pak® bag, seal bag and place in cooler.
- Remove Tool City® 4 inch cable tie from receptor and place receptor in Nasco Whirl-pak® bag.
- Make sure new receptor is still in location where water is flowing.
- Take water grab sample from stream as close to where the charcoal receptor sits as possible.
- Put water grab sample in cooler.
- Refrigerate samples and store out of direct sunlight until they are to be analyzed.

Instructions for dye receptor exchange at monitoring well location

- Put on new powder-free NDex® nitrile gloves.
- Write project name, receptor ID, location name, date and time, and initials of the collector on Nasco Whirl-pak® bag with black (no other color) Sharpie®.
- Remove well cap.
- Slowly pull up receptor line while wrapping the nylon rope around the palm of your hand. Do not allow rope to touch the ground or the outside of the well.
- Remove receptor and grab sample vial from bag.
- Attach new receptor to nylon rope without touching the old receptor then remove old receptor
- Remove zip tie from receptor and place receptor in Nasco Whirl-pak® bag.
- Lower a Voss® PVC weighted disposable bailer (1.5 inches by 36 inches) down the well to take a water grab sample.
- Pour water from well into 50 ml plastic water grab vial.
- Place water grab sample into Nasco Whirl-pak® bag with charcoal receptor
- Seal Nasco Whirl-pak® bag and place into cooler.
- Refrigerate samples and store out of direct sunlight until they are to be analyzed.

Laboratory instructions for sample analysis from Ozark Underground Laboratory

More extensive laboratory methods can be found in Ozark Underground Laboratory Lab Manual

Checking samples in

- Wear powder-free NDex® nitrile gloves when handling samples
- Check that all samples are on chain of custody
- Write lab number of each sample on chain of custody, every 20$^{th}$ lab number sample is to be used as a laboratory control blank (20, 40, 60, 80, 100)
- Write lab number on sample bag and water vial. Store samples vials in a rack until ready for use.
- Water samples may be required to be pH adjusted if fluorescein or eosine is being tested for.
- Water samples should have a pH greater than 8 to be analyzed. If pH is less than 8: put water samples on a rack with the lids off. Place samples in a cooler under a vent hood. Place Nalgene bottle with lid off with ¾ full with ammonia inside the cooler with the

samples that need to be adjusted. Samples need to stay in the ammonia environment for 3-4 hours to have enough time for their pH to adjust, though overnight is best.

Cleaning charcoal packet samples

- Plastic 2 ounce Solo® cups with lids are used to elute dye out of charcoal samples. Label eluting cups and storage vials with lab numbers, including lab blank numbers with black sharpie marker.
- Line cups up in number order under the vent hood with lids loosely placed on them.
- Long sleeve disposable gloves should be worn with latex gloves over them. A lab coat or plastic apron should also be worn.
- Charcoal blanks should be prepared by using an unused charcoal packet that is run under tap water for at least 15 minutes.
- At the lab sink, remove one sample from Nasco Whirl-pak® bag. Make sure only one sample is out at a time.
- Set Nasco Whirl-pak® bag to the side of sink in a tray for reference of the lab number
- Wash sample under the faucet until samples are clean while being careful to not splash dye all over.
- Shake packet to remove excess water and cut the top off the charcoal packet with clean scissors. Find the Solo®cup that has the same lab number as the sample and pour the charcoal into the cup over a trash can so as to not contaminate other samples. Secure lid on cup and place cup back on counter in designated spot.
- Repeat the previous 3 steps for every charcoal sample.
- Once samples are finished being washed, spray bleach and water solution on the sink and sink hood and rinse them off. Clean scissors with bleach and water solution and rinse them of.

Mixing Elutant

- The following glassware will be needed: One 1000 ml cylinder, one 1000 ml beaker, one 50ml cylinder, one 1000 ml Erlenmeyer flask and one 250 ml beaker.
- Fill 250 ml beaker with ammonia. Measure 50 ml of aqua ammonia from beaker into 50 ml cylinder.
- Pour aqua ammonia into 1000 ml cylinder. Fill the rest of the cylinder with 70 % Isopropyl Alcohol until the 1000 ml line is reached. Put stopped on cylinder and shake to mike the aqua ammonia and alcohol.
- Using a digital scale, measure our 15 grams of Potassium Hydroxide, using a plastic disposable spoon to scoop it. Place funnel on top of glass bottle and add 15 grams of Potassium Hydroxide (KOH) pellets
- Pour Aqua Ammonia and Isopropyl Alcohol solution into clear glass jug and label it 5 % aqua ammonia, 95% Isopropyl Alcohol and KOH.
- Label the glass bottle: 5 % aqua ammonia, 95% Isopropyl Alcohol and KOH.
- Clean all glassware with bleach and water solution, letting them soak for one hour.

Eluting Samples

- Start a one hour timer.
- Use an Erlenmeyer flask with a 15 ml delivery head to measure out 15 ml of elutant.
- Pour elutant into charcoal cup making sure flask does not enter the cup and contaminate the sample.
- Snap lid shut on sample cup.
- Repeat previous 3 steps for all samples.

- Samples must stay in elutant for exactly one hour so as to ensure all dye has been eluded and dye does not start to be adsorbed back into the charcoal.
- After one hour, pour elutant into sample vial with corresponding sample number. This should be done in the same order that you poured the elutant into the sample cups so each sample sits for one hour.
- Once samples are eluded and in vials, they are ready to be analyzed.

Analyzing Samples

- At Ozark Underground Laboratory, using a Shimadzu RF-5301 and SpecDrvr software, run samples through machine to produce results.
- Results will be printed once sample is done running.

Detailed geology descriptions:

The geologic units in this study are Permian limestones and shales from the Council Grove Group and Chase Group of the Wolfcampian Series (Figure 3; Jewett, 1941). The regional strata are nearly horizontal with a dip of 0.1-0.21$^0$ NW (Smith, 1991). This type a karst aquifer is likely classified as a discontinuous carbonate rock (Chen *et al*., 2017). The thicknesses listed are general and the actual thicknesses of the units are highly variable. The Cottonwood Limestone Member of the Beattie Limestone, the Morrill Limestone Member of the Beattie Limestone and the Eiss Limestone Member of the Bader Limestone are both within the Council Grove Group were the aquifers used in this study. For the purpose of this study, the Cottonwood Limestone, Morrill Limestone, and Eiss Limestone will all be referred to as aquifers. The Cottonwood Limestone member of the Beattie Limestone is the lowest unit monitored in this study. The Cottonwood Limestone is 1.8 m thick and is distinguished by massive ledges. Springs are common beneath these massive ledges (Jewett, 1941). The Florena Shale member overlies the Cottonwood Limestone. The Florena is 3 m thick and is a gray argillaceous shale. The Florena shale is overlain by the Morrill Limestone member of the Beattie Limestone. The Morrill limestone is approximately 1 m thick and is brownish gray with many distinct calcite crystals in it. The Morrill weathers into an irregularly pitted, granular brown limestone. The weathered pits

are partially filled in by crystalline calcite (Jewett, 1941). Because it is not very resistant to weathering, outcrops of the Morrill are difficult to find, but it can be identified by locating the Cottonwood Limestone, which the Morrill overlies by 3 m. The Morrill is overlain by the Stearns shale. The Stearns shale is overlain by the Eiss limestone. The Eiss Limestone is made up of three parts: 1) a lower gray, thinly bedded limestone unit which is 0.5 m thick, 2) a middle unit of gray shale which is 0.75 m thick, and 3) the upper limestone unit which is 0.9 m thick. The Hooser Shale Member of the Bader Limestone overlies the Eiss Limestone. The Hooser Shale can be up to 1.8 m thick and is green and gray. The Middleburg Limestone Member of the Bader Limestone overlies the Hooser Shale. The Middleburg limestone is composed of a lower limestone unit that has a thickness of 0.9 m and is dark at the top but its coloring is mostly yellow. Overlying the lower portion of the Middleburg is a 0.15 thick black shale. The upper portion of the Middleburg is 0.18 m thick and ranges from a yellow-brown limestone to a red and green brecciated limestone. The Easly Creek Shale overlies the Bader Limestone. The Easly Creek Shale ranges from 4.5 to 6 m thick and is mostly gray and green with bands of colored material above and below bands of yellow and red. The Crouse Limestone overlies the Easly Creek Shale. The Crouse Limestone is 3 m thick and its color ranges from gray to brown. The Blue Rapids shale overlies the Crouse Limestone. The Blue Rapids Shale is between 6 and 9 m thick and is mostly gray with some red banding in between with a layer of limestone towards the bottom. The Funston Limestone overlies the Blue Rapids Shale. The Funston Limestone averages 1.5 m thick and is composed of interbedded gray limestone and green shale. The Speiser Shale overlies the Funston Limestone. There are three units within the Speiser Shale. The lower unit is 4.2 m thick and has an array of gray, red, green, and purple material that make it up. The middle unit is a 0.3 m thick gray and crystalline limestone. The upper unit of the Speiser

Shale is 0.9 m thick and is gray and yellow in color. Above the Council grove group lies the Chase group. The Threemile Limestone Member of the Wreford Limestone is the lowermost member of this group. The Threemile Limestone is less than 2.7 m thick and consists of a lower light colored limestone bed. The upper bed is lighter in color. The Havensville Shale member of the Wreford Limestone. The shale is 3 m in thickness and gray in color. Overlying the Havensville Shale is the Schroyer Limestone Member of the Wreford Limestone. This unit is 5.4 m thick and is mostly flint rich except for the top meter. The Wymore Shale member of the Matfield Shale overlies the Schroyer limestone. This shale is 6 m thick and has various colors of gray, red, green, brown, and purple. The Kinney Limestone Member of the Matfield Shale overlies the Wymore Shale. The Kinney Limestone is fossiliferous and 1.2 m thick. Overlying the Kinney Limestone is the Blue Springs Shale member of the Wymore Shale. The Blue Springs Shale is approximately 8 m and is a brightly colored shale with variations of yellow, gray, red, purple, green, and chocolate throughout (Jewett, 1941). Quaternary deposits of alluvium and colluvium overlie these Permian units. A thin layer of loess covers most of the region (Smith, 1991).

Slug test data and calculations:

| Time Since Start (t) (s) | Depth to Water (DTW) | Head in Well (h) (ft) | Head Ratio ($h/h_o$) |
|---|---|---|---|
| 10 | 10.65 | -0.093 | 1.0000 |
| 20 | 10.63 | -0.073 | 0.7849 |
| 30 | 10.615 | -0.058 | 0.6237 |
| 40 | 10.61 | -0.053 | 0.5699 |
| 50 | 10.605 | -0.048 | 0.5161 |
| 60 | 10.6 | -0.043 | 0.4624 |
| 75 | 10.595 | -0.038 | 0.4086 |
| 90 | 10.59 | -0.033 | 0.3548 |
| 105 | 10.585 | -0.028 | 0.3011 |
| 120 | 10.58 | -0.023 | 0.2473 |
| 150 | 10.58 | -0.023 | 0.2473 |
| 180 | 10.576 | -0.019 | 0.2043 |
| 210 | 10.574 | -0.017 | 0.1828 |
| 240 | 10.572 | -0.015 | 0.1613 |
| 300 | 10.57 | -0.013 | 0.1398 |
| 360 | 10.567 | -0.010 | 0.1075 |
| 420 | 10.566 | -0.009 | 0.0968 |
| 480 | 10.563 | -0.006 | 0.0645 |
| 540 | 10.562 | -0.005 | 0.0538 |
| 600 | 10.562 | -0.005 | 0.0538 |
| 720 | 10.56 | -0.003 | 0.0323 |
| 840 | 10.56 | -0.003 | 0.0323 |
| 960 | 10.56 | -0.003 | 0.0323 |
| 1080 | 10.559 | -0.002 | 0.0215 |
| 1200 | 10.558 | -0.001 | 0.0108 |
| 1500 | 10.557 | 0.000 | 0.0000 |

Table 5: Slug test data for well 3-5-1M from February 2017.

| | |
|---|---|
| **Well Depth (m)** | 11.000 |
| **Initial depth to water ($DTW_i$) (ft)** | 10.557 |
| **Slug Width (ft)** | 0.030 |
| **Slug Length (ft)** | 1.020 |
| **Initial Displacement ($h_0$) (ft)** | 0.093 |
| **Volume of slug ($V_s$) ($ft^3$)** | 0.001 |
| **Length of screen ($L_e$) (ft)** | 1.000 |
| **length from WT to bottom of screen ($L_w$) (ft)** | 0.443 |
| **Saturated thickness* (b) (ft)** | 0.443 |
| **Diameter of casing ($d_c$) (ft)** | 0.051 |
| **Diameter of well bore (D) (ft)** | 0.051 |
| **$t_{0.37}$ (s)** | 85 |

Table 6: Slug test calculation parameters for well 3-5-1M from February 2017.

| **Hvorslev** | |
|---|---|
| **$R_e$** | 0.459 |
| **T** | 1.39E-05 |
| **K** | 3.15E-05 |

Table 7: Slug test results for well 3-5-1M from February 2017 (Hvorslev, 1951).

Table 8: Well log data showing limestone, gravel pack, and bentonite elevations.

| Elevations, m amsl | Ground elev | Top Morrill | Base Morrill | Top Stearns Ls | Base Stearns Ls | Top Eiss | Base Eiss | Top Lower Eiss (1) | Base Lower Eiss (1) | Top Upper Eiss (2) | Base Upper Eiss (2) | Depth below unit well was drilled to (m) | Unit thickness | Screened interval (m) | Gravel pack length (m) | Bentonite fill (m) | Unit the top of the gravel pack lies in |
|---|---|---|---|---|---|---|---|---|---|---|---|---|---|---|---|---|---|
| 1-3 Mor | 371.891 | 365.80 | 365.19 | 369.09 | 369.03 | 371.89 | 369.76 | | | | | | 0.61 | n/a | | | |
| 1-3 Eis | | | | | | | | | | | | | 2.13 | n/a | | | |
| | | | | | | | | | | | | | | | | | |
| 1-6 Mor | 372.184 | 365.78 | 364.87 | | | 372.18 | 370.05 | | | | | | 0.91 | n/a | | | |
| 1-6 Eis | | | | | | | | | | | | | | n/a | | | |
| | | | | | | | | | | | | | | | | | |
| 2-1 Mor | 368.345 | 366.82 | 366.21 | | | | | | | | | | 0.61 | n/a | | | |
| 2-3 Mor | 376.448 | 366.39 | 365.02 | 367.61 | 367.46 | 372.64 | 370.05 | | | | | | 1.37 | n/a | | | |
| 2-3 Eis | | | | | | | | | | | | | 2.59 | n/a | | | |
| 2-4 Mor | 366.231 | 365.62 | 365.32 | | | | | | | | | | 0.30 | n/a | | | |
| | | | | | | | | | | | | | | | | | |
| 2-5 Mor | 368.277 | 365.84 | 364.92 | | | | | | | | | | | n/a | | | |
| 2-6 Mor | 372.323 | 365.77 | 364.46 | 369.12 | 368.82 | 371.56 | 369.95 | | | | | | 1.31 | n/a | | | |
| 2-6 Eis | | | | | | | | | | | | | | n/a | | | |
| | | | | | | | | | | | | | | | | | |
| 3-2 Mor | 372.322 | 365.92 | 365.01 | | | 372.32 | 370.04 | | | | | 0.30 | 0.91 | 0.61 | 1.83 | 5.79 | Stearns Shale |
| 3-2 Eis | 372.319 | | | | | 372.32 | 370.03 | | | | | 0.09 | 2.29 | 0.61 | 1.22 | 1.16 | Eiss Limestone |
| 3-3 Mor | 375.801 | 365.74 | 364.83 | | | 372.14 | 369.71 | | | | | 0.15 | 0.92 | 0.61 | 1.83 | 9.30 | Stearns Shale |
| 3-3 Eis | 375.756 | | | | | 372.19 | 369.81 | | | | | 0.00 | 2.38 | 0.61 | 1.83 | 4.11 | Hooser Shale |
| | | | | | | | | | | | | | | | | | |
| 3-5 Mor | 370.588 | 365.10 | 364.19 | | | | | | | | | 0.30 | 0.92 | 0.61 | 0.91 | 5.79 | Stearns Shale |
| 3-5-1 Mor | 374.803 | 364.38 | 362.56 | 368.40 | 368.15 | 370.86 | 368.40 | | | | | | 1.82 | | | | |
| 3-6 Mor | 374.164 | 366.24 | 365.02 | | | 372.03 | 370.05 | | | | | 0.00 | 1.22 | 0.61 | 0.91 | 8.23 | Stearns Shale |
| 3-6 Eis | 374.149 | | | | | 372.17 | 369.73 | | | | | 0.30 | 2.44 | 0.61 | 0.91 | 3.81 | Eiss Limestone |
| 3-7 Mor | 393.438 | 365.45 | 364.48 | 369.94 | 369.63 | 372.07 | 369.94 | | | | | | 0.98 | n/a | | | |
| 3-7 Eis | 393.389 | | | | | | | | | | | | 2.13 | n/a | | | |
| | | | | | | | | | | | | | | | | | |
| 4-1 Mid | *375.756* | | | | | | | | | | | | | | | | |
| 4-2 Mor | 374.651 | 364.90 | 364.59 | | | 371.30 | 369.01 | | | | | 0.55 | 0.30 | 0.61 | 1.22 | 8.78 | Stearns Shale |
| 4-2 Eis 1 | 374.600 | | | | | 371.40 | 368.81 | 368.99 | 368.81 | 371.40 | 370.49 | 0.18 | 0.18 | 0.61 | 1.83 | 3.96 | Eiss 2 Limestone |
| 4-2 Eis 2 | 374.507 | | | | | | | | | 371.46 | 368.81 | 0.30 | 2.65 | 0.61 | 1.83 | 1.98 | Hooser Shale |
| 4-4 Stearns | 373.583 | | | 369.47 | 367.49 | 370.84 | 370.69 | | | | | | | | | | |
| | | | | | | | | | | | | | | | | | |
| 4-5 Stearns | 371.477 | | | 369.50 | 368.58 | | | | | | | | | | | | |
| 4-6 Mor | 375.816 | 365.00 | 363.78 | 368.20 | 367.43 | 371.40 | 368.81 | | | | | 0.61 | 1.22 | 0.61 | 1.83 | 10.82 | Stearns Shale |
| 4-6 Eis 1 | 375.783 | | | | | | | | | | | | n/a | 0.61 | 1.83 | 5.03 | ? |
| 4-6 Eis 2 | 375.795 | | | | | | | | | 371.07 | 370.13 | | 0.95 | 0.61 | 1.83 | 3.35 | Hooser Shale |
| 4-7-Mor | 400.385 | 365.03 | 363.81 | 367.47 | 365.03 | 370.21 | 367.47 | | | | | | | | | | |